Universidad Zaragoza
1542

Trabajo Fin de Grado

EVALUATION OF FATIGUE PROPERTIES OF THERMOPLASTIC ELASTOMERS (TPEs) FOR BIOMEDICAL APPLICATIONS

Autor/es

Paula Gracia Muñoz

Director/es

Miroslawa El Fray

Escuela de Ingeniería y Arquitectura (EINA)

2014-2015

West Pomeranian University of Technology in Szczecin

MECHANICAL ENGINEERING DEPARTMENT

Final Project

EVALUATION OF FATIGUE PROPERTIES OF THERMOPLASTIC ELASTOMERS (TPEs) FOR BIOMEDICAL APPLICATIONS

Author: Paula Gracia Muñoz

Supervisor: Prof. Dr. Habil. Miroslawa El Fray

JUNE 2015

To my family for being the best support during my life, teaching me how to work and fight to get what I want and believe in and doing myself a better person.

ACKNOWLEDGEMENTS

Hereby I would like to acknowledge first of all my supervisor, Prof. Dr. Habil. Miroslawa El Fray for her assistance and guidance during my work and let me do my research in the university.

I would like to thank a Polish PhD student, MSc. Michał Rybko, for his help in the laboratory, support and patience during all my project.

Furthermore, I would like to thank another colleagues in the university, Dr. Marta Piątek-Hnat, Joanna Gajowy and Zygmunt Staniszewski for their help and knowledge in different scientific fields.

CONTENTS

INTRODUCTION

1. AIMS OF THE STUDY

The major aim of this study is to assess the long-term behaviour of thermoplastic elastomers (TPEs) at different environmental conditions for biomedical applications.

These materials will be a member of someone's body, thus, they have to be studied under the same organism conditions (inside artificial body fluid at 37ºC (temperature of our body)).

Their function is to behave as heart assisting devices (artificial hearts). That is why their mechanical properties will be measured to determine how they will be influenced by time, blood, heartbeats … and see if they are appropriate for that because we are talking about a human life and everything should work as good as possible.

The main features to be studied will be strength, hardness, stiffness, loading and elongation in fatigue test, stress-strain curve, creep behaviour…

2. LITERATURE REVIEW

2.1. Review of tissue engineering

Biomedical engineering involves the application of engineering science and technology to problems arising in medicine and biology. The integration of each engineering discipline (electrical, mechanical, chemical, and so on) with each discipline in medicine (pathology, cardiology, neurology) or biology (biochemistry, pharmacology, molecular biology, cell biology, and so on) is a potential area of biomedical engineering application [1].

Tissue engineering is the use of a combination of cells, engineering and materials methods, and suitable biochemical and physico-chemical factors to improve or replace biological functions. While the application of engineering expertise to the life sciences requires an obvious knowledge of contemporary technical theory and applications, it also demands an adequate knowledge and understanding of relevant medicine and biology. It has been argued that the most challenging part of finding engineering solutions lies in the formulation of the solution in engineering terms. From a biomedical engineering point of view also this demands a full understanding of the life science substrates as well as the quantitative methodologies [1].

Langer and Vacanti [2] stated that tissue engineering is "an interdisciplinary field that applies the principles of engineering and life sciences

toward the development of biological substitutes that restore, maintain, or improve tissue function or a whole organ".

Also most definitions of tissue engineering cover a broad range of applications, in practice the term is closely associated with applications that repair or replace portions or whole tissues (bone, cartilage, blood vessels, bladder, and so on). Often, the tissues involved require certain mechanical and structural properties for their human applications.

2.2 Heart: physiology and function

"It has been shown by reason and experiment that blood by the beat of the ventricles flows through the lungs and heart and is pumped to the whole body…the blood in the animal body moves around in a circle continuously, and…the action or function of the heart is to accomplish this by pumping. This is the only reason for the motion and beat of the heart."—William Harvey (1628). *Exercitatio Anatomica de Mow Cordis et Sanguinis in Animalibus.* [3]

The heart is a central organ in the circulatory system, and is indispensable for normal organism homeostasis by providing a constant supply of blood to tissues, which carries oxygen and nutrients and removes carbon dioxide and waste products. The heart pumps blood through blood vessels, and to accomplish this, the heartbeats about 100,000 times every day, which adds up to 35 million beats in a year and about 2.5 billion times in an average lifetime, pumping 5 liters of blood each minute.

The unique heart structure ensures a continuous blood supply, at rest and in various stressful conditions. Due to the central function of the heart in sustaining life and normal homeostasis of the body, the diseases of the heart are a major concern in public health. [4]

2.2.1 Chambers of the heart

The four chambers in the heart (Fig. 2.1, A-B) can be segregated into the left and the right side, each containing an atrium and a ventricle. The right side is responsible for collecting oxygen-poor blood and pumping it to the lungs. The left side is responsible for collecting oxygen-rich blood front the lungs and pumping it to all tissues in the body. Within each side, the atrium is a site for the collection of blood, before pumping it to the ventricle. The ventricle is much stronger, and it is a site for the pumping of blood out and away from the heart.

The right ventricle is the site for the collection of ALL oxygen-poor blood. The large superior and inferior venae cavae, among other veins, carry oxygen-poor blood from the upper and lower parts of the body to the right atrium. The right ventricle pumps the blood out of the heart, and through the pulmonary trunk. The term *trunk,* when referring to a vessel, is a convention that indicates an artery that bifurcates. The pulmonary trunk bifurcates into the left and right pulmonary arteries that enter the lungs. It is important to note that the term

"artery" is always used for a vessel that carries blood AWAY from the heart. This is irrespective of the oxygen content of the blood that flows through the vessel.

Once oxygenated, the oxygen-rich blood returns to the heart from the right and left lung through the right and left pulmonary vein, respectively (“vein”—a vessel carrying blood TOWARD the heart). Each pulmonary vein bifurcates before reaching the heart. Thus, there are four pulmonary veins entering the left atrium. Oxygen-rich blood is pumped out of the heart by the left ventricle and into the aortic artery. The right side of the heart and the pulmonary artery and veins are part of the pulmonary circuit because of their role in getting blood to and from the lungs *(pulmo* = “lungs”). The left side of the heart, the aortic artery, and the venire cavae are part of the systemic circuit because of their role in getting blood to and from all the tissues of the body. [5]

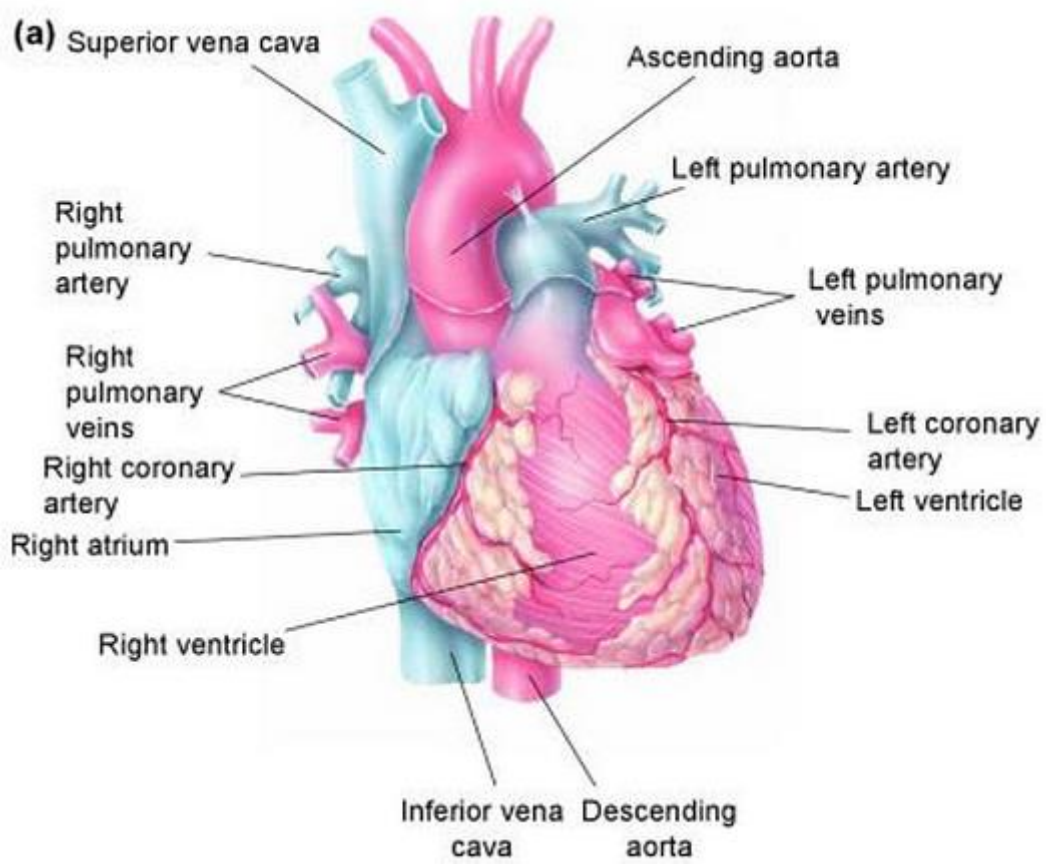

Fig. 2.1 A. Anterior external view of the heart showing major surface features. [4]

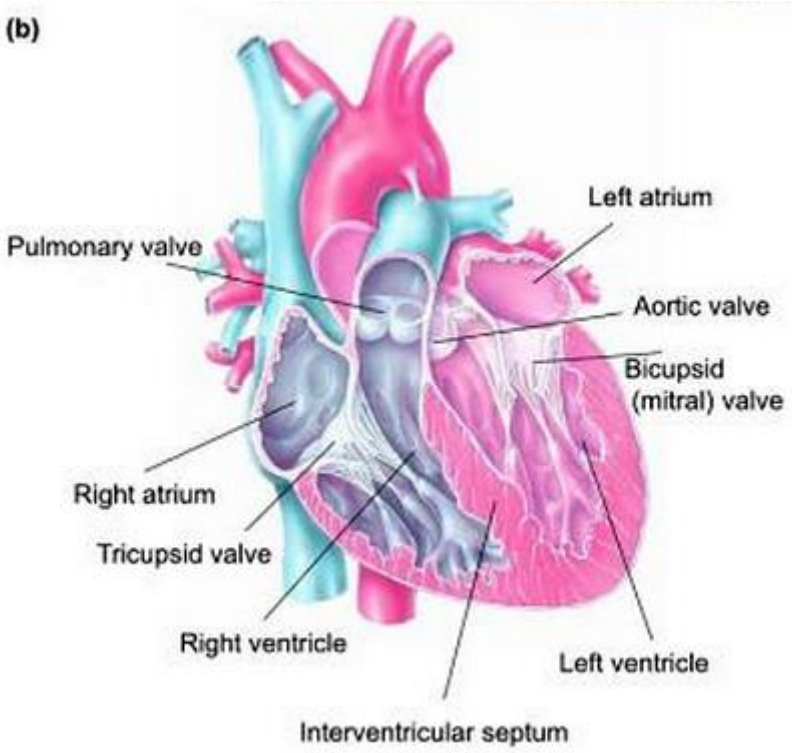

Fig. 2.1 B. Major internal features of the heart. Blood vessels that carry oxygenated blood are colored red, whereas those that carry deoxygenated blood are colored blue. [4]

2.2.2 Muscle tissues

The heart is composed of cardiac muscle which enable the heart to contract and allow the synchronization of the heartbeat. In order to best understand the heart wall, it is desirable to first know muscle tissue types. [6]

Muscle tissue contains numerous microfilaments composed of actin (an abundant 43-kd protein that polymerizes to form cytoskeletal filaments) and myosin (a protein that interacts with actin as a molecular motor - a protein that converts chemical energy in the form of ATP to mechanical energy, thus generating force and movement.), which are contractile proteins [7].

There are three major types of muscle tissue:

- *Cardiac Muscle*

Cardiac muscle is so named because it is found in the heart. Cells are joined to one another by intercalated discs which allow the synchronization of the heartbeat. Cardiac muscle is branched, striated muscle.

- *Skeletal Muscle*

Skeletal muscle, which is attached to bones by tendons, is associated with the body's voluntary movements. Skeletal muscle is striated muscle. Unlike

cardiac muscle, the cells are not branched.

• *Visceral (Smooth) Muscle*

Visceral muscle, is found in various parts of the body such as the arteries, the bladder, the digestive tract, as well as in many other organs.

Visceral muscle is also called smooth muscle because it doesn't have cross striations. Visceral muscle contracts slower than skeletal muscle, but the contraction can be sustained over a longer period of time. [6]

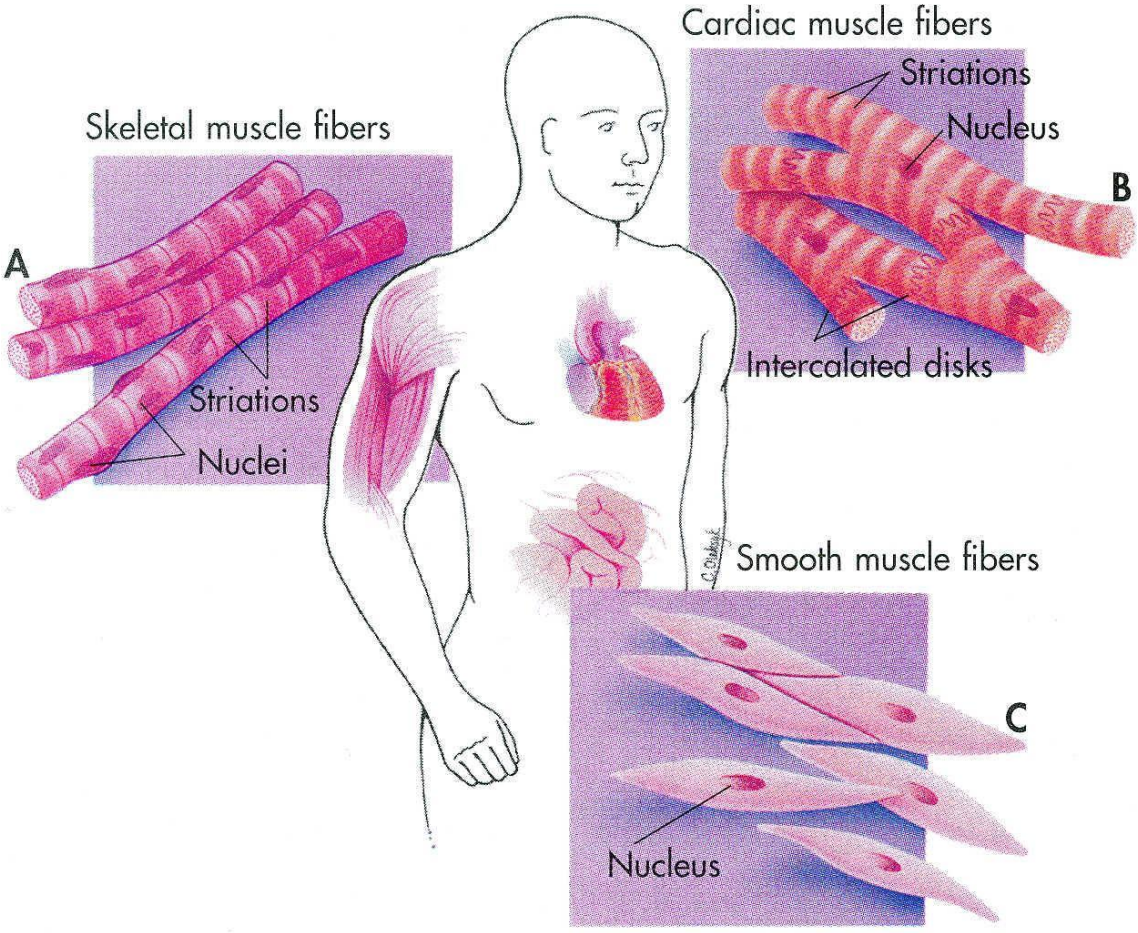

Fig. 2.2 Differences between muscle tissues

2.2.3 The heart wall

The wall of the heart consists of three layers: the epicardium (external layer), the myocardium (middle layer), and the endocardium (inner layer). Epicardium, the thin, transparent outer layer of the heart wall, is composed of mesothelium and delicate connective tissue that imparts a smooth, slippery texture to the outermost surface of the heart. The middle myocardium, which is the cardiac muscle tissue, constitutes about 95% of the heart mass and is responsible for its pumping action. The cardiac muscle fibers swirl diagonally

around the heart in bundles. The innermost endocardium is a thin layer of endothelium overlying a thin layer of connective tissue. It provides a smooth lining for the chambers of the heart and covers the valves of the heart. The endocardium is continuous with the endothelial lining of the large blood vessels attached to the heart, and it minimizes surface friction as blood passes through the heart and blood vessels.

The human myocardium consists of 2 to 3 billion cardiomyocytes (75% by volume, ~30% by number), the striated muscle cells found only in the heart that can be distinguished from the skeletal and smooth muscle cells. Apart from muscle cells, the heart tissue is mainly composed of fibroblasts (about two thirds in terms of numbers) and endothelial cells. Unlike skeletal muscle cells, cardiomyocytes are controlled by the autonomic (involuntary) rather than the somatic (voluntary) nervous system. Furthermore, cardiomyocytes can generate their own excitatory impulses, functioning as a biological pacemaker.

The myocardium assumes a unique structure, enabling it to synchronously contract (Fig. 2.3 C-D). As I mentioned earlier, compared with skeletal muscle fibers, the cardiac muscle fibers are shorter in length and less circular in the transverse section. They also exhibit branching, which gives the individual cardiac muscle fibers a "stair-step" appearance. A typical cardiac muscle fiber is 50-100 *μm* long and has a diameter of about 14 μm. The cardiomyocyte has one centrally located nucleus, although an occasional cell may have two nuclei. The ends of cardiac muscle fibers connect to neighboring fibers by irregular transverse thickenings of the sarcolemma called intercalated discs. The discs contain desmosomes, which hold the fibers together, and gap junctions, which allow the muscle action potentials to conduct from one muscle fiber to its neighbors. Gap junctions allow the entire myocardium of the atria or the ventricles to contract as a single, coordinated unit.

Myofibrils, the contractile structure of cardiomyocytes, are composed of repeating single contractile units known as sarcomeres (Fig. 2.3D). Electrical excitation of cardiomyocytes leads to contraction of the heart through the process of excitation-contraction coupling (ECC).The ubiquitous second messenger, Ca^{2+}, is essential for cardiac electrical activity and is the direct activator of the myofilaments, which cause contraction.

Myocyte mishandling of Ca^{2+} is a central cause of both contractile dysfunction and arrhythmias in pathophysiological conditions. The cardiomyocyte contraction machinery is based on two main proteins, myosin and actin, that build thick and thin filaments, respectively. During muscle contraction, actin fibers move toward the inner space of the sarcomere by sliding along the fixed myosin fibers. Each sarcomere is bounded by Z-lines formed by protein aggregates, situated at the edge of the sarcomere. Together, the protein complexes comprising the sarcomere enable the macroscopic movement associated with contractile activity (Fig. 2.3D)

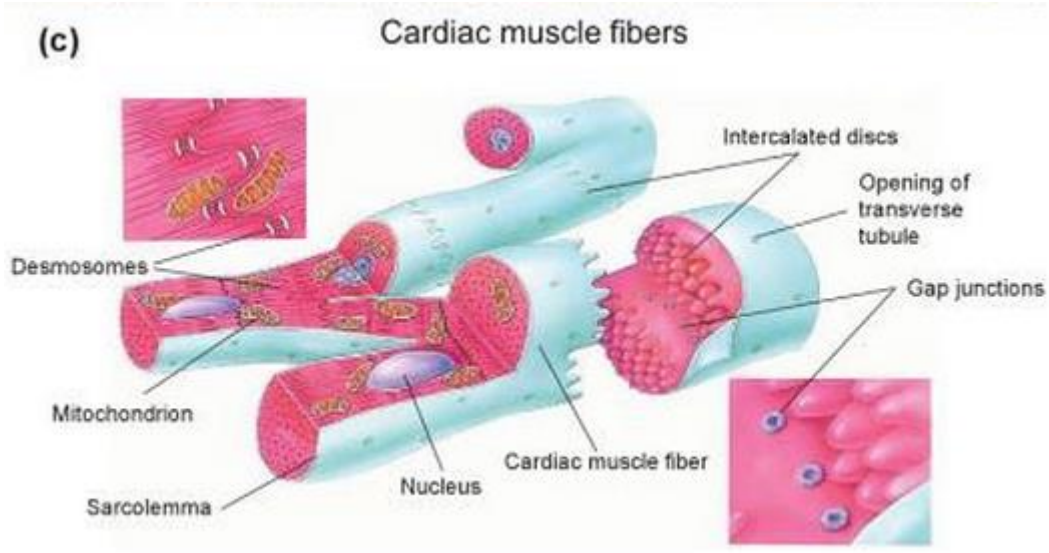

Fig. 2.3 C. Overall organization of cardiac muscle fibers. Sarcolemma is plasma membrane of a muscle cell. Sarcoplasmic reticulum (SR) is membranous sacs encircling each myofibril. In a relaxed muscle fiber, the sarcoplasmic reticulum stores calcium ions. Release of Ca^{2+} from the terminal cisterns of the SR triggers muscle contraction.

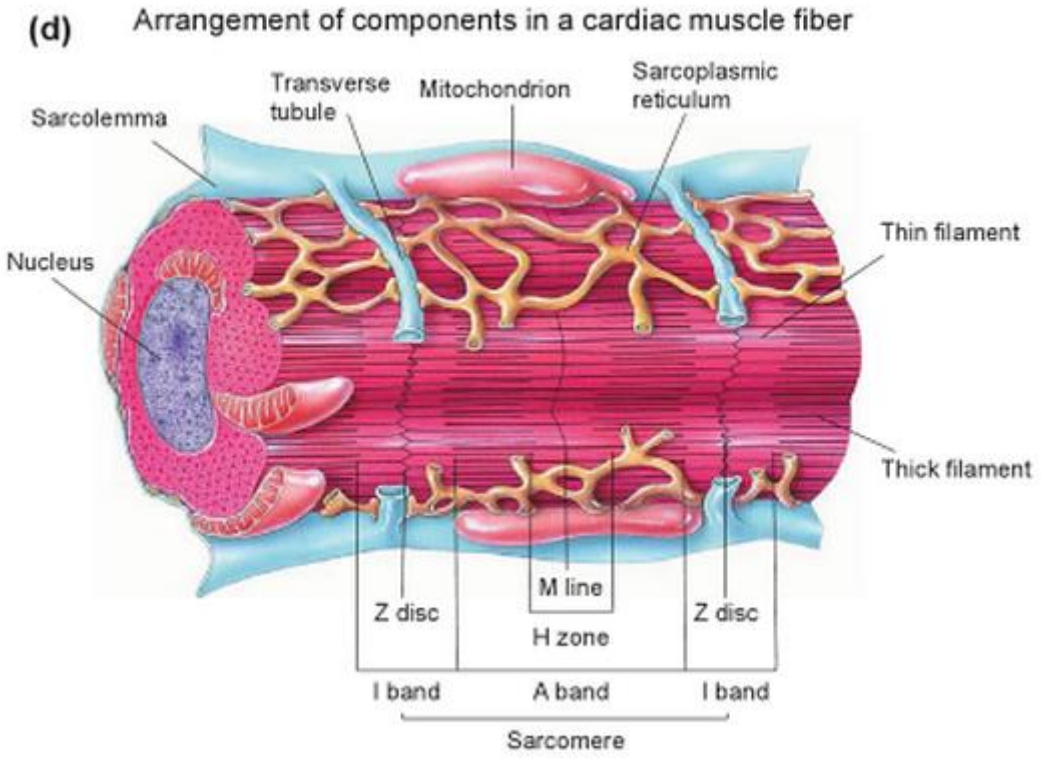

Fig. 2.3 D. Internal arrangement of the cardiac fiber showing basic sarcomere structure. The assembly of contractile proteins into sarcomeres is a complex process that requites coordinate synthesis of the constituent proteins, the polymerization of actin and myosin (and many associated proteins) into thin and thick filaments, respectively, and the association of the two filament systems into highly organized sarcomeres. Newly assembled sarcomeres consist of parallel arrays of ~1.0 µm-long thin filaments that interdigitate with laterally aligned 1.6 µm-long thick filaments. Narrow, plate-shaped regions of dense protein material called Z discs separate one sarcomere from the next. Thus, a sarcomere extends from one Z disc to the next Z disc. The thick and thin filaments overlap one another to a greater or lesser extent, depending on whether the muscle is contracted, relaxed, or stretched. The pattern of their overlap, consisting of a variety of zones and bands (I, A, and H), creates the striations that can be seen both in single myofibrils and in whole muscle fibers. The M line marks the middle of the sarcomere. [4]

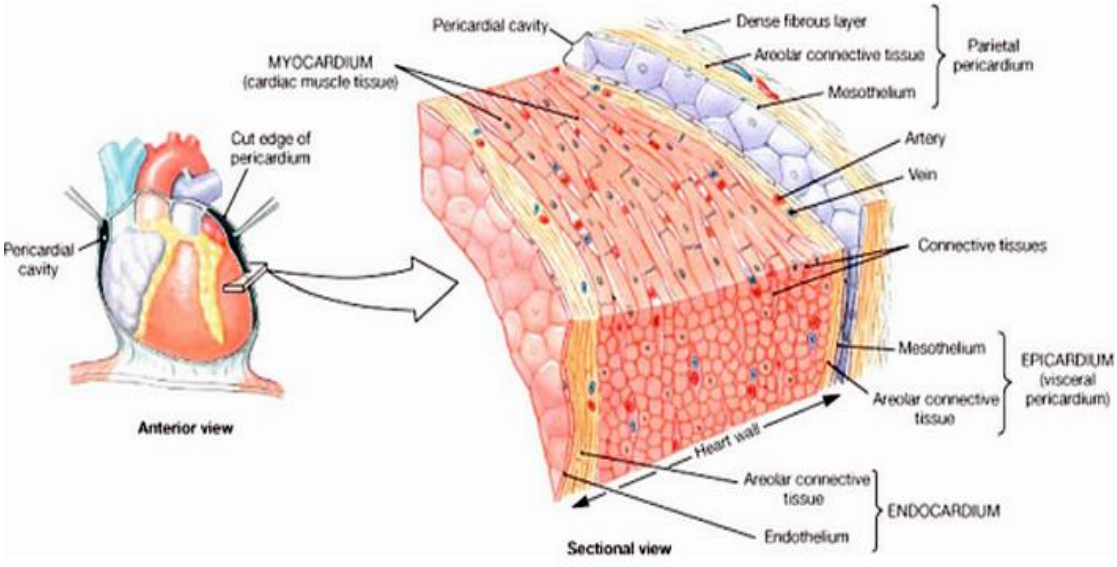

Fig. 2.4 Internal anatomy of the heart (Fig. 21.3a & b, p. 553 from HUMAN ANATOMY. 4th Edition by Frederic H. Martini, Michael J. Timmons and Robert B. Tullitsch 2003 by Frederic **H.** Martini. Inc. and Michael J. Timmons.) [5]

2.2.4 Cardiac cycle

A single cycle of cardiac activity can be divided into two basic phases - diastole and systole. (Fig. 2.5)

Diastole

Diastole represents the period of time when the ventricles are relaxed (not contracting).Throughout most of this period, blood is passively flowing from the left atrium (LA) and right atrium (RA) into the left ventricle (LV) and right ventricle (RV), respectively (see figure at right). The blood flows through atrioventricular (AV) valves (mitral and tricuspid) that separate the atria from the ventricles. The RA receives venous blood from the body through the superior vena cava (SVC) and inferior vena cava (IVC). The LA receives oxygenated blood from lungs through four pulmonary veins that enter the LA. At the end of diastole, both atria contract, which propels an additional amount of blood into the ventricles.

Systole

Systole represents the time during which the left and right ventricles contract and eject blood into the aorta and pulmonary artery, respectively. During systole, the aortic and pulmonic valves open to permit ejection into the aorta and pulmonary artery. The atrioventricular valves are closed during systole, therefore no blood is entering the ventricles; however, blood continues to enter the atria though the vena cavae and pulmonary veins.

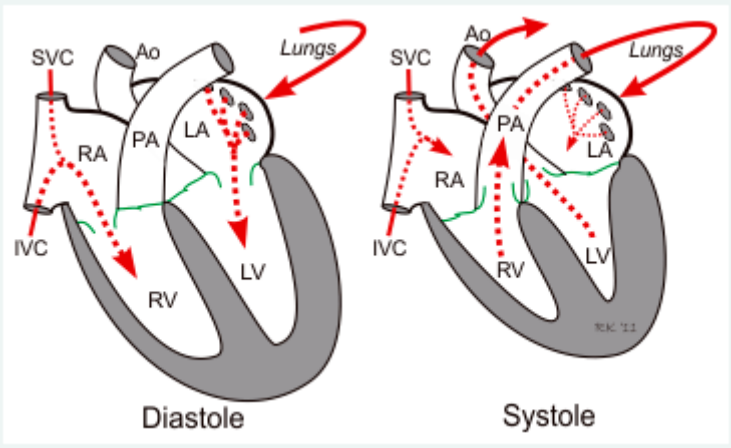

Fig. 2.5 Two basic phases of cardiac cycle

There are several mechanical events in the heart during the cardiac cycle including the arterial pulse, ECG (electrocardiogram), heart sounds, venous pulse, pressure and volume changes in the right atrium and in the left ventricle. [8]

The duration of the cardiac cycle is inversely proportional to the heart rate. The cardiac cycle duration increases with a decrease in the heart rate and on the other hand it shortens with increasing heart rate. At a normal heart rate of 75 beats per minute, one cardiac cycle lasts 0.8 second. Under resting conditions, systole occupies ⅓ and diastole ⅔ of the cardiac cycle duration. At an increasing heart rate (e.g. during an intensive muscle work), the duration of diastole decreases much more than the duration of systole. [9]

To analyse systole and diastole in more detail, the cardiac cycle is usually divided into several phases but first, it is better to know something about the electrocardiogram.

2.2.4.1 Electrocardiogram

Electrical activity recorded from the surface of the body represents the vector sum of action potentials recorded from many cardiac muscle fibers oriented in many different directions. A deflection away from the baseline observed on the surface electrocardiogram (EKG or ECG) indicates an electrical imbalance between the pair of recording electrodes, as a wave of activity moving within the heart produces current flow between the distant areas being monitored by the electrodes. The configuration of the electrocardiogram bears little resemblance to single fiber action potentials.

An electrocardiogram furnishes information about heart rate, conduction pathways, cardiac excitability, cardiac refractoriness, and some anatomical irregularities. It does not provide any information about mechanical actions of the heart, such as valve movements or contractile force of the myocardium. [9]

A "typical" ECG tracing is shown below (Fig.2.6 A). The different waves that comprise the ECG represent the sequence of depolarization (the term used for the release (discharge) of an electrical stimulus) and repolarization (the term for recharging) of the atria and ventricles. The ECG is recorded at a standardized speed of 25 mm/sec, and the voltages are calibrated so that 1 mV = 10 mm in the vertical direction (Amplitude). Therefore, each small 1-mm^2 represents 0.04 sec (40 msec) in time and 0.1 mV in voltage (Fig.2.6 B)

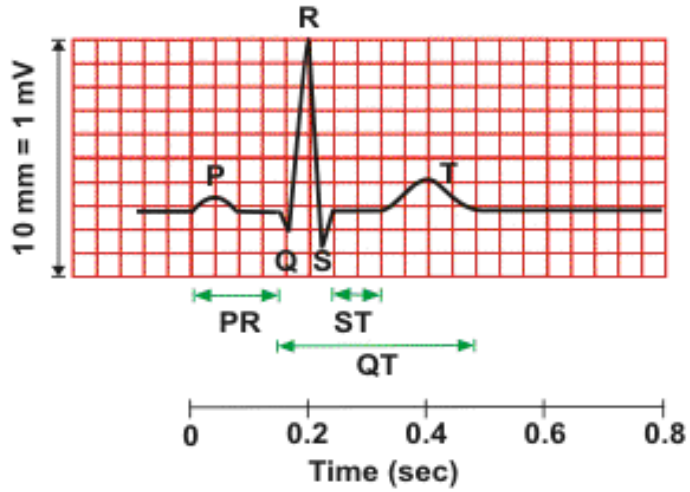

P wave (0.08 - 0.10 s) QRS (0.06 - 0.10 s)

P-R interval (0.12 - 0.20 s) Q-T_C interval (≤ 0.44 s)*

$*QT_C = QT/\sqrt{RR}$

Fig. 2.6 A- A typical ECG

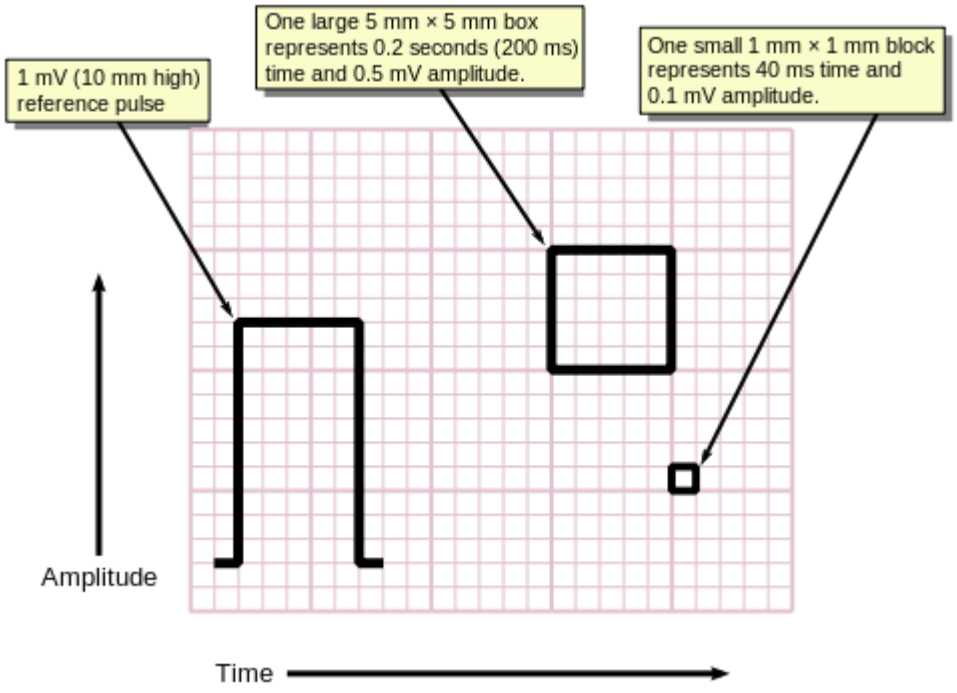

Fig.2.6 B- For ease of measuring the amplitudes and intervals, an ECG is printed on graph paper at a standard scale

P wave

The P wave represents the wave of depolarization that spreads from the SA (sinoatrial) node throughout the atria, and is usually 0.08 to 0.1 seconds (80-100 msec) in duration. The brief isoelectric (zero voltage) period after the P wave represents the time in which the impulse is traveling within the AV (atrioventricular) node (where the conduction velocity is greatly retarded) and the bundle of His.

QRS complex

The QRS complex represents ventricular depolarization. The duration of the QRS complex is normally 0.06 to 0.1 seconds. This relatively short duration indicates that ventricular depolarization normally occurs very rapidly.

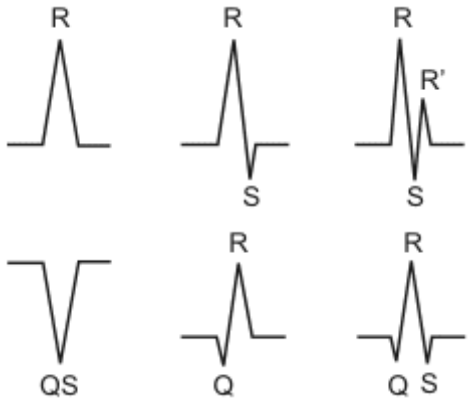

Fig. 2.7 The nomenclature used to define the different components of the QRS complex

The shape of the QRS complex in the above figure (Fig.2.6) is idealized. In fact, the shape changes depending on which recording electrodes are being used. The shape will also change when there is abnormal conduction of electrical impulses within the ventricles.

ST segment

The isoelectric period (ST segment) following the QRS is the time at which the entire ventricle is depolarized and roughly corresponds to the plateau phase of the ventricular action potential. The ST segment is important in the diagnosis of ventricular ischemia or hypoxia because under those conditions, the ST segment can become either depressed or elevated.

T wave

The T wave represents ventricular repolarization and is longer in duration than depolarization (i.e., conduction of the repolarization wave is slower than the wave of depolarization). Sometimes a small positive U wave may be seen following the T wave (not shown in figure 2.6). This wave represents the last

remnants of ventricular repolarization. Inverted or prominent U waves indicates underlying pathology or conditions affecting repolarization. [8]

2.2.4.2 Individual phases of the cardiac cycle

1- Atrial contraction

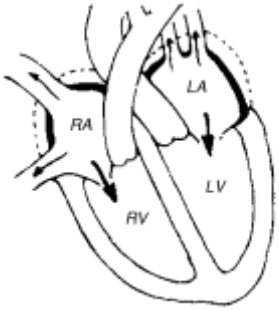

a. Preceded by P wave (atrial excitation)

b. Pressure rise in atrium, small, transient (venous "a" wave)

c. Increase ventricular volume, small, transient at rest

d. Mitral and tricuspid valves open at the beginning; may be closed at end

e. Little contribution to blood pumping at rest; may contribute 10-20% to ventricular filling in exercise when heart rate is higher

f. Decreasing aortic (and pulmonic) pressure because blood is flowing from the arteries into the peripheral vascular beds and no blood is being ejected from the heart

g. QRS begins

2- Isovolumetric contraction

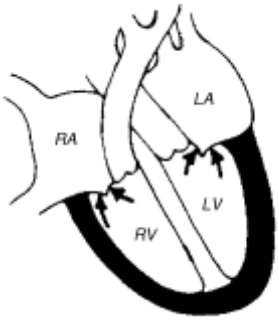

a. Initiated by ventricular excitation (QRS wave)

b. Mitral and tricuspid valves close because of pressure gradient (aortic and pulmonic valves already closed)

c. Rapid rise in ventricular pressure

d. No change in ventricular volume (isovolumetric = constant volume)

e. Decreasing aortic (and pulmonic) pressure

f. Atrial pressures may increase due to bulging of A-V valves (venous "c" wave)

g. First heart sound begins

3- Ventricular ejection

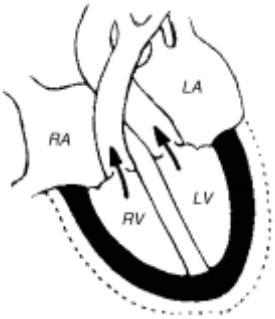

a. Begins when ventricular pressure exceeds aortic (or pulmonary artery) pressure

b. Aortic (and pulmonic) valves open

c. Initial rapid reduction of ventricular volume as blood is ejected from the ventricle followed by reduced ejection

d. Ventricular (and arterial) pressures increase to maximum ("systolic pressure") and then decrease slowly as the ventricular begin to relax

e. Initial low atrial pressure followed by increasing atrial pressure as the atria fill with blood returning via the veins from the peripheral vascular beds

f. Ventricular repolarization begins (T wave)

4- Isovolumetric relaxation

a. Begins when ventricular pressure drops below aortic (or pulmonary artery) pressure

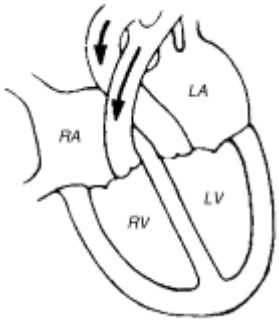

b. Aortic (and pulmonic) valve closes (mitral and tricuspid already closed)

c. Rapid fall in ventricular pressure

d. No change in ventricular volume

e. Decreasing arterial pressure

f. Increasing atrial pressure (venous "v" wave)

g. Second heart sound begins

5- Ventricular filling

a. Begins when ventricular pressure drops below atrial pressure

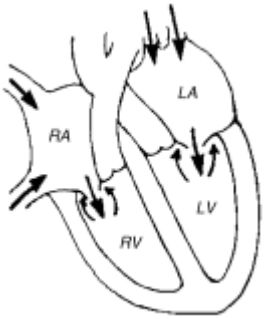

b. Mitral (and tricuspid) valves open

c. Flow of blood from atrium to ventricle, initially rapid, then slower as the ventricles fill

d. Ventricular pressure decreases and then rises slowly as the ventricles fill

e. Atrial pressure decreases initially as blood flows from the atria to the ventricles, then slowly increases

f. Arterial pressure decreases

In cardiovascular physiology, the Pressure-volume loop diagram is often applied to the left ventricle, and it can be mapped to specific events of the cardiac cycle.

- **A** is the end-diastolic point; this is the point where contraction begins.
- Segment **AB** is the contraction phase. This phase is called isovolumetric contraction.
- At point **B**, pressure becomes higher than the aortic pressure and the aortic valve opens, initiating ejection.
- **BC** is the ejection phase, volume decreases. At the end of this phase, pressure lowers again and falls below aortic pressure. The aortic valve closes.

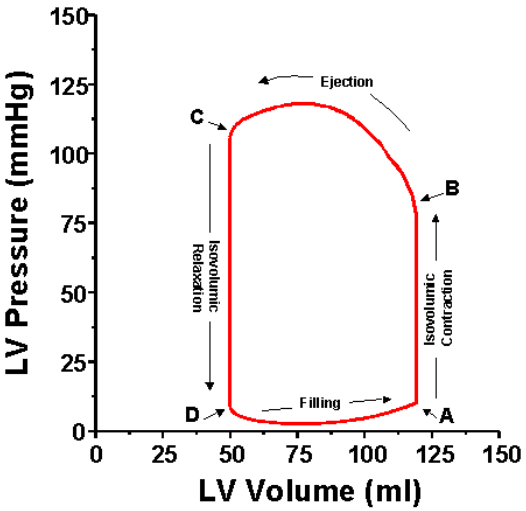

- Point **C** is the end-systolic point.
- Segment **CD** is the isovolumetric relaxation. During this phase, pressure continues to fall.
- At point **D** pressure falls below the atrial pressure and the mitral valve opens, initiating ventricular filling.
- **DA** is the diastolic filling period. Blood flows from the left atrium to the left ventricle. Atrial contraction completes ventricular filling. [10, 11]

2.2.5 Cardiac conduction system

As a pump needs electricity to work, the human heart has a similar need for a power source and also uses electricity.

The cardiac conduction system is a group of specialized cardiac muscle cells in the walls of the heart that send signals to the heart muscle causing it to contract. [12]

Step 1: Pacemaker Impulse Generation

The sinoatrial (SA) node (also referred to as the pacemaker of the heart) contracts generating nerve impulses that travel throughout the heart wall. This causes both atria to contract. The SA node is located in the upper wall of the right atrium (Fig. 2.8). It is composed of nodal tissue that has characteristics of both muscle and nervous tissue.

Step 2: AV Node Impulse Conduction

The atrioventricular (AV) node lies on the right side of the partition that divides the atria, near the bottom of the right atrium. When the impulses from the SA node reach the AV node they are delayed for about a tenth of a second. This delay allows the atria to contract and empty their contents first.

Step 3: AV Bundle Impulse Conduction

The impulses are then sent down the atrioventricular bundle. This bundle of fibers branches off into two bundles and the impulses are carried down the center of the heart to the left and right ventricles.

Step 4: Purkinje Fibers Impulse Conduction

At the base of the heart the atrioventricular bundles start to divide further into Purkinje fibers. When the impulses reach these fibers, they trigger the muscle fibers in the ventricles to contract. The right ventricle sends blood to the lungs via the pulmonary artery and the left ventricle pumps blood to the aorta.

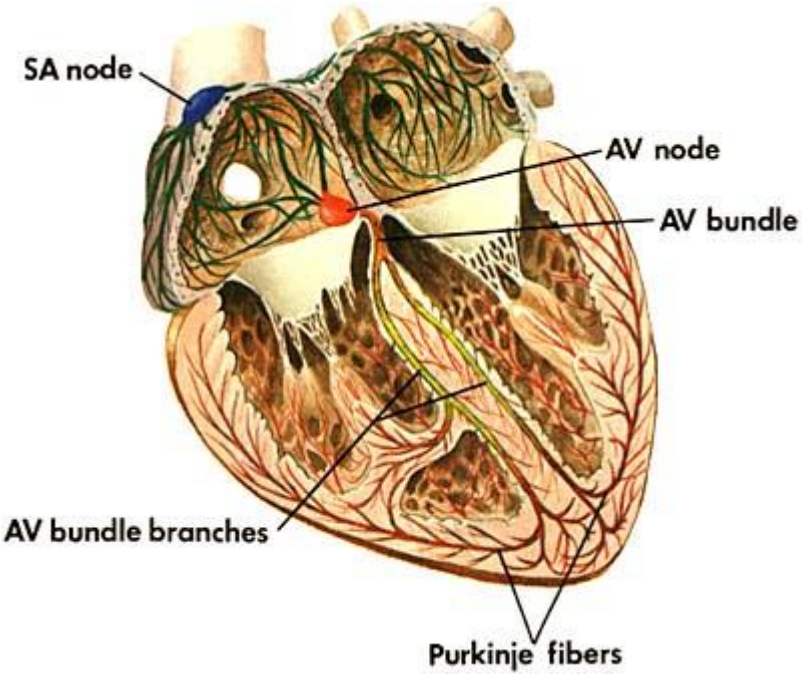

Fig. 2.8 Main elements of cardiac conduction system [13]

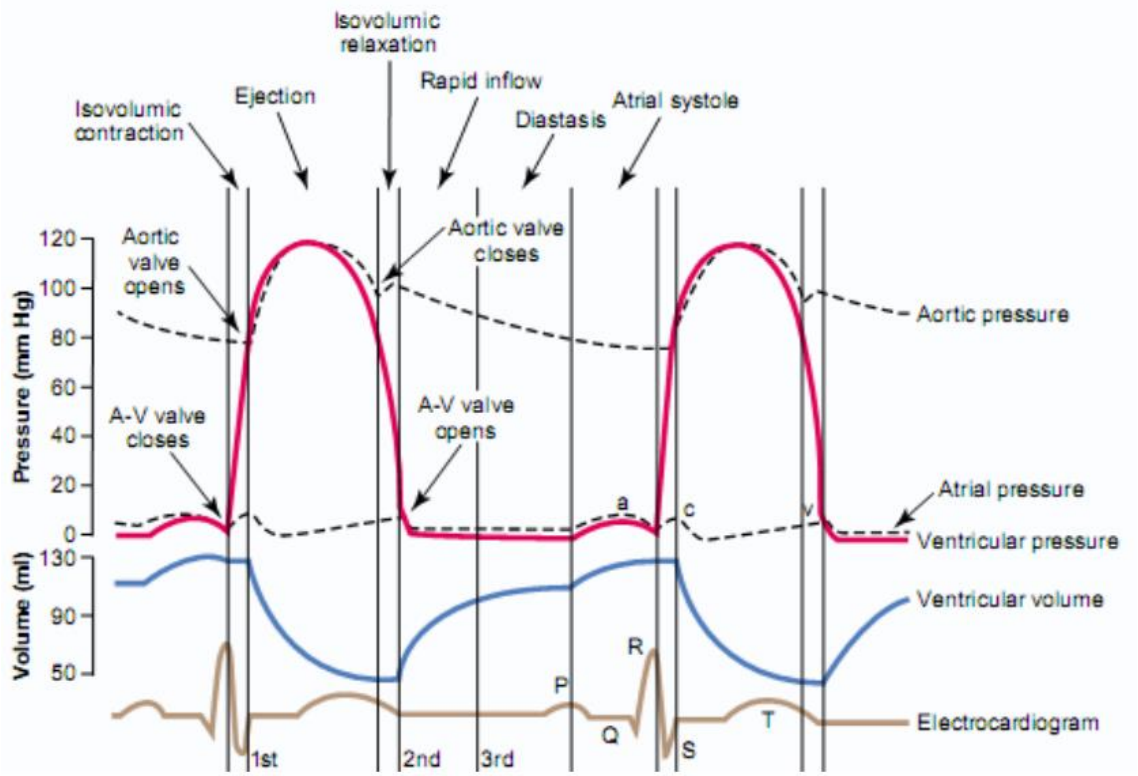

Fig. 2.9 Wiggers diagram - Events of the cardiac cycle

2.2.6 Heart rate

Once we know that the heart produces electrical pulses to work, it is also important to talk about these pulses which are called heart rates.

Heart rate, or heart pulse, is the speed of the heartbeat measured by the number of poundings of the heart per unit of time — typically beats per minute (bpm) (Table 1). [14]

The heartbeat rate is controlled by the autonomic nervous system, which is composed of two parts: the sympathetic system speeds up the heartbeat rate while the parasympathetic system slows it down.

Heart rate is not a stable value and it increases or decreases in response to the body's need in a way to maintain an equilibrium (basal metabolic rate) between requirement and delivery of oxygen and nutrients. Activities that can provoke change include physical exercise, sleep, anxiety, stress, illness, ingesting, and drugs. [15]

Abbreviation	Meaning
Bpm	Beats per minute
HR	Heart rate
THR	Target heart rate
HR_{max}	Maximum heart rate
HR_{rest}	Resting heart rate

Table 1: Different metrics to describe heart rate.

Resting heart rate

The basal or resting heart rate (HR_{rest}) is defined as the heart rate when a person is awake, in a neutrally temperate environment, and not having recently exerted himself or any form of stimulation, such as stress or surprise.

A normal resting heart rate for a man is between about 64 and 72 beats per minute; with strenuous exercise the heart rate can jump to more than twice its resting rate. The better a man's fitness level, the lower his resting heart rate and the more efficiently his heart is pumping. A man who has a high fitness level might have a resting heart rate between 50 and 60 beats per minute; a man whose lifestyle is sedentary might have a resting heart rate of 80-90 beats per minute. [16]

Target heart rate

For healthy people, the target heart rate or training heart rate (THR) is a desired range of heart rate reached during aerobic exercise which enables one's heart and lungs to receive the most benefit from a workout. This theoretical range varies based mostly on age; however, a person's physical condition, sex, and previous training also are used in the calculation. To calculate THR there is an element called "intensity" which is expressed as a percentage. However, it is crucial to derive an accurate HR_{max} to ensure these calculations are meaningful. [17]

Maximum heart rates vary significantly between individuals and they have been reported as varying from 160 to 220. [18]

Example for someone with a HR_{max} of 180 (age 40, estimating HR_{max} as 220 − age):

65% Intensity: (220 − (age = 40)) × 0.65 → 117 bpm

85% Intensity: (220 − (age = 40)) × 0.85 → 153 bpm [19]

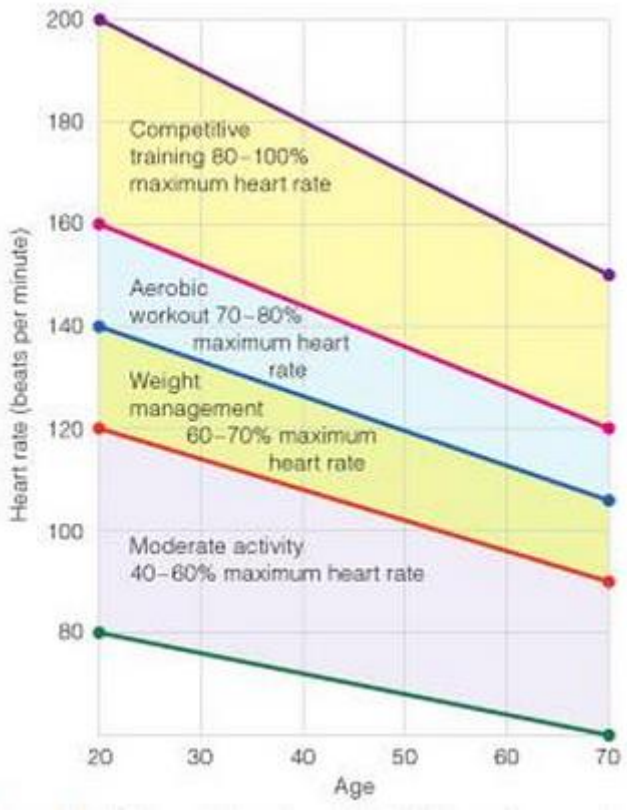

Fig. 2.10 Target heart rate for different ages and various levels of activity [17]

Maximum heart rate

The maximum heart rate (HR_{max}) is the highest heart rate an individual can achieve without severe problems through exercise stress, [20] and generally decreases with age. Since HR_{max} varies by individual, the most accurate way of measuring any single person's HR_{max} is via a cardiac stress test. In this test, a person is subjected to controlled physiologic stress (generally by treadmill) while being monitored by an ECG. The intensity of exercise is periodically increased until certain changes in heart function are detected on the ECG monitor, at which point the subject is directed to stop. Typical duration of the test ranges ten to twenty minutes.

It is very important to know that the typical maximum heart rate is 220 minus your age because for the future fatigue test I will perform, it will be necessary to set proper parameters such as amplitude, frequency…

Frequency is denoted as the number of times a regularly recurring phenomenon occurs in one second. The number of times a heart beats in one minute is divided by 60 seconds to obtain the frequency in Hertz. [21] Therefore, if the heart rate is 200 bpm then the frequency will be ~3.34 Hz (200 (bpm)/60=3.333333 Hz)

Bibliographic Entry	Result (surrounding text)	Standardized Result
[22]	"It beats or contracts about 70 times per minute."	1.17 Hz
[23]	"so the resting heart rate (70 beats per minute)"	1.17 Hz
[24]	"It beats roughly 70 times a minute throughout one's life"	1.17 Hz
[25]	"A baby's heart beats 120 times a minute. A man's heartbeats 72."	2.00 Hz 1.20 Hz
[26]	"The normal heart rate at rest is usually between 60 and 100 beats per minute."	1.00 to 1.67 Hz

Table 2: Operations to calculate frequencies (bpm/60)

Thus, I will not be able to set a higher frequency than an actual heart rate because the test will not be successful but I will look at this subject again in the future.

2.2.6.1 Heart rate variability (HRV)

It is the physiological phenomenon of variation in the time interval between heartbeats. It is measured by the variation in the beat-to-beat interval.

Other terms used include: "cycle length variability", "RR variability" (where R is a point corresponding to the peak of the QRS complex of the ECG wave (Fig.2.11); and RR is the interval between successive Rs), and "heart period variability". [27]

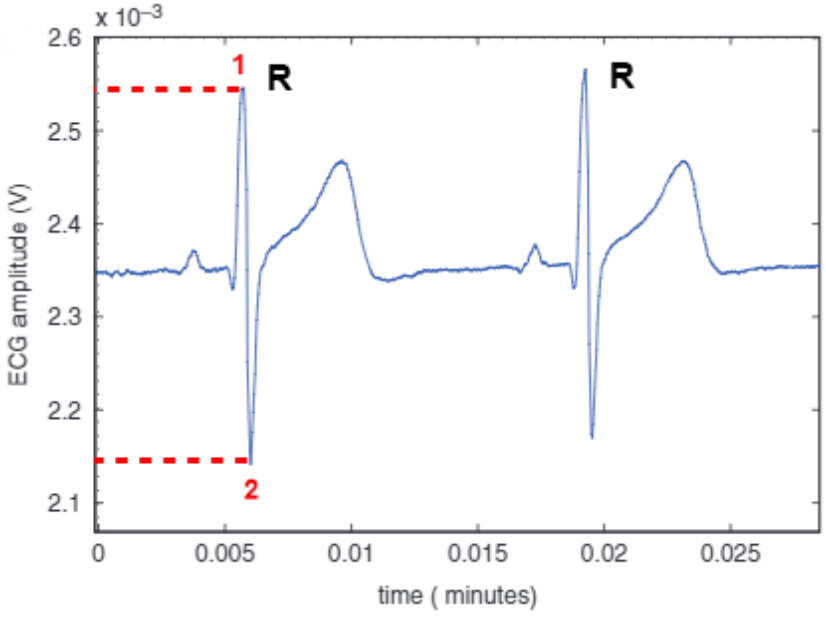

Fig.2.11 ECG signal without noise [28]

For purpose of analyse the amplitude of the heart rate we can use the ECG signals. In the figure above, we see heart rate varies between point 1 and 2. If we subtract 2 from 1 we arrive at a HRV “amplitude” of 0.40mV [2.55 (mV) – 2.15 (mV) = 0.40 mV].

The SA node receives several different inputs and the instantaneous heart rate or RR interval and its variation are the results of these inputs.

The main inputs are the sympathetic and the parasympathetic nervous system (PSNS) and humoral factors.

Decreased PSNS activity or increased SNS (only sympathetic nervous system) activity will result in reduced HRV. High frequency (HF) activity (0.15 to 0.40 Hz), especially, has been linked to PSNS activity. Activity in this range is associated with the respiratory sinus arrhythmia (RSA), a mediated modulation of heart rate such that it increases during inspiration and decreases during expiration.

Less is known about the physiological inputs of the low frequency (LF) activity (0.04 to 0.15 Hz). Though previously thought to reflect SNS activity, it is now widely accepted that it reflects a mixture of both the SNS and PSNS. [29]

2.2.7 Mechanical properties of heart

The mechanical properties of cardiac muscle are like those of skeletal muscle with two important differences. First, the cardiac action potential persists for approximately 70% of the duration of mechanical contraction, lasting past the time when peak contractile force is generated. During this time muscle cells are refractory to further stimulation, so cardiac muscle cannot undergo tetanic contraction. The duration of contraction of cardiac muscle is primarily a function of the duration of the action potential. Second, because there are more elastic components in cardiac muscle than in skeletal muscle, cardiac muscle exhibits a significant amount of passive tension at normal resting length. In skeletal muscle the force of contraction is determined by the number of fibers that contract. On the other hand, in cardiac muscle contraction strength is graded by direct adjustment of the intracellular contractile mechanism of myocardial cells. This adjustment is controlled by mechanical, humoral, and neural factors. Force of contraction also varies with the length of cardiac fibers at the moment of initiation of contraction. Passive stretching of muscle fibers causes an increase in contractile strength which is seen to a more limited extent in skeletal muscle (Fig. 2.12). This relationship is known as the Frank-Starling law and should not be confused with the concept of contractility. [30]

Contractility refers to a change in the ability to generate force at a given initial length. Thus, there are two ways to increase the force of cardiac contraction; 1) increase the initial muscle length (Frank-Starling law), or 2)

increase the strength of contraction at a given muscle length. Digitalis glycosides increase contractility presumably by inhibiting Nat-Kt ATPase of cell membranes. Catecholamines increase contractility via 13-adrenergic receptors and cyclic AMP.

The Frank–Starling law of the heart (Fig. 2.13) states that the stroke volume ((SV) is the volume of blood pumped from the left ventricle of the heart per beat) of the heart increases in response to an increase in the volume of blood filling the heart (the end diastolic volume) when all other factors remain constant. The increased volume of blood stretches the ventricular wall, causing cardiac muscle to contract more. The stroke volume may also increase as a result of greater contractility of the cardiac muscle during exercise, independent of the end-diastolic volume. The Frank–Starling law appears to make its greatest contribution to increasing stroke volume at lower work rates, and contractility has its greatest influence at higher work rates.

This allows the cardiac output to be synchronized with the venous return, arterial blood supply and humoral length [31] without depending upon external regulation to make alterations.

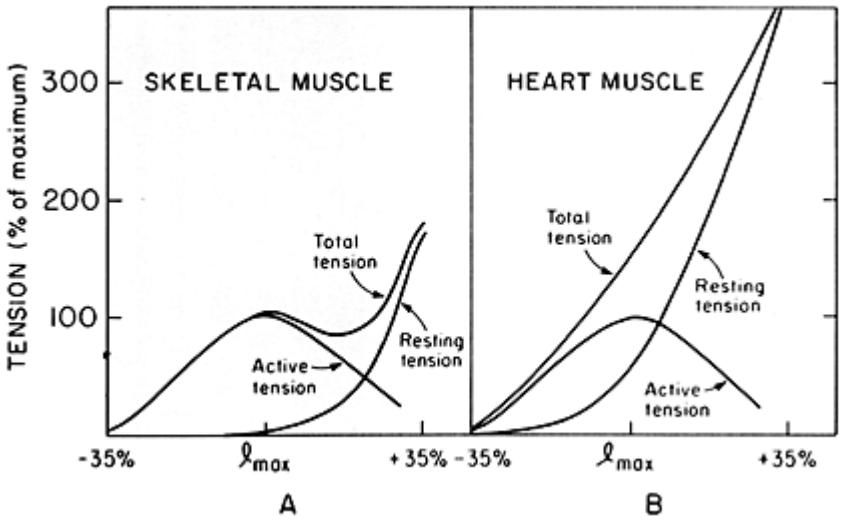

Fig. 2.12 Cardiac muscle experiences elastic tension even at resting length (skeletal muscle does not). In addition, the maximum developed tension in cardiac muscle occurs, not at the resting length, but when it is stretched beyond resting length.

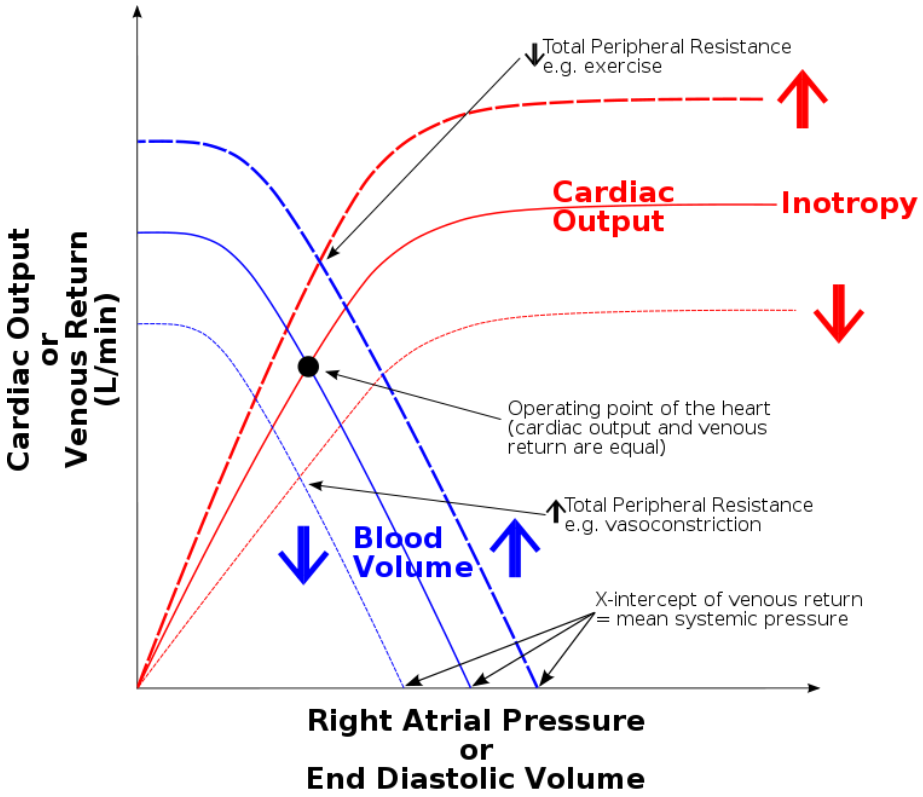

Fig. 2.13 Cardiac function curve. In diagrams illustrating the Frank–Starling law of the heart, the Y axis often describes the stroke volume, stroke work, or cardiac output. The X axis often describes end-diastolic volume, right atrial pressure, or pulmonary capillary wedge pressure. The three curves illustrate that shifts along the same line indicate a change in preload, while shifts from one line to another indicate a change in afterload or contractility.

Pressure-volume loops, described in section 2.2.4.2, are among the best of the current methods for estimating the contractility of the intact heart.The Pressure-volume parameters are:

Stroke volume (SV)

It is the volume of blood ejected by the right/left ventricle in a single contraction. It is the difference between the end-diastolic volume (EDV) and the end-systolic volume (ESV).

SV = EDV – ESV

Stroke work (SW)

Ventricular stroke work is defined as the work performed by the left or right ventricle to eject the stroke volume into the aorta or pulmonary artery, respectively. The area enclosed by the PV loop is a measure of the ventricular stroke work, which is a product of the stroke volume and the mean aortic or pulmonary artery pressure (afterload), depending on whether one is considering the left or the right ventricle.

The stroke work output of the heart is the amount of energy that the heart converts to work during each heartbeat while pumping blood into the

arteries. The general expression of external work done when a mass is lifted a certain distance is W = force x distance.

For pressure moving a volume, the external work is: $dW = P \cdot dV$

Cardiac output (CO)

It is defined as the amount of blood pumped by the ventricle in unit time.

CO = SV x heart rate

CO is an indicator of how well the heart is performing its function of transporting blood to deliver oxygen, nutrients, and chemicals to various cells of the body and to remove the cellular wastes.

Ejection fraction (EF)

It is defined as the fraction of end-diastolic volume that is ejected out of the ventricle during each contraction.

EF = SV/EDV.

Healthy ventricles typically have ejection fractions greater than 0.55.

dP/dt_{min} & dP/dt_{max}

These represent the minimum and maximum rate of pressure change in the ventricle.

An increase in contractility is manifested as an increase in dP/dt_{max} during isovolumetric contraction…

Likewise, an increase in diastolic function or an increase in relaxation (lusitropy) causes increased dP/dt_{min} during isovolumetric relaxation.

Isovolumetric relaxation constant (Tau)

Tau represents the exponential decay of the ventricular pressure during isovolumetric relaxation. Several studies have shown that Tau is a preload-independent measure of isovolumetric relaxation.

The accurate estimation of Tau is highly dependent on the accuracy of ventricular pressure measurements. Thus, high fidelity pressure transducers are required to obtain real time instantaneous ventricular pressures.

Calculation of Tau (Glantz method) (Fig. 2.14)

$$P(t) = P_0 e^{-t / \tau_E} + P_\alpha$$

where

- P = pressure at time t
- P0 = amplitude constant
- τ_E = Glantz relaxation constant

- P_α = non zero asymptote due to pleural and pericardial pressure [32,33]

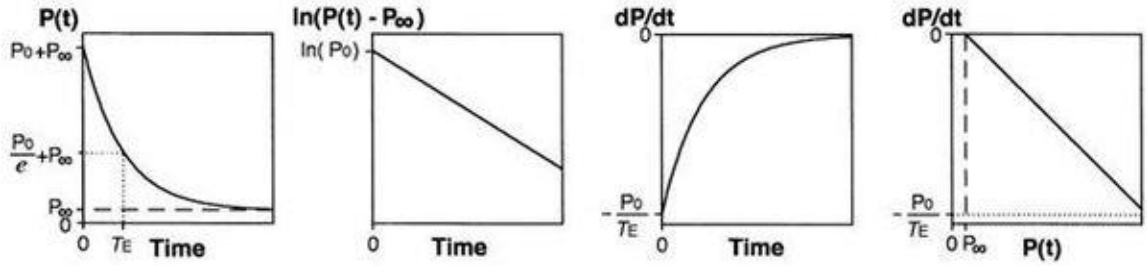

Fig. 2.14 Calculation of Tau (Glantz method)

Tissue	Young's Modulus (MPa)	Strain at Break (%)
Relaxed smooth muscle	0.006	300
Contracted smooth muscle	0.01	300
Aortic valve leaflet	15 ± 6	21 ± 12
Pericardium	20.4 ± 1.9	34.9 ± 1.1
Cerebral vein	6.85	83
Myocardium	0.2–0.5 (at the end of diastole)	>20

Fig. 2.15 Mechanical properties of some human soft tissues

3. ELASTOMERS IN BIOMEDICAL APPLICATIONS

3.1 Elastomers: definition and classification

ASTM (American Society for Testing and Materials) defines an elastomer as a macromolecular material (natural or synthetic) that returns rapidly to approximately its initial dimensions and shape after substantial deformation by weak stress and release of the stress. [35]

While they are members of the broad family of polymers, elastomers behave differently than plastic materials or plastomers. For materials to be considered elastomers they must be:

- Flexible: i.e... Have low rigidity (several megapascals (MPa))
- Highly deformable. i.e... Are able to withstand strong deforming forces without rupturing and have an elongation at rupture over 200%, while possessing relatively high tensile strength at ultimate elongation
- Elastic or resilient, i.e., are able to return to their original shape and size after the deforming force is removed and quantitatively release the energy used to deform them. [36]

The current classification system separates elastomers into four categories (the acronyms are based on the ISO 1629:1995 standard):

-*General-use elastomers*. Includes natural rubber (NR), synthetic polyisoprene (IR), styrene butadiene co-polymers (SBR), and polybutadienes (BR)

-*Special elastomers*. Includes ethylene propylene and diene copolymers (EPM, EPDM), isobutylene and chloro- and bromoisobutylene isoprene copolymers (HR, STIR. CUR), nitrite butadiene copolymers (NBR), and polychloroprenes (CR)

-*Very special elastomers*. High thermal and/or chemical resistance elastomers, including silicone elastomers (VMQ), fluoroelastomers (FPM), chloropolyethylenes and chlorosulfonyl polyethylenes (CM, CSM), polyacrylates (ACM), ethylene vinyl acetate elastomers (EVA), ethylene methyl acrylate (EAM), hydrogenated nitrile elastomers (HNBR), and epichlorhydrin elastomers (CO, ECO, GECO)

-*Thermoplastic elastomers*. A separate category indicating that they do not need to be vulcanized since they can be used like any thermoplastic material. [37]

A standard formulation contains several additives like fillers, plasticizers, protective agents, a crosslinker and various other ingredients such as colorants, conditioning agents…

It is clear that the release of additives by biomedical elastomers may have a significant impact on host tissues.

Silicones (a contraction of silicon ketone) make up a vast family of polymers with remarkable properties due to the presence of both silicon-oxygen and silicon-carbon bonds (Fig. 3.1). Today, silicone elastomers are the most widely used polymers in medical applications [38] because of the strong, very mobile bonds of their Si —O—Si (siloxane) catenary backbone, which provide elevated chemical inertness and exceptional flexibility. They are also very stable over time and at body temperature, show little tissue reactivity, and are highly resistant to chemical attack and heat, which allows them to be autoclaved. They also have exceptional mechanical properties such as high tear strength, outstanding elasticity, and high gas permeability, which makes them suitable for many medical applications such as contact lenses, special dressings and air/blood filter membranes.

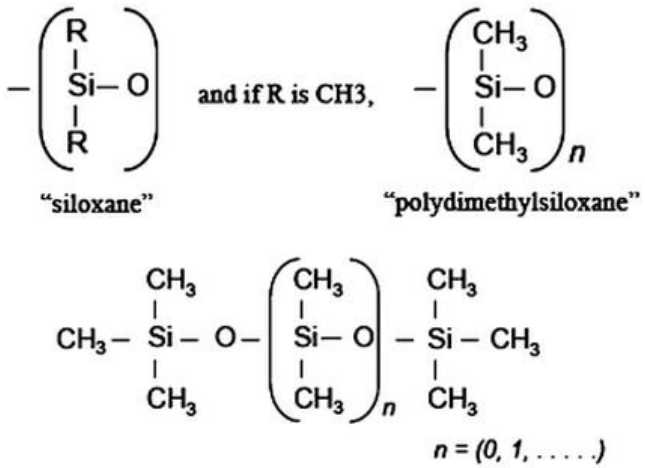

Fig. 3.1 Synthesis of silicone from its monomer (polydimethylsiloxane)

Polyvinyl chloride (PVC) is a widely used polymer, and PVC products can be produced with a broad range of properties (flexible, rigid, cellular). It has been widely used in the medical field for some 40 years (gloves, tubes, tubing, catheters, bags, etc.) because of its low cost and ease of processing.

Natural rubbers are the most elastic and resistant of all biomedical elastomers but are also the least hemocompatible due to the release of accelerator (dithiocarbamate) residues [39]. Many attempts have been made to improve their blood compatibility. Untreated natural rubbers are mainly used to manufacture latex gloves, while treated natural rubbers are used to produce catheters and tubing. Hydrosoluble proteins are responsible for allergies associated with latex products. Simple washing is sufficient to completely remove the proteins and eliminate the risk of allergic reactions [40]

3.2 Biocompatibility of elastomers

A material used for medical devices and implants should possess good biocompatibility, biostability and mechanical properties. By biocompatibility it means that the material should not be harmful or cause severe allergic reactions in patients or individuals. At the same time its mechanical, physical and chemical properties should not be adversely affected by the biological environment in which it is used (i.e. biostability and biodurability). In addition the mechanical properties should be such as to withstand the predominant loading conditions to which the medical device or implant is subjected without the risk of premature failure. [41]

Specially, mechanical properties of elastomeric blends and composites used for medical applications should be rigorously and adequately measured and characterised. It is very important in the case of elastomers since the mechanical properties of many of these materials are temperature, humidity and strain rate dependent. This means that the properties of a medical device once inside the host environment can significantly change from those measured in a laboratory setting under room temperature conditions. Therefore, when measuring these properties one should always choose test conditions that are as representative

of the in vivo conditions as possible. Thus, in the experimental part I need to test the samples with the proper temperature (37 ºC) inside the correct fluid: SBF (simulated body fluid).

Elastomers are very important in the manufacture of medical devices that may come into contact with host tissues for varying periods of time. Exposure times have been arbitrarily divided into three categories: limited exposure (<24 h), prolonged exposure (24 h to 30 days), and permanent exposure (>30 days). The tests used to evaluate biocompatibility depend on exposure time. It is thus easy to understand why elastomers used to make implants have to meet stricter standards than those used for dental impressions [37].This classification system is only a guide; since elastomers may be used for short, but repeated periods, biocompatibility testing must be based on the maximum exposure time. It must also take into account how the material will be used and the type of contact.

Differing standards apply to medical devices that are:

-In contact with surfaces like the skin or mucous membranes other than the skin

-In direct or indirect contact with other tissues, including blood

-Implantable devices

4. THERMOPLASTIC ELASTOMERS (TPEs)

Thermoplastic elastomers are generally low modulus, flexible materials that can be stretched repeatedly to at least twice their original length at room temperature with an ability to return to their approximate original length when stress is released. The grandfather materials with this property are thermoset rubbers, but many families of injection-mouldable thermoplastic elastomers (TPEs) are replacing traditional rubbers [42] and above their melt or softening temperatures, are melt processable via thermoplastic processing methods.

4.1 Structure of TPEs

The dual capability of elastomeric properties and recyclability are achieved using one of several approaches to prepare the TPE. The three major types of TPEs are:

-block copolymers

-rubber/plastic blends

-dynamically vulcanised rubber/plastic alloys, called thermoplastic vulcanisates.

4.1.1 Block copolymers

The earliest TPEs were made by preparing tailored copolymer molecules consisting of a multi-block or tri-block copolymer structure. The end

block of the copolymer molecules will crystallise. So these copolymer molecules are linked together when below the melting temperature, thus forming a virtually crosslinked network. Between these crystallised ends is the centre block which is amorphous and has rubber-like properties across the ambient temperature range. These block copolymers can he divided into classes based on their chemistry. They include:

- styrene block copolymers (SBC)
- copolyesters (COPE)
- thermoplastic polyurethanes (TPU)
- copolyamides (COPA)

A simple picture of the structure of a TPE block copolymer, shown in Figure 4.1, illustrates how the rigid crystalline regions act as virtual crosslinks with the flexible rubbery blocks providing the overall flexibility of these copolymers. The rubbery blocks do not crystallise with the crystalline blocks.

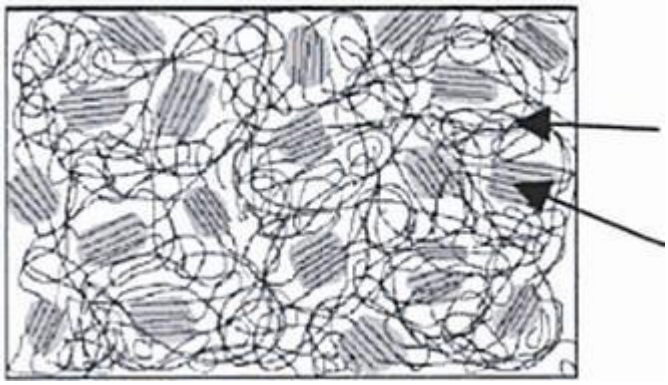

Fig. 4.1 Block copolymer morphology — illustration of hard blocks crystallised into domains with soft rubber block regions between them

They form a continuous domain of softer, rubbery chains. These are held together by the crystalline domains which have the copolymer chains locked together in a crystalline structure. When these copolymers are deformed the hard blocks remain crystalline and do not deform. The soft rubber domain is easily deformed and provides rubbery behaviour. The recovery of these materials is good as long as the domains are not strained too greatly and the temperatures are well below the crystallisation temperature. Above the crystalline melt temperature the block copolymer chains are no longer locked into position and all the chains are free to flow. In the melt temperature range a block copolymer will process easily in typical thermoplastic processing equipment. This behaviour is exhibited by all the block copolymer TPEs.

4.1.2 Rubber/Plastic blends

One of the early type thermoplastic elastomers was prepared by blending a rubber and a thermoplastic polymer. The rubber and plastic polymers

need to be somewhat incompatible with each other so that separate phases are formed.

The most popular rubber/plastic blend is polypropylene with EPDM or ethylene-propylene copolymer (EP) rubber and is called a thermoplastic olefin (TPO). These polymers form separate phases. In some TPOs the EPDM rubber is partially or lightly crosslinked. The plastic phase is the continuous phase. The EPDM phase is generally discrete particles as shown in Figure 4.2.

In some situations the rubber phase can be a continuous phase. It is important to note that the TPO rubber phase morphology is not fixed. Without full crosslinking the rubber phase undergoes coalescence or rupture during high shear processing. The rubber particles also change shape freely. This allows a TPO to flow freely and results in good processing characteristics. Injection moulded and extruded TPOs also have a smooth surface appearance as a result.

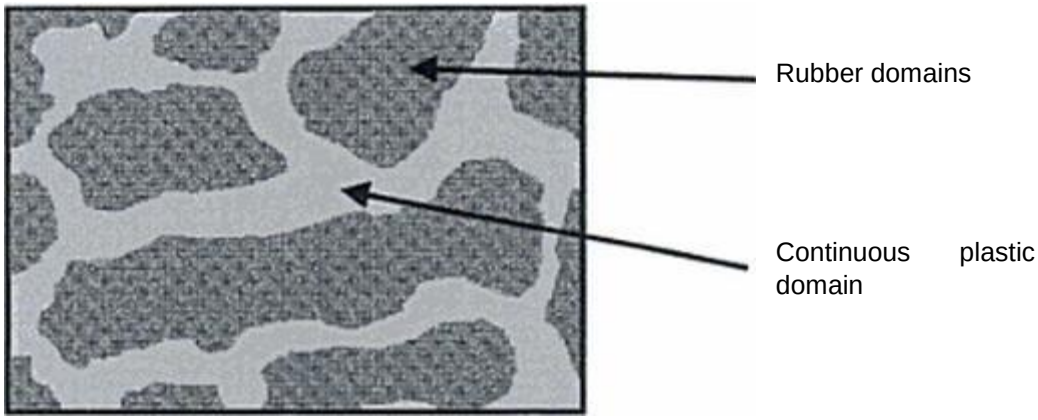

Fig. 4.2 TPO rubber/plastic blend morphology

Nitrile rubber (NBR) and polyvinyl chloride (PVC) thermoplastic are other rubber/plastic blends that have commercial utility.

4.1.3 Thermoplastic Vulcanisates

A TPV is a blend of thermoplastic with fully crosslinked. i.e., vulcanised, rubber. The thermoplastic is the continuous phase and the crosslinked rubber is a dispersed particulate phase. TPVs are prepared by dynamic vulcanisation where the rubber phase is crosslinked during the mixing process when the polymers are mixed together. The rubber phase crosslinking is nearly 100% and must exceed 95% to have good fluid resistance, recovery and seal stress retention. The properties of TPVs approach those of a thermoset rubber because of the complete vulcanisation of the rubber phase. The best physical properties are achieved when the particles are about 1 µm in diameter as shown in Figure 4.3.

TPVs are made with a variety of rubber and plastic pairs. The most common are the EPDM/PP TPVs. Butyl rubber and polypropylene is used for an isobutylene-isoprene rubber (IIR)/PP TPV. A compatibilised thermoplastic vulcanisate of nitrile rubber (NBR) and PP (NBR/PP TPV) is a higher fluid

resistant TPE which has the same upper temperature limits as the EPDM/PP TPVs.

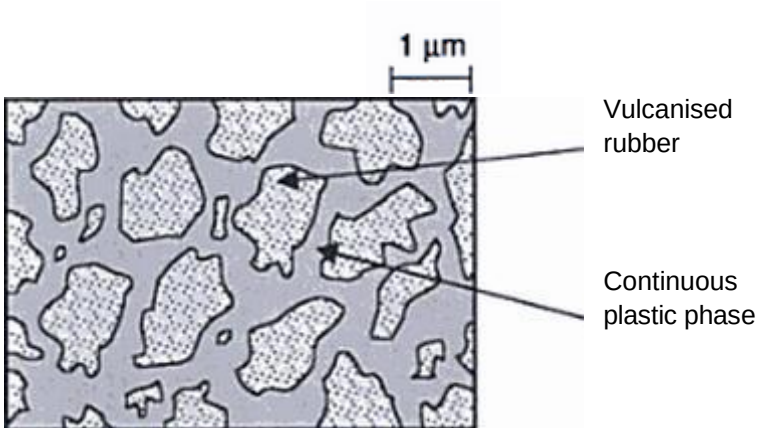

Fig. 4.3 Thermoplastic vulcanisate morphology with continuous plastic phase and discrete rubber panicles

There are new developments in TPVs based on the dynamic vulcanisation of the higher temperature rubber and plastic combination ethylene-acrylate rubber and polyester (polyethylene terephthalate (PET) or polybutylene terephthalate (PBT). These new TPV developments have recently been commercialised by DuPont. Another new TPV based on silicone rubber called TPSiV has been developed and commercialised. These TPVs provide higher temperature and/or higher fluid resistance than the PP based TPVs [43].

4.2 Processing techniques

Thermoplastic processing operations involve the process of moving melted (viscous) materials with thermoplastic characteristics (soften when heated) into some form or mould and then cooling (solidifying) the materials for the purpose of making desired shapes. [44]

The five major thermoplastic processes used to form thermoplastic materials are:

Injection Moulding

Injection moulding is by far the most used processing technique of producing parts from thermoplastic elastomers due to its high productivity. Injection moulding machines and moulds are very expensive because of the high pressures required and complexity of the process control. However, the shortcoming of this technique is balanced by its ability to produce a complex finished part in a single and rapid operation.

The principle of injection moulding is very simple (Fig. 4.4). The plastic material is fed into the injection barrel by gravity through hopper. Upon entrance into the barrel, the polymer is heated to the melting temperature. It is then forced into a closed mould that defined the shape of the article to be produced. The

mould is cooled constantly to a temperature that allows the molten to solidify and the mould is opened, the finished product is ejected and the process continues. [45,46]

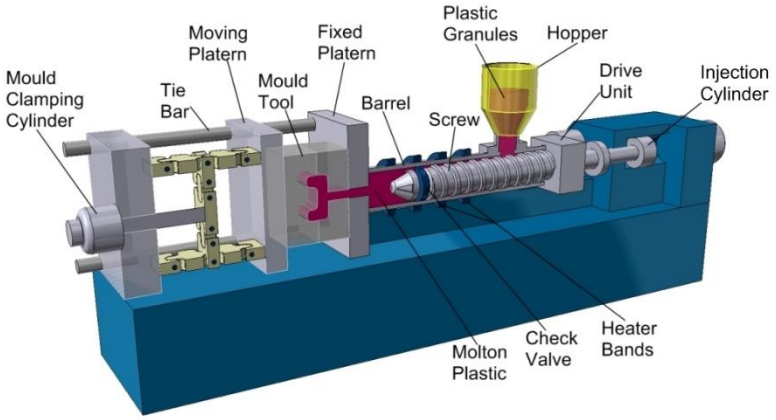

Fig. 4.4 Typical machine for injection moulding

Blow Moulding

Blow moulding is a manufacturing process that is used to produce hollow plastic parts. There is a wide variety of materials can be used in this process, including but not limited to high density polyethylene (HDPE), low density polyethylene (LDPE), polypropylene (PP), Poly(vinyl chloride) (PVC) and Poly(ethylene terephthalate) (PET). The basic process begins with the melting of thermoplastic and extruding it through a die head to form a hollow tube called a parison. The parison is then clamped between two mould halves, which close around it and the parsion is inflated by pressurized air until it conforms to the inner shape of the mould cavity. Lastly, the moulds open and the finished part is removed.

Basically, there are three types of blow moulding used to form the parison. In extrusion blow moulding, plastic is melted and extruded using a rotating screw to force the molten through a die head that forms the parsion. Injection blow moulding is part injection moulding and part blow moulding where the molten plastic is injection moulded around the core pin and then the core pin is transferred to a blow moulding station to be inflated. There are two stretch moulding techniques. In one-stage process, the preform is injection moulded which is then transferred to the blow mould where it is blown and ejected from the machine. In the two-stage process, preform is injection-moulded, stored for a short period of time, and blown into container using a reheat blow machine. The figure 4.5 shows one type of process:

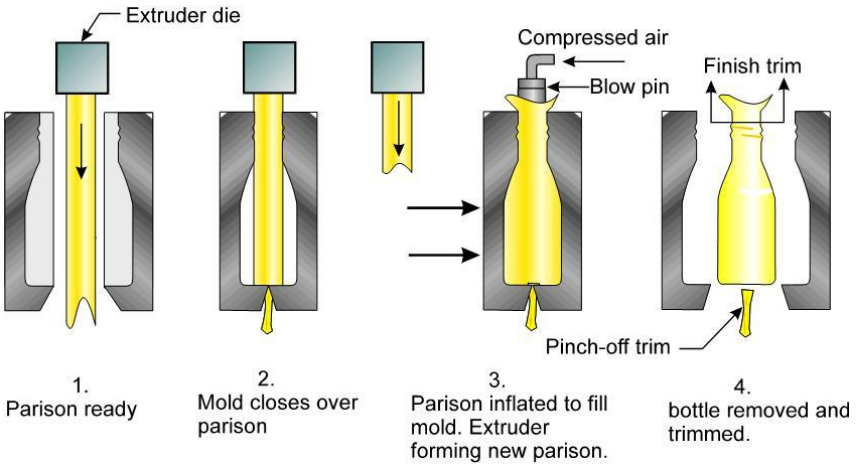

Fig. 4.5. Blow moulding to make plastic bottles

Extrusion

Extrusion is a high volume manufacturing process for fabricating parts from thermoplastic elastomers. This processing technique is essential in the melting of raw materials and shaping them into different continuous profiles. The most common extrusion methods are film and sheet extrusion, blow film extrusion, cast film extrusion, coextrusion, tubing extrusion and extrusion coating. The end products made by extrusion are pipe/tubing, wire insulation, film, sheets, adhesive tapes and window frames.

Basically, the extrusion process (Fig. 4.6) involves heating a thermoplastic above its melting temperature and forcing it through the die. The extruder is a heating and pressurizing device involves one or more screws operating in a heated barrel. The key determinant of an extruder's performance is the screw. It has three main functions to perform: feeding and conveying the raw material feed; melting, compressing and homogenizing the material; and metering and pumping it through the extrusion die at a constant rate. Raw thermoplastic elastomer material is fed into the barrel of the extruder and comes into contact with the screw. As a melt delivery device, the rotating screw forces the polymer forward into barrel which is heated at a desired temperature. After leaving the screw, the molten travels through a screen pack/plate breaker, where the contaminants in the melt are removed. Breaker plate also creates back pressure in the barrel which is needed for uniform melting and proper mixing of polymer. After that, the molten enters the die, where the cross section of the extruded product is determined.

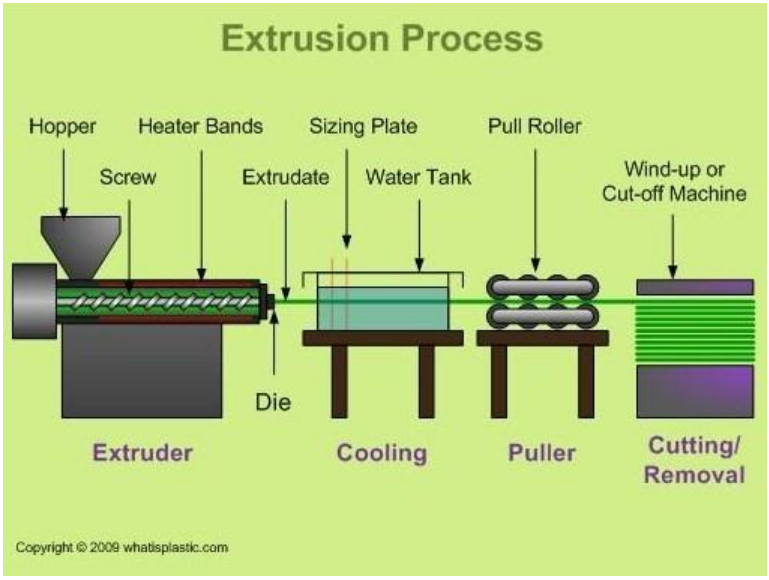

Fig. 4.6. The picture shows how the extrusion process is

Compression moulding

Compression moulding was among the first method of moulding to be used to produce plastic parts. However, it is by far less used than injection moulding. Generally, this method involves four steps. First of all, the raw polymer materials in pellets or powder form are placed in a heated and open mould cavity. The mould is closed with another half of the mould and at the same time, pressure is applied to force the materials into contact with all mould areas. The materials soften under high pressure and temperature, flowing to fill the mould. The part is hardened under pressure by cooling the mould before removal so the part maintains its shape.

There are six important considerations that should be bear in mind, they are the proper amount of material, the minimum energy required to heat the material, the minimum time required to heat the material, the proper heating technique, the force needed to ensure that shots attains the proper shape, the design of the mould for rapid cooling. Compression moulding of TPEs usually requires longer heating and cooling time due to their high melting points. Separate platens can be used to solve this problem where one is hot press that is electrically heated and another one is cold press that is water cooled. The part is hot pressed under pressure and then transferred immediately to the cold press to chill it under pressure. The hot press is usually preheated to reduce the total cycle time.

Transfer moulding

Transfer moulding is a process which the polymer is melted in a separate chamber known as pot then forced into a preheated mould through a sprue, taking a shape of the mould cavity. The mould is cooled down before opening. Thermoplastic elastomers usually have high viscosity and longer transfer time is needed. The temperature of the mould should be maintained at above melting temperature of the polymer to avoid premature cooling or freezing before the

completion of transfer. The important variables during the process of transfer moulding are the type of polymer, melting point of the polymer, pot hold time, transfer pressure, transfer rate and the mould cooling time

Thermoforming

Thermoforming is a process which uses heat and pressure or vacuum to transform thermoplastic flat sheet into a desired three-dimensional parts. The sheet is drawn from large rolls or from an extruder and then transferred to an oven for heating to its softening temperature. The heated sheet is then transferred to a preheated, temperature-controlled mould. Vacuum is applied to remove the trapped air and deform the sheet into the mould cavity, where it is cooled to retain the formed shape. After that, a burst of reverse air pressure is applied to break the vacuum and assist the formed part out of the mould. The principal factors in this process include the forming force, mould type, sheet prestretching, the material input form and the process phase condition. These factors have a critical effect on the quality and properties of the final products.

Calendaring

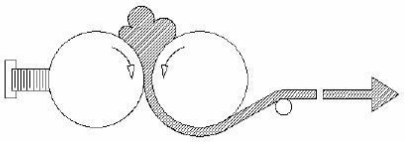

Calendaring is a process where a large amount of molten plastic is fashioned into sheets by passing the polymer between a set of rollers. The rollers are hot and keep the polymer in its semi-molten state. This allows the molten to be rolled many times until the desired thickness is reached. The sheet is then rolled through cold rollers to enable it to go hard and then wound up into rolls. Calendar for thermoplastics generally operates in four-roll units made up of three banks, each bank being wider than the preceding one. The advantages of calendar over extruder are the possibility of calendar to produce embossed films, sheets and laminates and the higher output than extruder. Examples of the final products are cling film, shrink film, clear, translucent rigid sheets for blister packaging and opaque flexible film. [45]

EXPERIMENTAL PART

1. MATERIALS

The research investigated the use of bioactive, biocompatible granulated biomaterials using different techniques in order to produce heart assisting devices. This means that the structures will mimic the natural tissue by design and internal structural changes, in order to replicate as much as possible the heart tissue.

The main materials to be used for comparative purposes in analysis of mechanical, and particularly fatigue behaviour under certain conditions were PU and PET-DLA.

Additional materials were used for the preparation of simulated body fluid (SBF) for in vitro bioactivity tests. They will be mentioned in section 2.2.

DSM is a global science-based company active in health, nutrition and materials [47]. It is our supplier for both main materials which I mentioned before.

Polyurethanes (PU) are important polymers used in biomedical applications, specifically for blood contacting devices, including artificial heart and heart valves, left ventricular assist devices and blood pumps. Good blood compatibility, biostability and biodurability are the major factors that determine their use for such specific applications. Unfortunately, due to high susceptibility to bacterial colonization and high creep in vivo, these materials require continuous modifications.

The trade name of our polyurethane is Bionate® PCU (Thermoplastic Polycarbonate Polyurethane). It is an industry-leading medical grade polymer for use in long-term implants. DSM provided this material in the form of pellets to the University in order to prepare the future samples. The type of Bionate® PCU which was used in this research was “55D”. The company delivered some physical properties of this material (Table 1.1):

Typical Property	Test Method	Bionate® PCU 55D
Color	Visual	Clear to amber colored pellets
Hardness, Durometer	ASTM D2240	56D
Density, g/cm^3	ASTM D792	1.21
Ultimate Tensile Strength	ASTM D1708	8782 psi / 60.5 MPa
Ultimate Elongation (%)	ASTM D1708	365
Tensile Stress at 50% elongation at 100% elongation at 300% elongation	ASTM D1708	 1772 psi / 12.2 MPa 2467 psi / 17.0 MPa 6963 psi / 48.0 MPa
Flexural Modulus, 1% Secant Modulus	ASTM D790	7000 psi / 48.3 MPa
Flexural Stress, at 5% Deflection	ASTM D790	300 psi / 2.1 MPa
Tear Strength, Die ‘C’, pli	ASTM D624	780
Coefficient of Linear Thermal Expansion x 10-6/˚C x 10-6/˚F	 ASTM E831 ASTM E1545	 137.1 76.2
Water Absorption (%)	ASTM D750	0.9
Dielectric Strength (V/mil)	ASTM D149	530
Dielectric Constant, k’, 60 Hz	ASTM D150	4.5
Coefficient of Friction (Kinetic)	ASTM D1894	0.81
Taber Abrasion, 1000g wt.	ASTM D1044	7.4

Weight Loss, mg/1000 cycles	H-18 wheel	
Vicat Softening Temp. ºC ºF	ASTM D1525	 98 208
Melt Flow Rate g/10 min at 224˚C	ASTM D1238	(2160g) 20
Mold Shrinkage, % 4.0” Disk Flame Bar	ASTM D955	 1.2 0.5-2.0
Recommended Extrusion Conditions ˚F ˚C		 370-428 190-220

Table 1.1. Physical properties of Bionate® PCU

These data are for general information purposes only, and may not be relied upon in individual situations but I will be able to compare my results with them and take this material as a reference.

The company also delivered representative biological test results (Table 1.2):

Biological test	Results
Ames Mutagenicity	Non-mutagenic
Chronic Toxicity: USP Muscle Implantation	Macroscopic reaction not significant
Complement Activation	Less activation of the complement system than ePTFE
USP Cytotoxicity (MEM Elution)	Non-cytotoxic
Humoral Immunological Study	No humoral (serological) immune response
Hemolysis	Non-hemolytic
USP Pyrogenicity	Non-pyrogenic
Platelet Deposition (ex vivo shunt)	No difference in thrombogenicity when compared to ePTFE control
Sensitization: Magnusson and Kligman	No dermal sensitization
Acute Systemic Toxicity	No significant systemic toxicity
USP Implantation Test: 7 days in rabbits	Macroscopic reaction not significant
Intracutaneous Toxicity	No significant irritation or toxicity
Carcinogenicity: 2 years in rats	Non-carcinogenic

Table 1.2. Biological test results of Bionate® PCU

In order to determine the bioactive features and biocompatible properties of this material in the laboratory, the samples were immersed in simulated body fluid (SBF), prepared in the lab, according to Kokubo’s formulation (I will talk about it in section 2.2).

The another material is a multiblock polyester copolymers composed from hard segments of ethylene terephthalate sequences as in PET (70%) and soft

segments of ethylene dilinoleate composed of dimmer fatty acid, here dilinoleic acid (DLA) (30%).It is 36-Carbon dicarboxylic acid formed by the catalytic dimerization of linoleic acid [48], light yellow viscous liquid and its density is 0.921 g/cm^3 (100ºC) [49].

Biodegradable polymers have much potential for applications such as implantable carriers for drug delivery systems as well as for surgical repair materials. Especially, polylactides have been applied for these purposes based on their good biodegradability, biocompatibility, high mechanical strength, and excellent shaping and moulding properties.

Poly(lactide)s exist in several enantiomeric forms, L, D, DL and *meso*. For instance, the polymers derived from the L and D monomers are semi-crystalline, while those from the DL (racemic mixture of L and D) are amorphous [50]. The chemical composition of PET-DLA is:

PET (=hard segment)

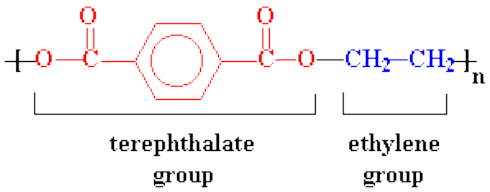

DLA (=soft segment)

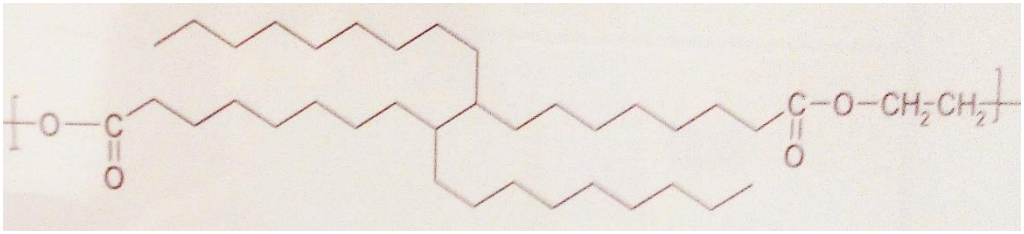

Polyethylene terephthalate is the most common thermoplastic polymer resin of the polyester family and is used in fibers for clothing, containers for liquids and foods, thermoforming for manufacturing, and in combination with glass fiber for engineering resins. It may also be referred to by the brand name Dacron; in Britain, Terylene [51]; or, in Russia and the former Soviet Union, Lavsan.

PET consists of polymerized units of the monomer ethylene terephthalate, with repeating ($C_{10}H_8O_4$) units. Depending on its processing and thermal history, polyethylene terephthalate may exist both as an amorphous (transparent) and as a semicrystalline polymer. The semicrystalline material might appear transparent (particle size < 500 nm) or opaque and white (particle size up to a few micrometers) depending on its crystal structure and particle size. Its monomer bis(2-hydroxyethyl) terephthalate can be synthesized by the esterification reaction between terephthalic acid and ethylene glycol with water as a byproduct, or by transesterification reaction between ethylene glycol and dimethyl terephthalate with methanol as a byproduct. Polymerization is through a polycondensation reaction of the monomers (done immediately after

esterification/transesterification) with water as the byproduct. Table 1.3 shows some special properties of this material:

Properties	
Chemical formula	$(C_{10}H_8O_4)_n$ [52]
Molar mass	Variable
Density	1.38 g/cm^3 (20 °C), [53] amorphous: 1.370 g/cm^3, [52] single crystal: 1.455 g/cm^3 [52]
Melting point	> 250 °C, [53] 260 °C [52]
Boiling point	> 350 °C (decomposes)
Young's modulus (E)	2800–3100 MPa [52]
Tensile strength (σ_t)	55–75 MPa [52]
Elastic limit	50–150% [52]
Notch test	3.6 kJ/m^2 [52]
Glass transition temperature (Tg)	67 to 81 ºC [52]
Vicat B	82 ºC [52]
Linear expansion coefficient (α)	7×10^{-5}/K [52]
Water absorption (ASTM)	0.16 [52]
Solubility in water	Practically insoluble [53]
Thermal conductivity	0.15 [54] to 0.24 W m^{-1} K^{-1} [52]
Refractive index (n_D)	1.57–1.58, [54] 1.5750 [52]
Specific heat capacity (C)	1.0 kJ/(kg·K) [52]

Table 1.3. Several properties for PET. Except where noted otherwise, data is given for materials in their standard state (at 25 °C (77 °F), 100 kPa)

An oligomer of polyethylene terephthalate (PET) was obtained in a separate unit, and was then reacted with dilinoleic acid (DLA) but DSM also supplied these materials in the form of pellets to the University.

2. EXAMINATION OF MATERIAL PROPERTIES

2.1 Samples preparation

Samples for static and fatigue testing were prepared by injection moulding using a pressure around 60 MPa for PET-DLA (70/30) and 40MPa for PU (Bionate 55D). Die temperatures were approximately 230 ºC for PET-DLA (70/30) and 240ºC for PU (Bionate 55D). The mould was kept at 14ºC for PET-DLA (70/30) and at 40ºC for PU (Bionate 55D). Samples were in the shape of dog-bones (samples S-2) with a thickness of 2.1 mm and a cross-section area of 8.6 mm2. Dumbbells for mechanical testing were prepared by injection moulding according to the ASTM D 1897-77 Standard (S2 geometry).

2.2 Simulated body fluid (SBF)

Simulated Body Fluid is an accellular solution that has inorganic ion concentrations similar to those of human extracellular fluid. It is often used to

reproduce the formation of apatite on bioactive materials in vitro. It was first developed by Kokubo and his colleagues [55] and is since known as SBF or Kokubo solution.

SBF has demonstrated its effectiveness via the surface modification of various materials [55]. Initially it was applied as a test to bio-ceramics which were part of bone implants. There are ceramics that bond to the bone through a bone-like apatite layer which forms on the ceramics or modified polymers surfaces. Currently the formation of the apatite-layer is not fully understood. It is known that the biomaterial surface must express OH groups, in order to attract the positive ions from the solution and create nucleation sites. On the surface of organic polymer the apatite layer formation takes place in a two-step biomimetic process [56]. Table 2.1 shows the concentrations of body plasma and SBF [57].

Ion	Concentration (mmol/dm^3)	
	Simulated body fluid (SBF)	Human blood plasma
Na^+	142.0	142.0
K^+	5.0	5.0
Mg^{2+}	1.5	1.5
Ca^{2+}	2.5	2.5
Cl^-	147.8	103.0
HCO_3^-	4.2	27.0
HPO_4^{2-}	1.0	1.0
SO_4^{2-}	0.5	0.5

Table 2.1. Ion concentrations of the simulated body fluid and human blood plasma

The pH of SBF is adjusted to pH 7.25 at 37 ºC, by using 50 mM (=mmol/dm3) of tris(hydroxymethyl)aminomethane and approximately 45 mM of HCl. Table 2.2 shows a brief overview about how to prepare SBF [57].

Order	Reagent	Amount of SBF (1000 mL)
#0	Ultra-pure water	750 mL
#1	NaCl	7.996 g
#2	$NaHCO_3$	0.350 g
#3	KCl	0.224 g
#4	$K_2HPO_4 \cdot 3H_2O$	0.228 g
#5	$MgCl_2 \cdot 6H_2O$	0.305 g
#6	1 kmol/m^3 HCl	40 cm^3
#7	$CaCl_2$	0.278 g
#8	Na_2SO_4	0.071 g
#9	$(CH_2OH)_3CNH_2$	6.057 g
#10	1 kmol/m^3 HCl	Appropriate amount for adjusting pH

Table 2.2. Amounts of reagents for preparation of SBF

2.3 Thermal properties of multiblock copolymers

The Differential scanning calorimetry (DSC)) method were recorded on a TA Instruments (DSC Q100) apparatus. The samples were examined in a triple cycle (heating-cooling-heating) in the temperature range from -90 ^{o}C to +300 ^{o}C. The heating and cooling rates were 10 ^{o}C/ min.

Procedure:

1. Ramp 10 ^{o}C/min from 25 ^{o}C to 300 ^{o}C - (First Heating)
2. Isothermal in 300 ^{o}C for 1 min
3. Ramp 10 ^{o}C/min from 300 ^{o}C to (-90 ^{o}C) - (Cooling)
4. Isothermal in (-90 ^{o}C) for 3 min
5. Ramp 10 ^{o}C/min from (-90 ^{o}C) to 300 ^{o}C - (Second Heating)

2.4 Mechanical characterization

When considering a material for an application, it is important to understand whether the material will be subjected to static or dynamic conditions. For example, if the material is subjected to dynamic forces then the application details required would include whether it is a rotary, reciprocating or vibrating environment. It would also be important to understand whether the application would be subjected to thermal cycling, as this small amount of dynamic movement may also need to be considered in selecting the correct material.

2.4.1 Static tensile testing

This test method is used to assess the behaviour of plastics when subjected to uniaxial tensile stress.

During testing of a material sample, the stress-strain curve is a graphical representation of the relationship between stresses, derived from measuring the load applied on the sample, and strain (Fig.2.1.a) derived from measuring the deformation of the sample, i.e. elongation, compression, or distortion. The nature of the curve varies from material to material.

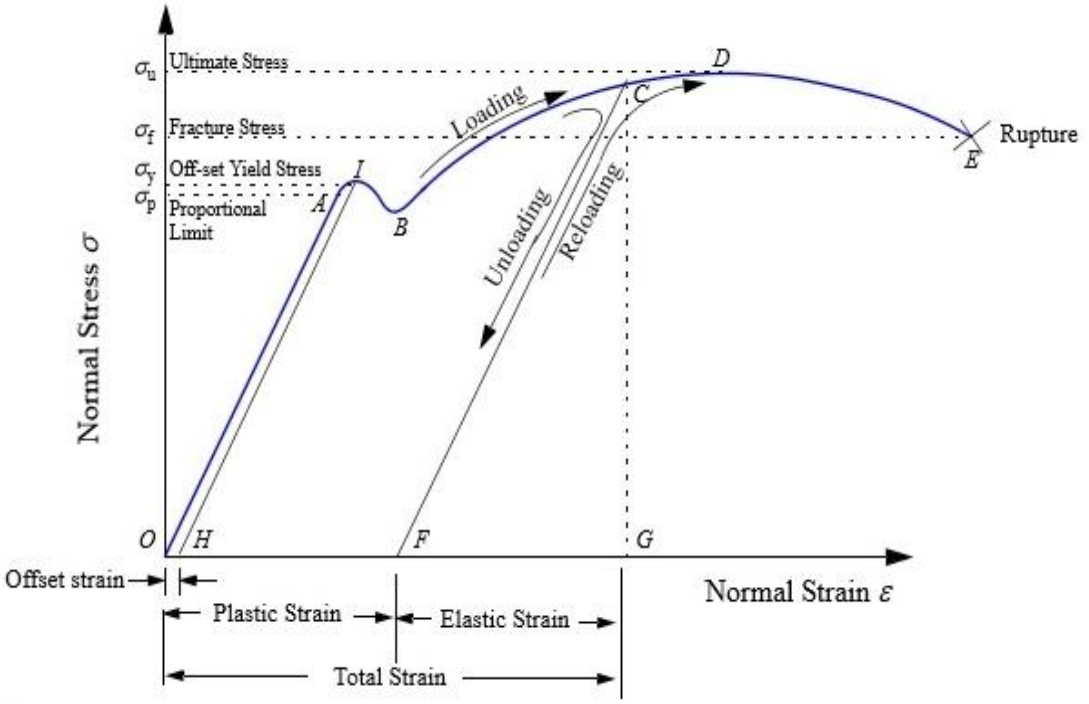

Figure 2.1.a. shows a typical stress–strain (σ-ε) curve for a metal, but in my materials (elastomers) the curve will be quite different (Fig. 2.1. b)

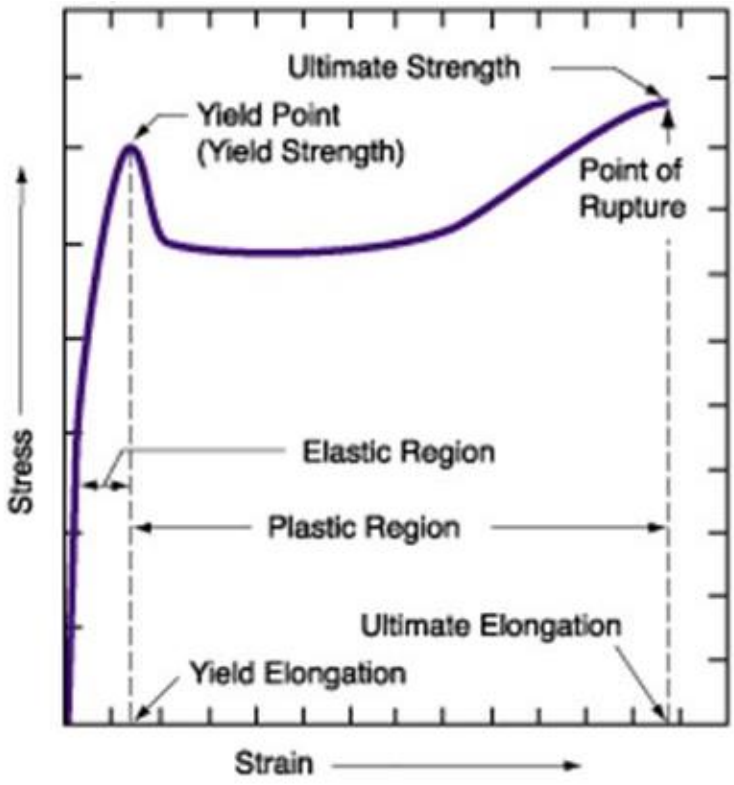

Fig. 2.1.b. shows a typical stress-strain curve of a thermoplastic polymer

In the Fig. 2.1.a., as the force is applied, initially a straight line (OA) is obtained. The end of this linear region is called the proportional limit. For some

metals, the stress may then decrease slightly (the region *AB*), before increasing once again.

The largest stress (point *D* on the curve) is called the ultimate tensile strength. In a force-controlled experiment, the specimen will suddenly break at the ultimate tensile strength. In a displacement-controlled experiment we will see a decrease in stress (region *DE*). The stress at breaking point *E* is called fracture or rupture stress.

-Elastic and plastic regions:

If we load the specimen up to any point along line *OA*—or even a bit beyond—and then start unloading, we find that we retrace the stress–strain curve and return to point *O*. In this elastic region, the material regains its original shape when the applied force is removed.

If we start unloading only after reaching point *C*, however, then we will come down the straight line *FC*, which will be parallel to line *OA*. At point *F*, the *stress* is zero, but the *strain* is nonzero. *C* thus lies in the plastic region of the stress-strain curve, in which the material is deformed permanently, and the permanent strain at point *F* is the plastic strain. The region in which the material deforms permanently is called plastic region. The total strain at point C is sum the plastic strain (*OF*) and an additional elastic strain (*FG*)

The point demarcating the elastic from the plastic region is called the yield point. The stress at yield point is called the yield stress. In practice, the yield point may lie anywhere in the region *AB*, although for most metals it is close to the proportional limit.

In my case, for my materials it wasn't clearly defined, thus I marked a prescribed value of offset strain to get point *H* in Figure 2.1. Starting from *H* it is drawn a line (*HI*) parallel to the linear part (*OA*) of the stress–strain curve. Offset yield stress would correspond to a plastic strain at point *I*. Usually the offset strain is given as a percentage. For instance, a strain of 0.2% equals $\varepsilon = 0.002$.

It should be emphasized that *elastic* and *linear* are two distinct material descriptions. Figure 2.2.a shows the stress–strain curve for a soft rubber that can stretch several times its original length and still return to its original geometry [58]. Soft rubber is thus *elastic* but *nonlinear* material.

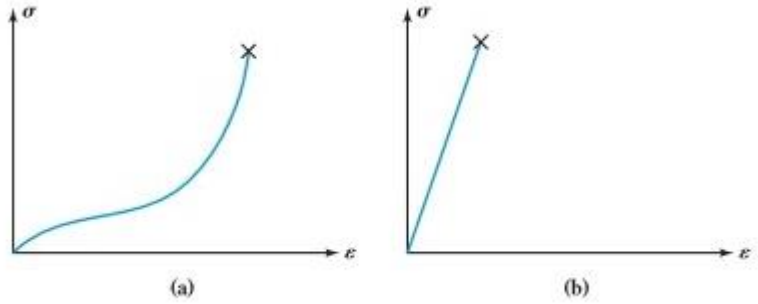

Fig. 2.2. Examples of nonlinear and brittle materials. (a) Soft rubber. (b) Glass.

Hooke's law gives the relationship between normal stress and normal strain for the linear region:

$$\sigma=\varepsilon*E$$

Where E is called modulus of elasticity or Young's modulus. It represents the slope of the straight line in a stress–strain curve, as shown in Figure 2.3 and serves as a parameter for comparing different materials and is a measure of stiffness.

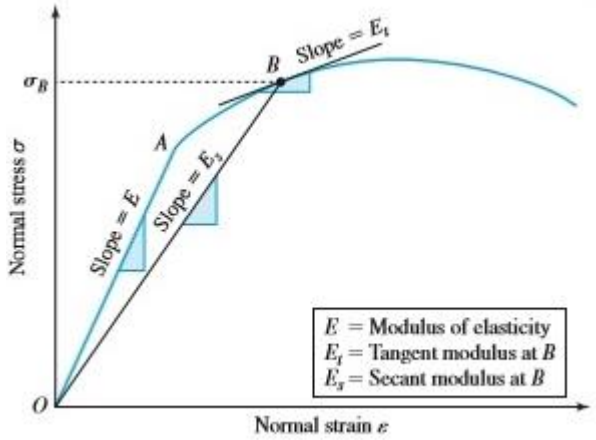

Fig.2.3. Different material moduli

In the nonlinear regions, the stress–strain curve is approximated by a variety of equations. The choice of approximation depends on the need of the analysis being performed. The two constants that are often used are the slope of the tangent drawn to the stress–strain curve at a given stress value which is called the tangent modulus and the slope of the line that joins the origin to the point on the stress–strain curve at a given stress value which is called the secant modulus. Organic tissues exhibit nonlinearity [59] in the stress–strain relationship, even at small strains.

Standard specimens were placed in a tension-test machine, where they were gripped at each end and pulled in the axial direction.

The static tensile data were collected at room temperature (22 ºC) with an Instron TM-M tensile tester (serial number 61093) (Fig. 2.4. a) equipped with a 500 N static load cell employing a crosshead speed of 10 mm/min. The strain (%) was measured using the clamp displacement (the starting clamp distance was 25 mm) and the stress data (MPa=N/mm^2) was calculated by dividing the force by the initial cross-section area (σ=F/A). The results obtained were averaged from 4-6 specimens for each material (test was performed according to ISO 527-1:1998). All measurements were registered in a software package called BlueHill. This available software drew all stress-strain curves during each measurement (Fig. 2.4. b).

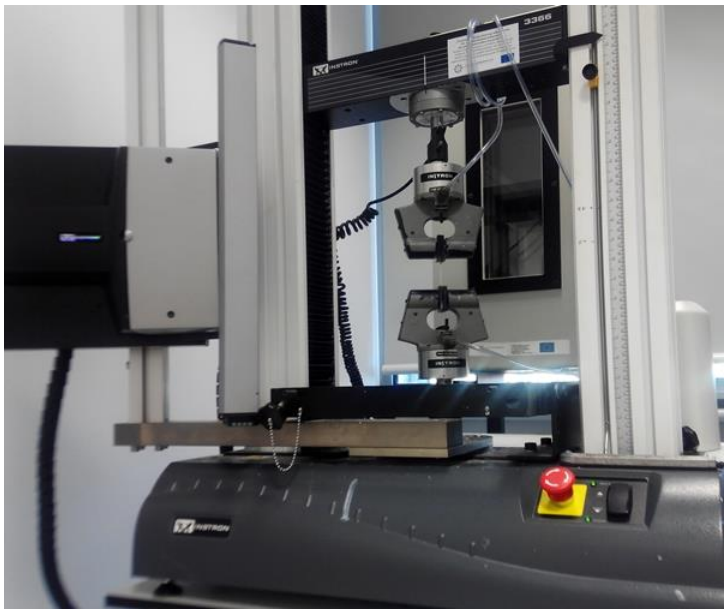

Fig.2.4. a. Static tensile test was performed in this machine

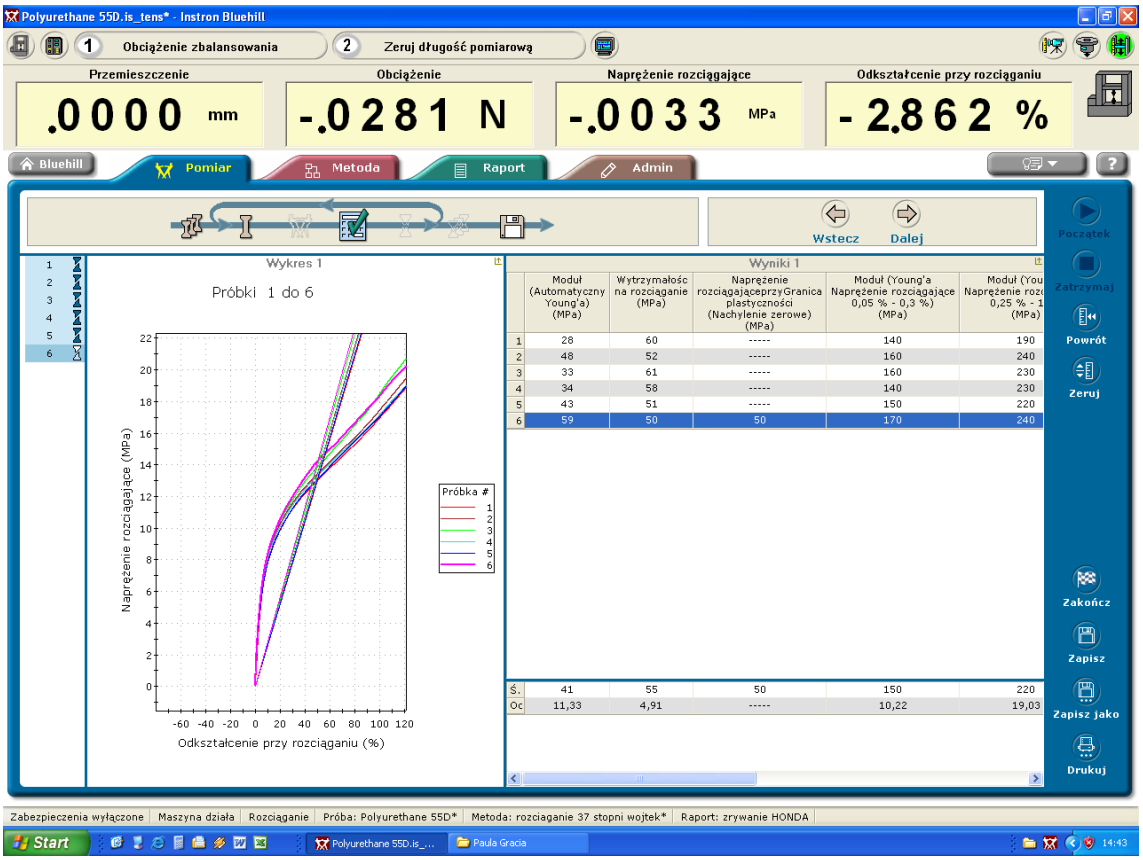

Fig. 2.4. b. Running of BlueHill

2.4.2 Fatigue testing via hysteresis measurements

Fatigue is the condition whereby a material cracks or fails as a result of repeated (cyclic) stresses applied below the ultimate strength of the material [60]. Fatigue life prediction is based on knowledge of both the number of cycles

the part will experience at any given stress level during that life cycle and other influential environmental and use factors.

As a function of the cyclic fatigue loading or straining conditions by hysteresis measurements, structural changes and fatigue behaviour of the material are able to be investigated. This method digitalizes the hysteresis loop and also determines some parameters such as stress and strain, the stored and lost energy, dynamic creep behaviour and damping.

The investigated materials are subjected to sinusoidal loading (Fig. 2.5). There are three basic factors necessary to cause fatigue: (1) a maximum tensile stress of sufficiently high value, (2) a large enough variation or fluctuation in the applied stress, and (3) a sufficiently large number of cycles of the applied stress. There are many types of fluctuating stresses. Several of the more common types encountered are shown in Fig. 2.6.

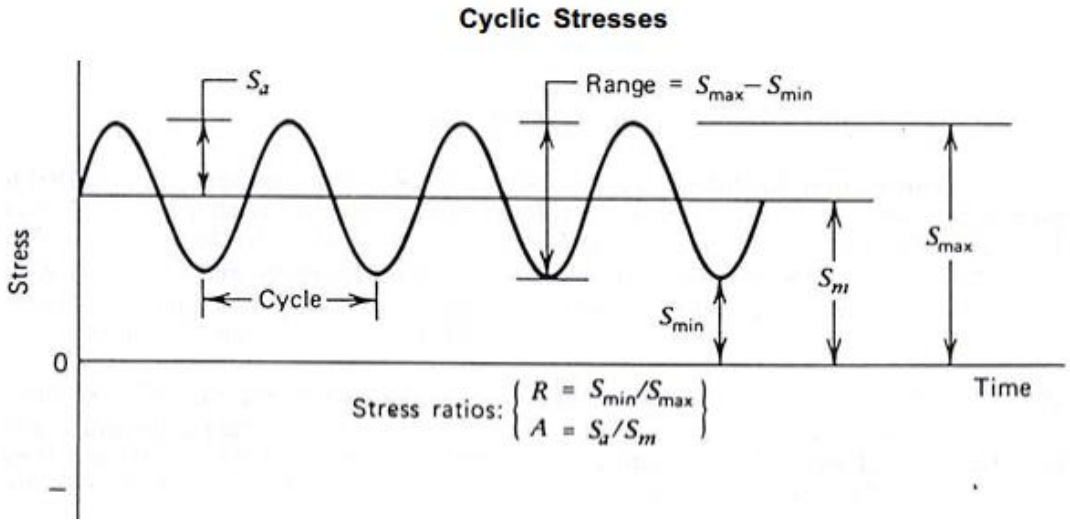

Fig. 2.5. Schematic Illustrating Cyclic Loading Parameters [61].

The following parameters are utilized to identify fluctuating stress cycles:

-Mean Stress (σ_m): $\sigma_m = (S_{max} + S_{min})/2$
-Stress Range (σ_r): $\sigma_r = \sigma_{max} - \sigma_{min}$
-Stress Amplitude (σ_a): $\sigma_a = (S_{max} - S_{min})/2$
-Stress Ratio (R): $R = S_{min}/S_{max}$
-Amplitude ratio (A): $A=S_a/S_m$

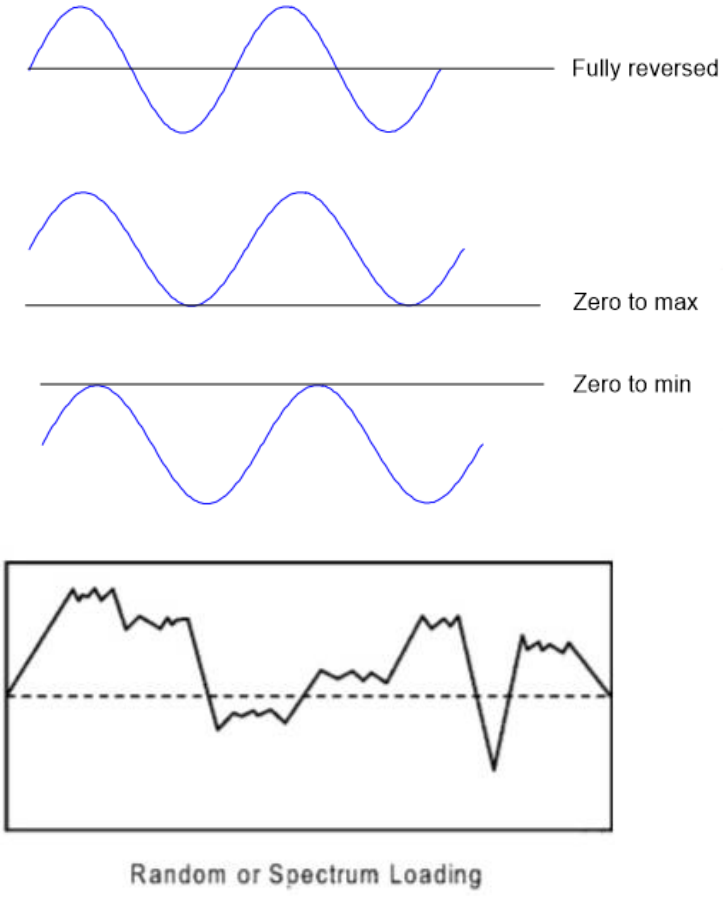

Fig. 2.6. Typical loading cycles [62]

The simplest fluctuating stress is completely reversed constant amplitude where the alternating stress varies from a maximum tensile stress to a minimum compressive stress of equal magnitude. The second type, termed repeated constant amplitude, occurs when the maxima and minima are asymmetrical relative to the zero stress level. Lastly, the stress level may vary randomly in amplitude and frequency which is merely termed random cycling.

Fully reversed: R= -1; A =∞

Zero to max: R= 0; A=1

Zero to min: R= ∞; A=0

During loading, the specimen absorbs energy, which is not completely recovered during unloading. This difference is called the energy loss w_1 and corresponds to the area enclosed by the hysteresis loop (Fig. 2.7) (σ_u,ε_u: upper stress and strain, respectively; σ_1, ε_1: lower stress and strain, respectively; σ_m, ε_m: mean stress and strain at mean stress, respectively; σ_{mc}: mean stress curve). If a material behaves as a linear-viscoelastic solid, the hysteresis loop takes the form of an ellipse.

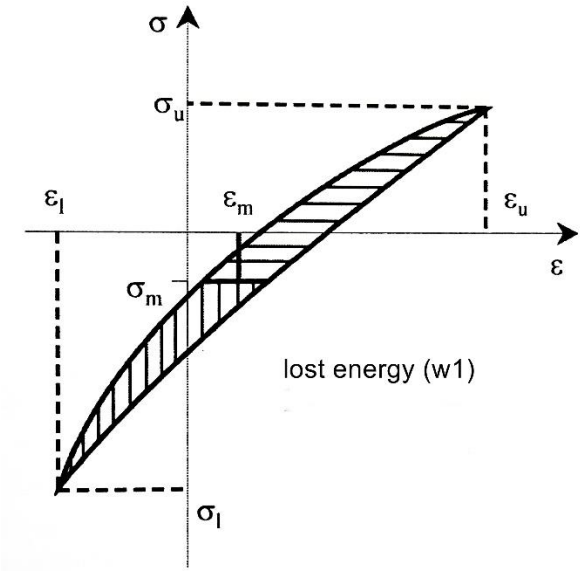

Fig. 2.7 Definition of the loss energy on a hysteresis loop

The strain (stored) energy, w_s is obtained from the area between the mid-curve and the mean stress (Fig. 2.8). By means of the relative coordinate system, the total energies can be divided into the corresponding upper (u) and lower (l) energies.

The ratio of energy loss to strain energy is the damping factor:

$$\Lambda = w_l / w_s$$

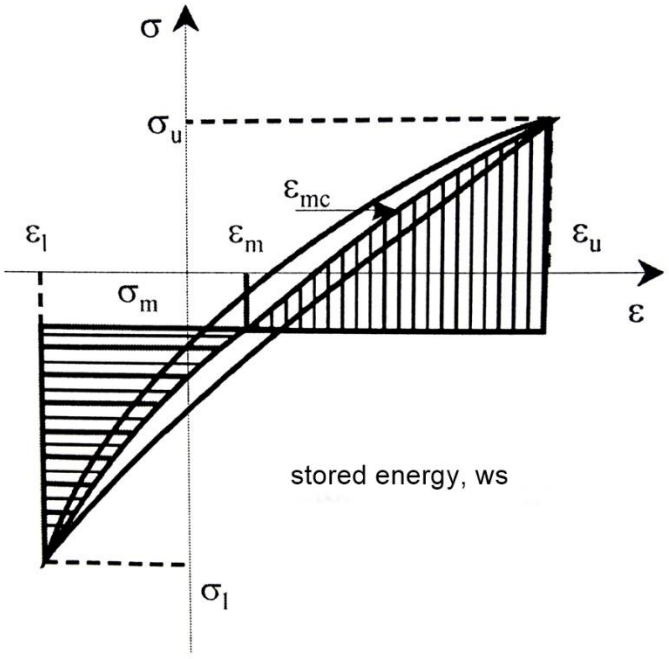

Fig. 2.7 Definition of the strain (stored) energy on a hysteresis loop

A very useful quantity to determine changes in the loop shape is the stiffness ratio of the upper and the lower modulus, E_u and E_l, respectively (Fig. 2.8):

$$E_u / E_l = \tan \alpha_u / \tan \alpha_l$$

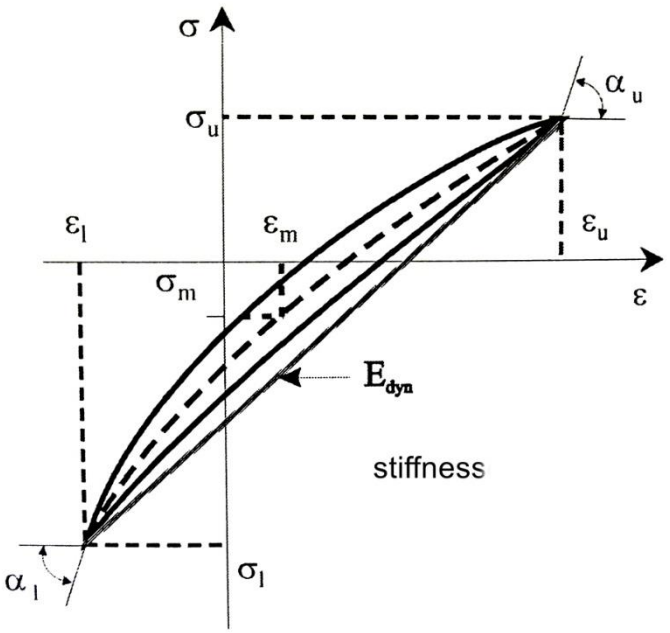

Fig. 2.8 Definition of the stiffness on a hysteresis loop

A very important basic property is the dynamic modulus, Edyn, defined as a quotient of the stress and the strain under vibratory conditions [63]:

$$E_{dyn} = (\sigma_u - \sigma_l) / (\varepsilon_u - \varepsilon_l)$$

From all these quantities, we can evaluate the total fatigue behaviour of the material.

Investigated samples with the same geometry characteristic for static tensile testing were subjected to cyclic sinusoidal loading. An ElectroPuls machine with a digital controller (Instron E3000 – Fig.2.9) and a software package for the evaluation of the hysteresis loop (WaveMatrix™) was used. The testing machine was equipped with a 5 kN cylinder and 250 N load cell.

Fig. 2.9. Fatigue test machine used in the investigation

The available software package digitalizes the hysteresis loop of any polymer material, which is measured continuously, and calculates a mid-curve in the hysteresis loop. The mid-curve is intersecting the hysteresis loop for equal strain. By this it is possible, also in the case of non-linear viscoelastic material behaviour, to determine strain-, stiffness- and energy-related material properties [63]. During the dynamic fatigue test it is desirable not only to determine the fatigue strength, but also to characterize the damage in the material. Furthermore, tiny changes in material damping can be detected by this method and used as a damage criterion to understand the behaviour of the material.

For hysteresis measurements, two test protocols have been used:

-A stepwise increasing load test (SILT)

-A single load test (SLT)

During the stepwise increasing load testing procedure (SILT), the dynamic load increases after a certain number of cycles, while the load ratio remains constant.

In other words, the amplitude of the load is stepwise increased and held constant within each step for a definite number of cycles [63].

The samples were subjected to a stress controlled sinusoidal oscillation which was set by me and the frequency, *f*, was in a range of 1‑4 Hz. The SILT method was performed in order to get load limits for a long time dynamic loading. The maximum stress was set at a value corresponding to one of ten prescribed stress levels in the range 5‑50% of the ultimate tensile strength (UTS) at 5% increments (Fig. 2.10). The stress was kept constant during a period of

1000 cycles and set to the next higher-level then. An interval of 50 cycles has been implemented between every step to allow the controller to reach a higher loading level (Fig. 2. 11 and 2.12) and when it has been reached, another 50 cycles in each step has had the same purpose. That means a maximum of 1050 cycles can be reached in each step. The frequency of the cyclic loading was varied according to the stress levels such as:

- at stress levels of 5, 10 and 15% of the UTS the frequency was 4 Hz,
- at stress levels of 20, 25 and 30% of the UTS the frequency was 3 Hz,
- at stress levels of 35 and 40% of the UTS the frequency was 2 Hz,
- at stress levels of 45 and 50% of the UTS the frequency was 1 Hz.

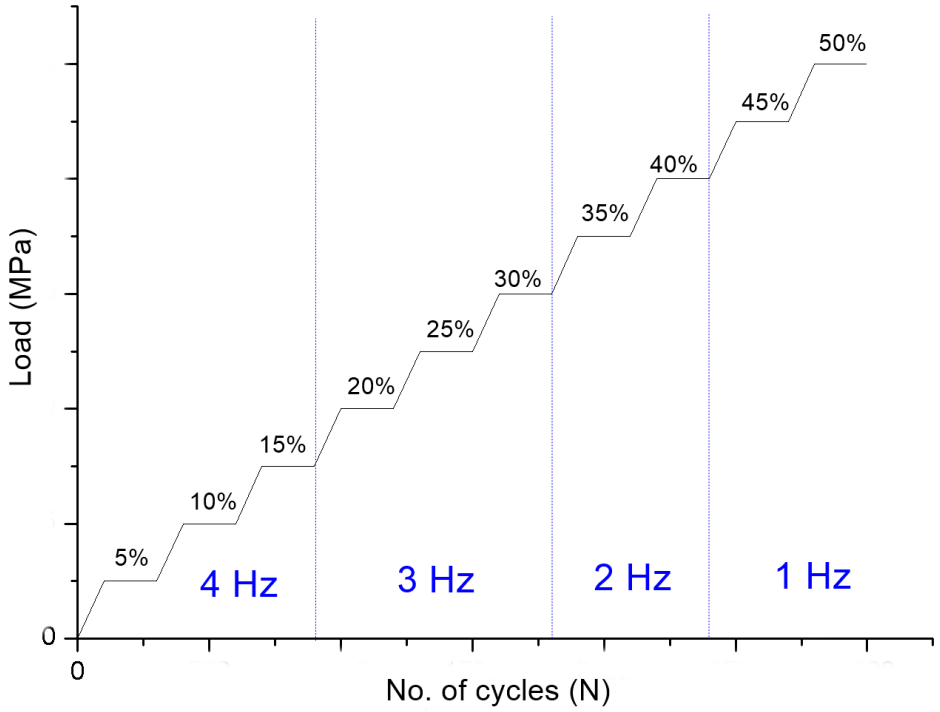

Fig. 2.10 The presumed ultimate load, estimated from previous test (static tensile test) is divided into 10 equal parts. This is the proper protocol followed to determine the main load in each step for SILT and set the parameters needed in the sinusoidal oscillation afterwards.

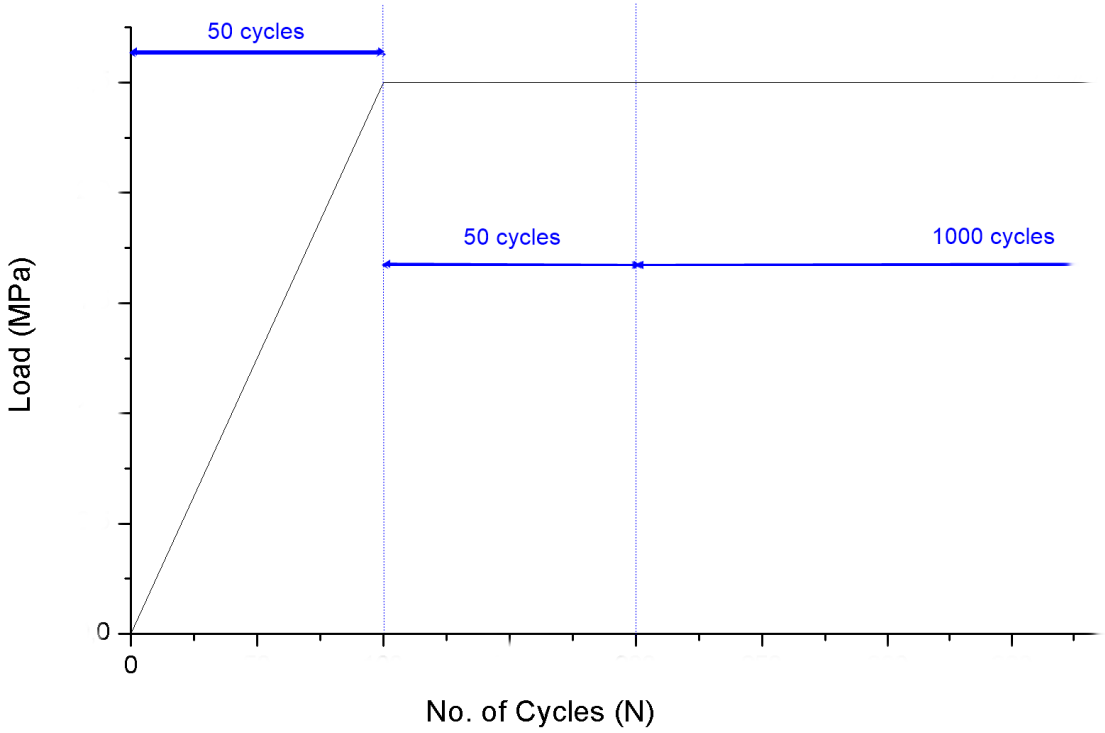

Fig. 2. 11. Representation of first step (5%) to show how all steps behave. One step can have 1050 cycles but there are 50 cycles before each step to allow the controller to reach a higher loading level. Next 50 cycles have the same task (Fig. 2.12).

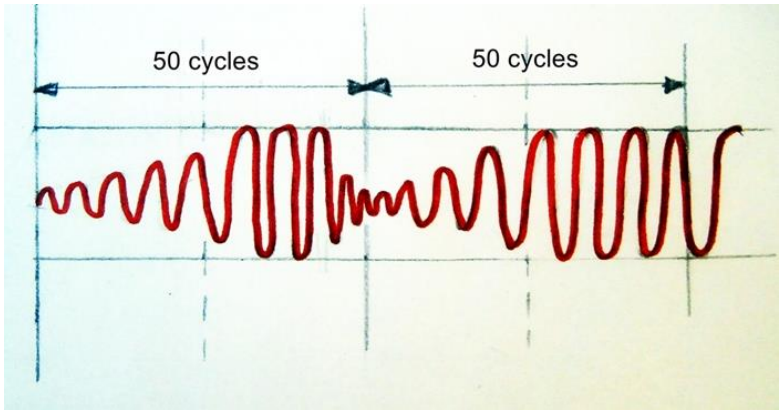

Fig. 2.12. Changes in the sinusoidal oscillation in the first 100 cycles

The load levels for the single load test (SLT) were determined by results obtained from SILT, where the applied waveform was a sinusoidal at a constant minimum-to-maximum load ratio, R, of 0’1. Thus, sinusoidal oscillations are cyclic repetitious in tension mode.

The digital controller was used to keep the load level constant at each stress level with an accuracy of 5%. Using the formula for dynamic modulus (E_{dyn}) described before, the controller is able to compare from cycle no. 100 to cycle

no. 1050, in every step, if the difference of E_{dyn} between them is higher than 5%. If this occurs, the machines will stop and the test will be finished. Nonetheless, I calculated that difference manually to be sure of the results. The test can also stop if the samples break or if the distance between clamps are higher than 29 mm (because I set that parameter in the machine according to the protocol used).

All measurements were performed at a room programmed temperature (23 ºC).

RESULTS AND DISCUSSION

1. THERMAL CHARACTERIZATION OF POLYMERS AS STUDIED BY DSC

DSC compares the exothermic and endothermic reactions of samples with a reference while subject to controlled heating. The technique enables the accurate determination of cure characteristics, glass transition temperature, crystallisation and melting point.

When elastomers are cooled to sufficiently low temperatures they exhibit the characteristics of glass, including hardness, stiffness and brittleness, and do not behave in the readily deformable manner usually associated with elastomers. As temperatures are raised, the segments of the polymer chain gain sufficient energy to rotate and vibrate. At high enough temperatures full segmental rotation is possible and the material behaves in the characteristic rubbery way. The usefulness of an elastomer at low temperatures is dependent on whether the material is above its glass transition temperature (Tg), where it will still behave elastically, or below its Tg, where the material will be hard and relatively brittle.

All non-cross-linked polymers, whether amorphous or semicrystalline, tend to change their mechanical stiffness, or rigidity, by several orders of magnitude upon passing through one or more temperature regions. The temperature location of the major softening regions depends upon the intra- and intermolecular forces that are operative for the particular polymer and varies greatly with the specific composition.

The study disclosed the following information about the materials (Fig. 1.1 and 1.2):

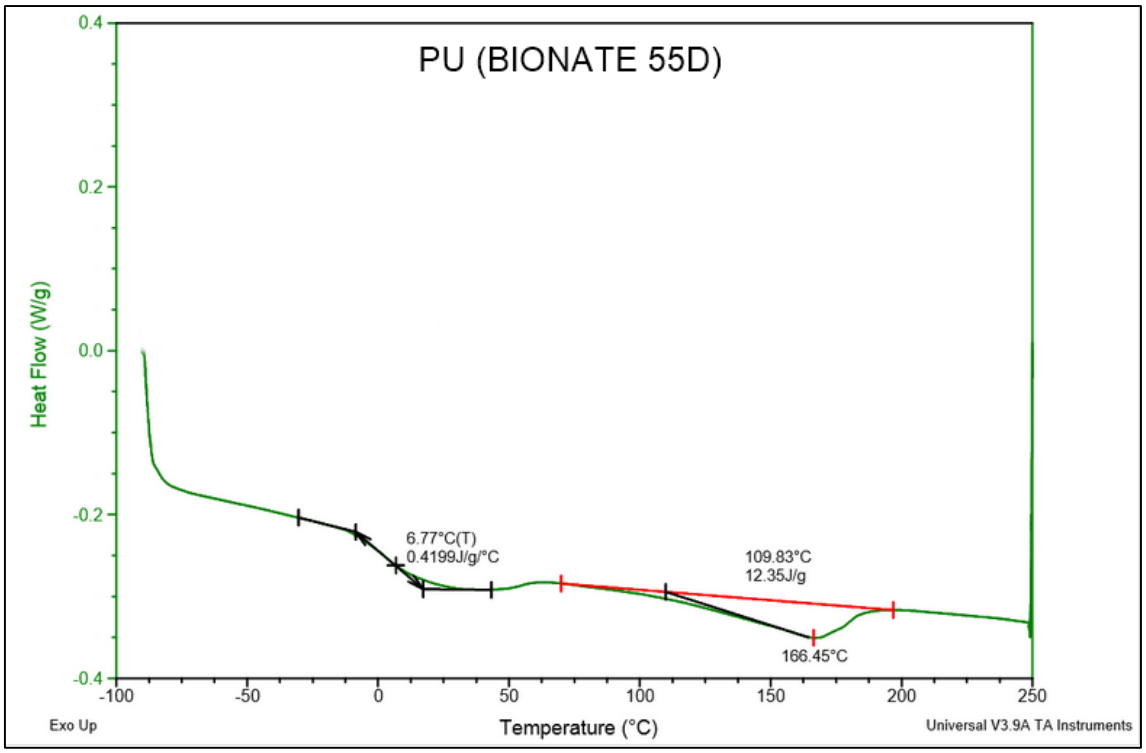

Fig. 1.1. DSC thermogram from second heating of PU (Bionate 55D)

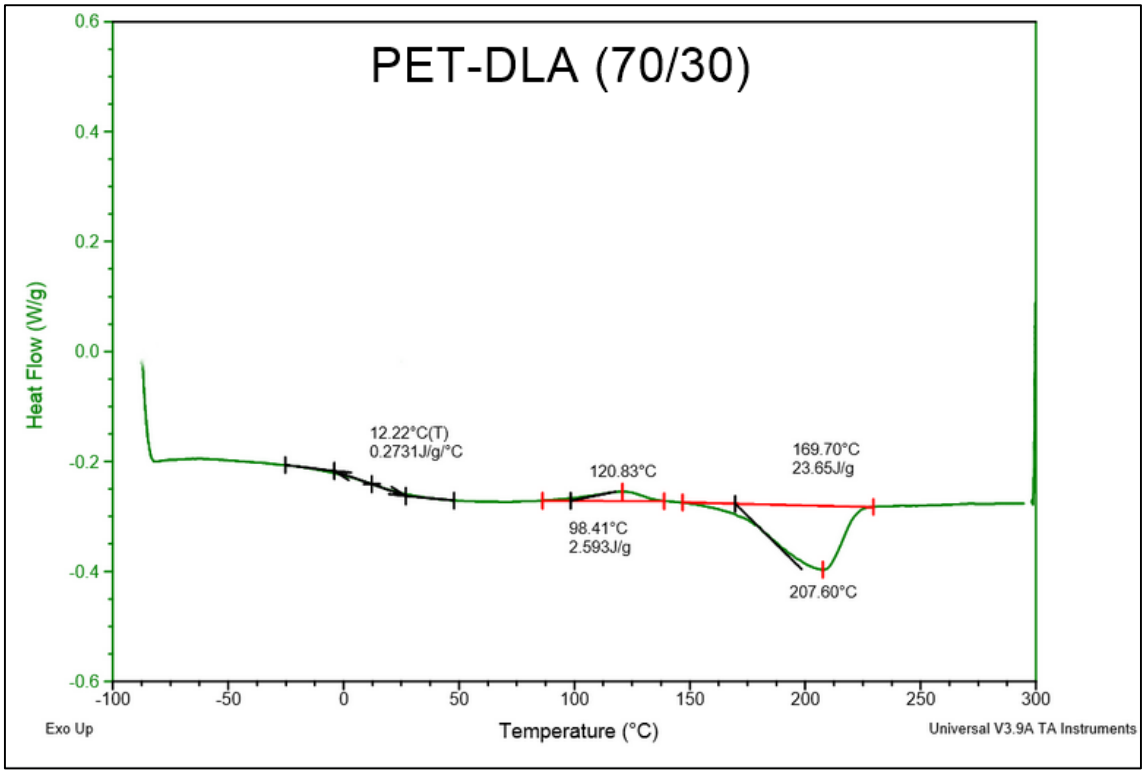

Fig. 1.2. DSC thermogram from second heating of PET-DLA (70/30)

The most important information extracted from the graphs are shown in Table 1.1:

Material	T_g [ºC]	ΔC_p [J/g/ºC]	T_m [ºC]
PU (Bionate 55D)	6.77	0.4199	166.45

PET-DLA (70/30)	12.22	0.2731	207.60

2. STATIC MECHANICAL PROPERTIES OF PET/DLA (70/30) AND PU (BIONATE 55D) MATERIALS

The general viscoelastic behaviour of PU (Bionate 55D) and multiblock copolymer PET-DLA (70/30) has been evaluated to determine the load levels for the future fatigue tests and define the tensile properties. To get these data, static tensile experiments have been carried out.

The specimens has been preheated in the oven before testing at 40ºC (below their T_g) during 4-5 h, because they were cooled in the injection moulding to sufficiently low temperatures that they exhibit the characteristics of glass, including hardness, stiffness and brittleness, and don't behave in the readily deformable manner usually associated with elastomers.

Specially in semi crystalline polymers, the annealing causes alteration of the crystallinity degree, the crystal structure, promotes the improvement of the crystals, increases the lamellae thickness, decreases the concentration of defect and generally induces alterations in the orientation of the crystalline and amorphous parts of the materials

Related to PET-DLA (70/30), this multiblock copolymer shows the stress-strain features which are very characteristic for thermoplastic elastomers as shown in Fig. 2.1.

For this material I don't need to keep in mind the last part of the graph, that means the point of rupture, because the yield point is well defined and from here on the specimen's cross-sectional area begins to decrease. This process is called necking and after that, the samples break.

In fact, that event happens because PET-DLA is a semi crystalline polymer and it is well recognized that kind of polymers consist of lamellar crystals which are separated from each other by layers of amorphous polymer and are held together by tie molecules through the amorphous phase. It is also characterized by a linear elastic region; a yielding followed by a drop in stress, a formation of a neck, an increase in stress due to straightening of polymer chain, and finally fracture.

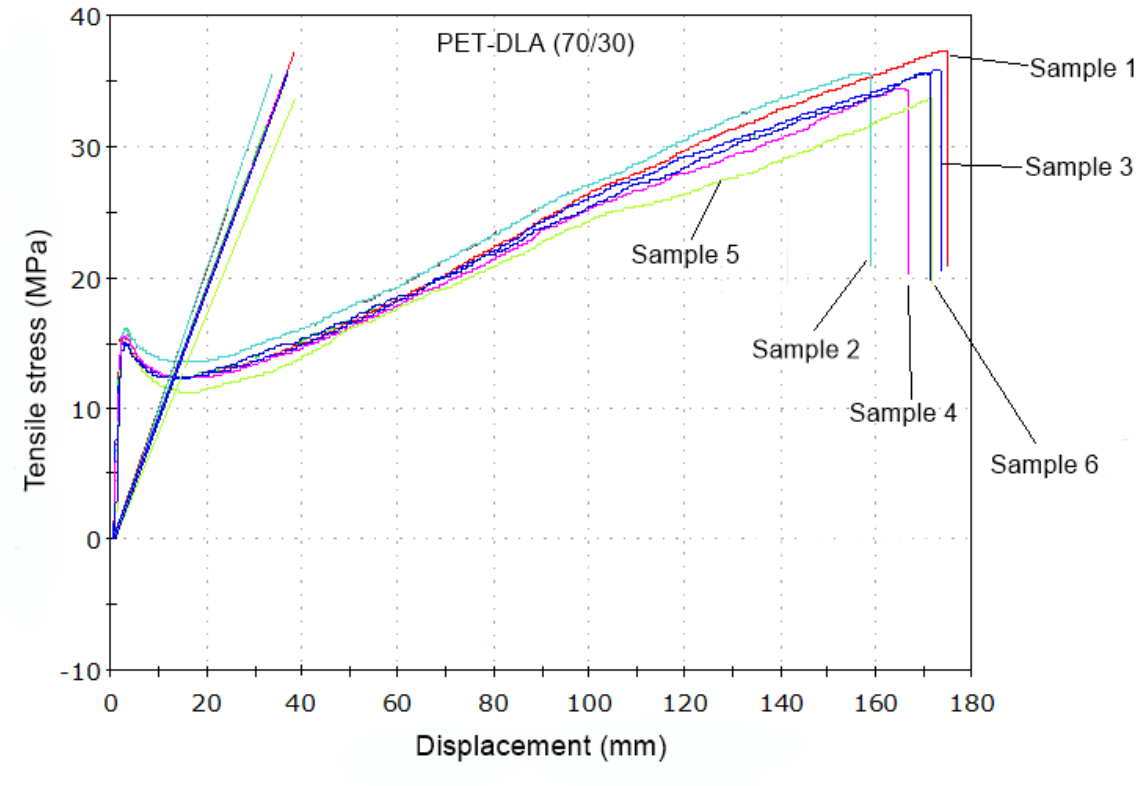

Fig. 2.1 Stress-strain curves for PET-DLA (70/30) (measurements performed with a crosshead speed of 10 mm/min)

As we can see in Fig. 2.1, the specimens with higher stresses show stronger yielding and necking. Once the yield strength is exceeded the polymer deforms plastically, thus, the specimens exhibit “irreversible” plastic deformations with increasing strain. Plastic deformation is the result of chains sliding, stretching, rotating, and disentangling under load. This causes permanent deformation. The drop in stress beyond the yield point is because the initially tangled and intertwined chains become straight and untangled. Once the chains are straighten, additional stress causes necking, in which there is the continued sliding and deformation of the chains. At this point strong covalent bonding between the more closely aligned chains requires higher stress in order to complete the deformation and fracture process.

Hence, it might be concluded that the stress–strain behaviour is related to strong morphological changes.

As I mentioned before, it is important to focus attention on the elastic region (before the yield point) because after that the specimen starts to creep and it is not convenient for the future purpose of the material. For that reason I redrew the graph (Fig 2.2) to have a better view for all parameters needed.

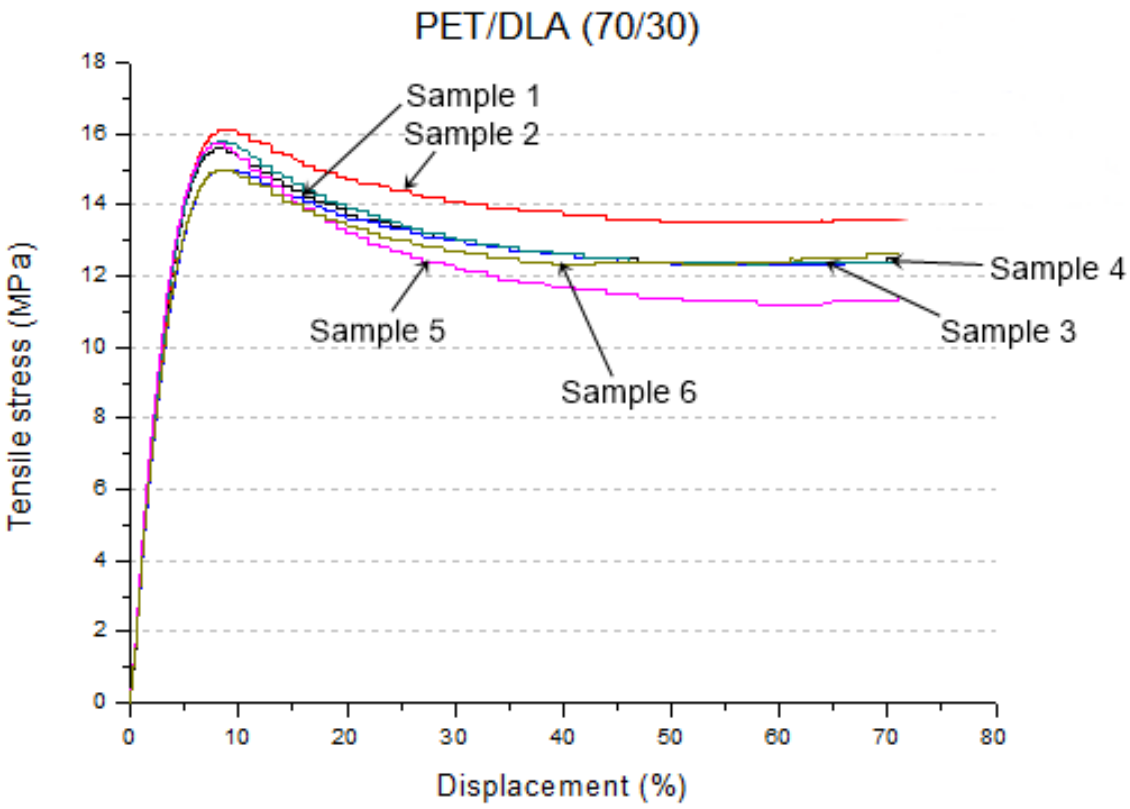

Fig. 2.2. Stress-strain curves for PET-DLA (70/30) focusing on the elastic region (measurements performed with a crosshead speed of 10 mm/min)

The next table (Table 2.1) shows the most important data which are in the graph:

Sample	Young Modulus (MPa)	Tensile strength (MPa)	Elongation at break (%)	Tensile at yield point (MPa)
1	390	37	690	16
2	380	36	630	16
3	360	36	690	15
4	390	35	660	16
5	410	34	680	16
6	370	36	670	15
Average	**383.33**	**35.67**	**670**	**15.6**

Sample	Young Modulus at 0,05 % - 0,3 % of elongation) (MPa)	Young Modulus at 0,25 % - 1 % of elongation) (MPa)	Young Modulus (at 100 % of elongation) (MPa)	Young Modulus (at 50 % of elongation) (MPa)
1	410	510	13	25
2	400	500	14	27

3	400	500	13	25
4	410	560	13	25
5	410	560	12	23
6	370	490	13	25
Average	**400**	**520**	**13**	**25**

Table 2.1. Values which have been collected from the static tensile test for PET-DLA (70/30)

The most important data are the first 4 columns. This material has a high Young's Modulus because of their 70% of hard segments but at the same time the 30% of dilinoleic acid (DLA) provides elasticity as we can see in the graphs. That will be perfect for the future biomedical device, as it will have to withstand certain loads and perpetual movements, without breaking, for the heart. But this study is only static, thus only tensile properties can be investigated and it will be necessary to perform a fatigue test to see how the material will behave with perpetual movements and loads.

Values for the ultimate tensile strength vary between 34 and 37 MPa, while elongation at break happens between 630 and 690%. The most important part is the tensile at yield point, which varies from 15 to 16 MPa, because the average will be the value I will use to set in the fatigue test as the UTS (Ultimate Tensile Strength) and calculate all parameters needed in that method.

If Table 2.5 (from section *2.2.7 Mechanical properties of heart)* is taken into consideration, I can ensure that this material shows a very good mechanical properties because they are above the values which are in that table:

Myocardium: Young's Modulus = 0.2 – 0.5 MPa and elongation at break = >20%.

In the case of PU (Bionate 55D) the graph that I obtained (Fig. 2.3) shows a different behaviour in the stress-strain curve:

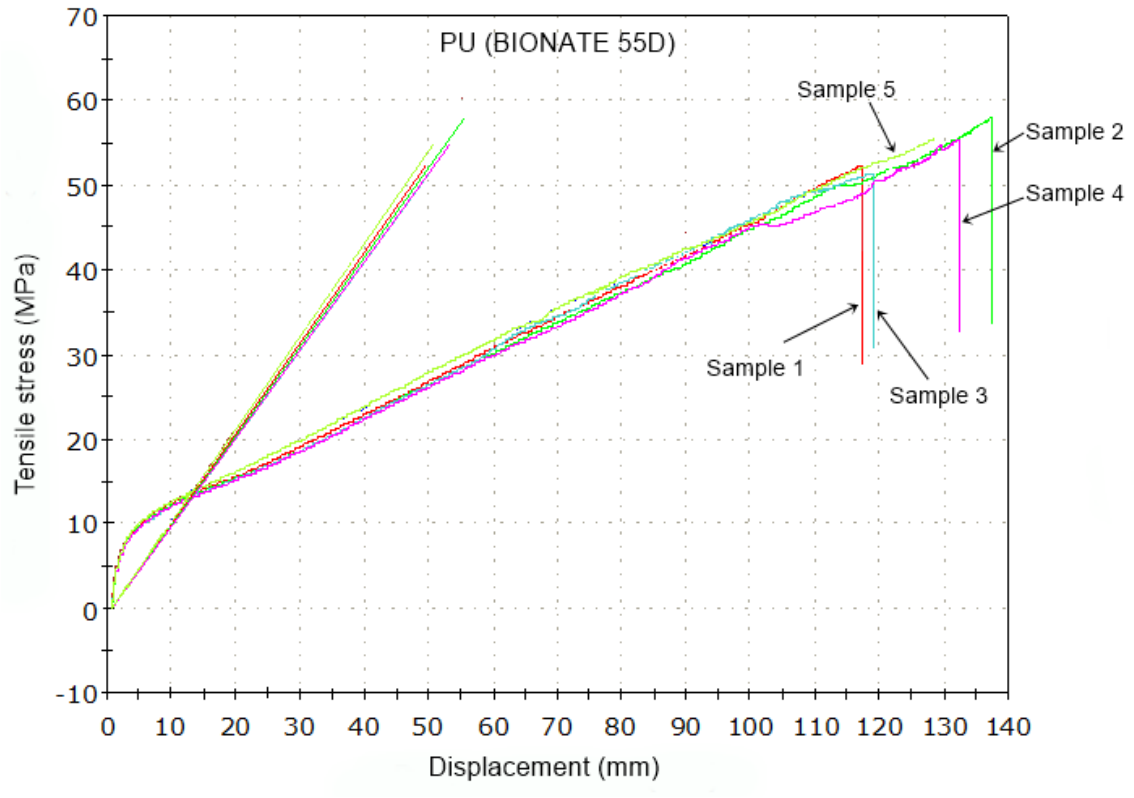

Fig. 2.3. Stress-strain curves of PU (Bionate 55D) (measurements performed with a crosshead speed of 10 mm/min)

This material, unlike the PET-DLA (70/30), doesn't show a yield point which is easy to identify. For that, although I don't want my material to reach the fracture point, the tensile strength will be considered as the UTS to the future fatigue test. The Table 2.2 indicates the values for the tensile properties of PU:

Sample	Young Modulus (MPa)	Tensile strength (MPa)	Elongation at break (%)
1	48	52	470
2	34	58	540
3	43	51	470
4	37	55	530
5	43	56	510
Average	**41**	**54.4**	**504**

Sample	Young Modulus at 0,05 % - 0,3 % of elongation) (MPa)	Young Modulus at 0,25 % - 1 % of elongation) (MPa)	Young Modulus (at 100 % of elongation) (MPa)	Young Modulus (at 50 % of elongation) (MPa)
1	160	240	17	27
2	140	230	17	27

3	150	220	17	26
4	130	200	17	26
5	140	200	18	28
Average	**144**	**218**	**17.2**	**26.8**

Table 2.2. Values which have been collected from the static tensile test for PU (Bionate 55D)

Young's Modulus is lower than the first material because, as it is shown in the Fig. 2.3, the elastic region is more curved, thus the slope of Young Modulus isn't so steep.

The elongation at break occurs between 470 and 540 % and values of the ultimate tensile strength vary between 51 and 58 MPa. The average will be the main parameter to set all values needed in the fatigue test. If I compare the tensile strength which I obtained with the one that DSM provides in his specifications of his supply, the difference between values are 6 MPa. As I said before, those data are for general information purposes only, and may not be relied upon in individual situations but that difference is not negligible. That doesn't mean that my results are wrong, merely the processing method (injection moulding) may have changed the internal structure due to the presence of dust, tiny cracks… Anyway, I chose the best samples to make all measurements; all the specimens with a transparent surface.

In comparison with PET-DLA (70/30), polyurethane has a very high tensile strength because of the presence of hydrogen bonds in it (Fig. 2.4). Due to the incompatibility between the hard and soft segments, polyurethane copolymers undergo micro-phase separation resulting in hard-segment-rich domains, a soft-segment-rich matrix, and an interphase between them. The elastic behaviour of polyurethanes are directly related to the stability of the hydrogen-bonded hard-segment-rich domains, acting as junction points in the network. In the same way as PET-DLA (70/30), this material reveals excellent mechanical properties.

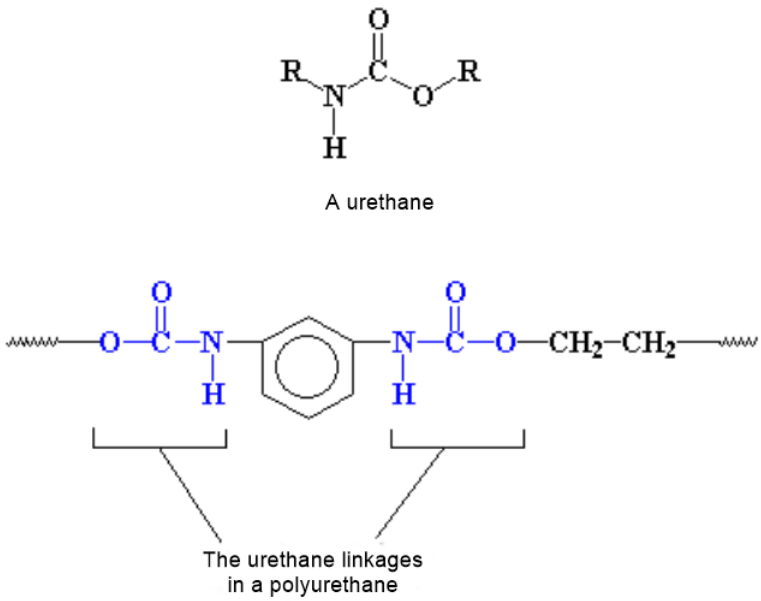

Fig. 2.4. Chemical structure of PU

3. FATIGUE PROPERTIES EVALUATED USING THE HYSTERESIS METHOD

Many loads are cyclic in nature [63], as in the case of heart muscle. It is of great interest the characterisation of deformation and fracture properties of materials, particularly if they are under fluctuating loads (fatigue).

When a polymer system is subjected to an applied stress, a great variety of chemical and rheological events may occur in a given polymer. The net effect of the several competing processes depends on many factors, including temperature, environment, and basic molecular properties of the polymer [63, 64].

In a fatigue test, specified mean load and an alternating load are applied to a specimen and the number of cycles required to produce failure (fatigue life) is recorded. Generally, the test is repeated with identical specimens and various fluctuating loads. Depending on amplitude of the mean and cyclic load, net stress in the specimen may be in one direction through the loading cycle, or may reverse direction. Data from fatigue testing often are presented in an S-N diagram which is a plot of the number of cycles required to cause failure in a specimen against the amplitude of the cyclical stress developed. The cyclical stress represented may be stress amplitude, maximum stress or minimum stress. Each curve in the diagram represents a constant mean stress [65].

Besides, with fatigue test, hysteresis method also gives extra information about structural changes of the material. Different properties can be determined simultaneously–stress, strain amplitude, stiffness and stored and lost energies, material damping and the cyclic creep behaviour [66, 67, 68, 69]. These properties are defined from the slope of the hysteresis loop, which is affected by the cyclic degradation [70].

A wide range of different polymeric systems like polymer blends, block and graft copolymers, and also composites have already been investigated for the evaluation of fatigue properties [63, 70, 71]. Especially, thermoplastic multiblock elastomers (TPEs) are a very interesting kind of polymeric materials but their fatigue properties are not widely studied via this new hysteresis measurement method [71].

3.1 Stepwise increasing load test (SILT)

As it was pointed in the experimental part, SILT was modified to simulate loading patterns reported *in vivo* for human hearts. The applied loading pattern consisted of a stepwise increasing load applied at the physiological frequency range from 1 to 4 Hz. 4Hz amount to 240 bpm, thus, this value overcomes the maximum real heart rate (220 bpm).

The results related to PET-DLA (70/30) have been the following:

The settings that I used to set the loading protocol are shown in Table 3.1. The value of UTS was obtained from the static tensile test (15.6 MPa).

UTS		4Hz 5%	4Hz 10%	4Hz 15%	3Hz 20%	3Hz 25%	3Hz 30%	2HZ 35%	2HZ 40%	1HZ 45%	1HZ 50%
15,6	Load	0,78	1,56	2,34	3,12	3,90	4,68	5,46	6,24	7,02	7,80
	Amplitude	0,638	1,276	1,915	2,553	3,191	3,829	4,467	5,105	5,744	6,382
	Fmax	1,418	2,836	4,255	5,673	7,091	8,509	9,927	11,345	12,764	14,182
	Fmin	0,142	0,284	0,425	0,567	0,709	0,851	0,993	1,135	1,276	1,418

Table 3.1. Parameters calculated and introduced in the stepwise increasing load test (SILT). All values are in MPa.

The load in every step, shown in “Load” boxes in the previous table (Table 3.1), appears in the following Fig. 3.1. a-b to observe the loading pattern in that material. These figures also illustrate the pattern of changes at the maximum stress and strain and the dynamic modulus during SILT.

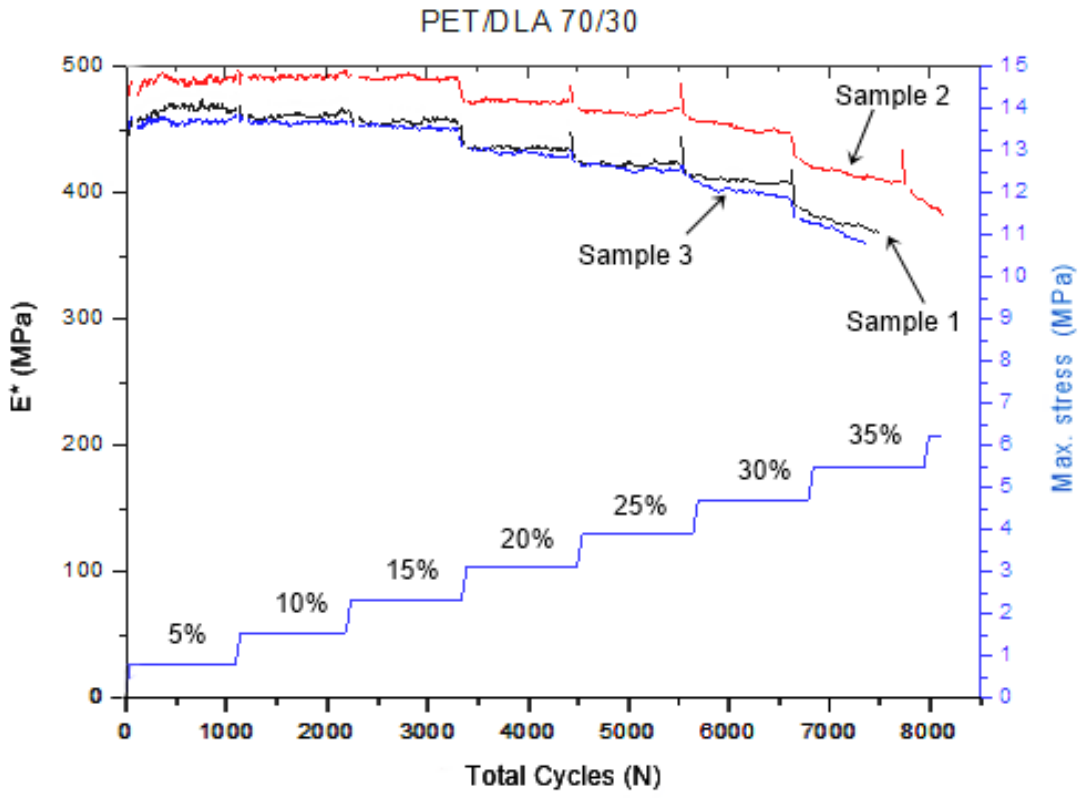

a) Pattern of change in the stress and dynamic modulus

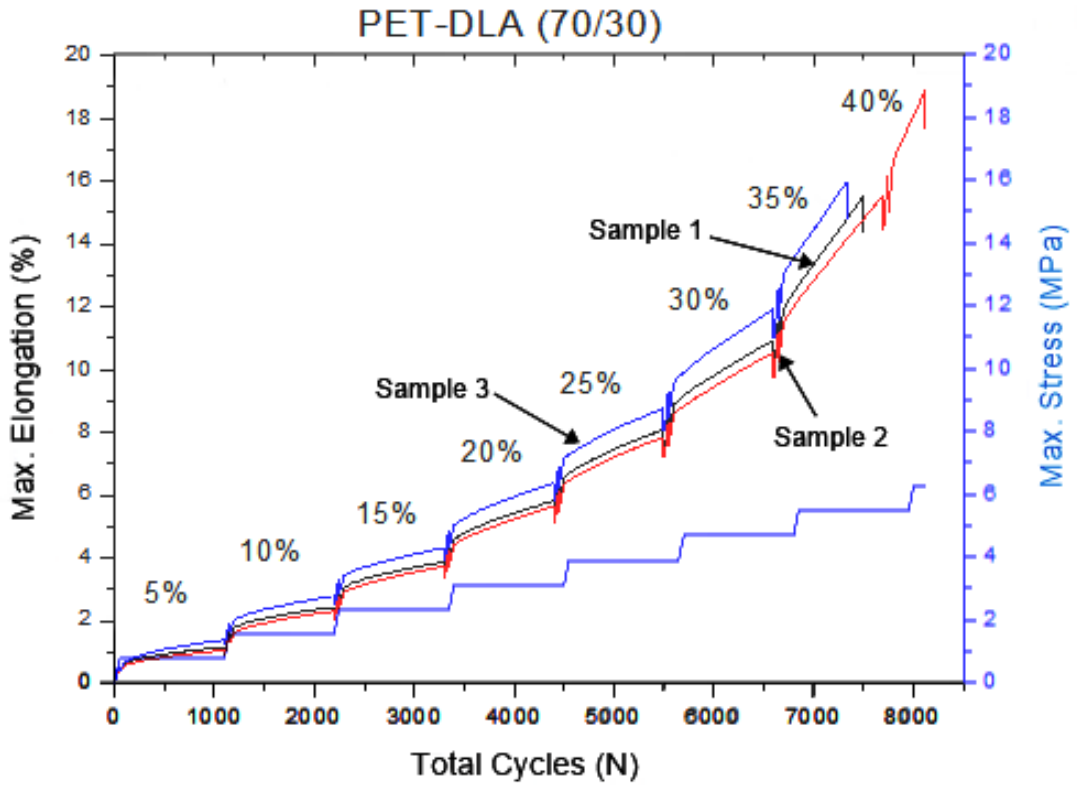

b) Pattern of change in the stress and strain

Fig. 3.1 a-b. Patterns of change in the stress, strain and dynamic modulus for PET-DLA (70/30) at room temperature T= 23ºC.

As shown in Fig. 3.1 a-b, for all samples, the dynamic modulus exponentially decreases with increasing load level and number of cycles (N). On the other hand, the maximum stress (σ_{max}) and maximum strain (max. elongation = ε_{max}) grow stagedly with increasing cycles number.

Although all samples reach the 7th step (35% of UTS) (Fig. 3.1.a), the dynamic modulus finishes to be stable in the 5th step (25% of UTS) because after that it starts to drop. There are also noise at the beginning of the 1st step (5% of UTS) and one of the main factors which cause that is the investigated area of the sample. It might has a bad surface, inclusions inside it, tiny cracks…interfering in the measures but, that noise can be ignored in this case because the specimens hadn't reached more than 5% of the dynamic modulus. There is a big error between samples no. 2 in comparison with 1 and 3. This might be due to the existence of tiny defects in sample no. 2, which have affected the results.

In Fig. 3.1.b, it can be seen that the material gradually creeps and it is stable until the 3rd step but it significantly increases at 25% of UTS or even at 20%.

The difference of dynamic modulus (E*) has been calculated for every step and as can be seen (Fig.3.2), each step has a vertical line. This line, surrounded by a dotted circle, is the point where the difference is higher than 5%, that means, the machine stops and the test finishes.

E*1 = dynamic modulus at the beginning of every step

E*2 = dynamic modulus at the end of every step

The samples no. 1 and 3 reach the 7th step (35%) and stop because the difference of dyn. modulus has been higher than 5%. Sample no. 2 reaches the last step and also stops because of the same reason.

Calculations are shown in Table 3.2 a-c, to know if I reached more than 5% of dyn. modulus.

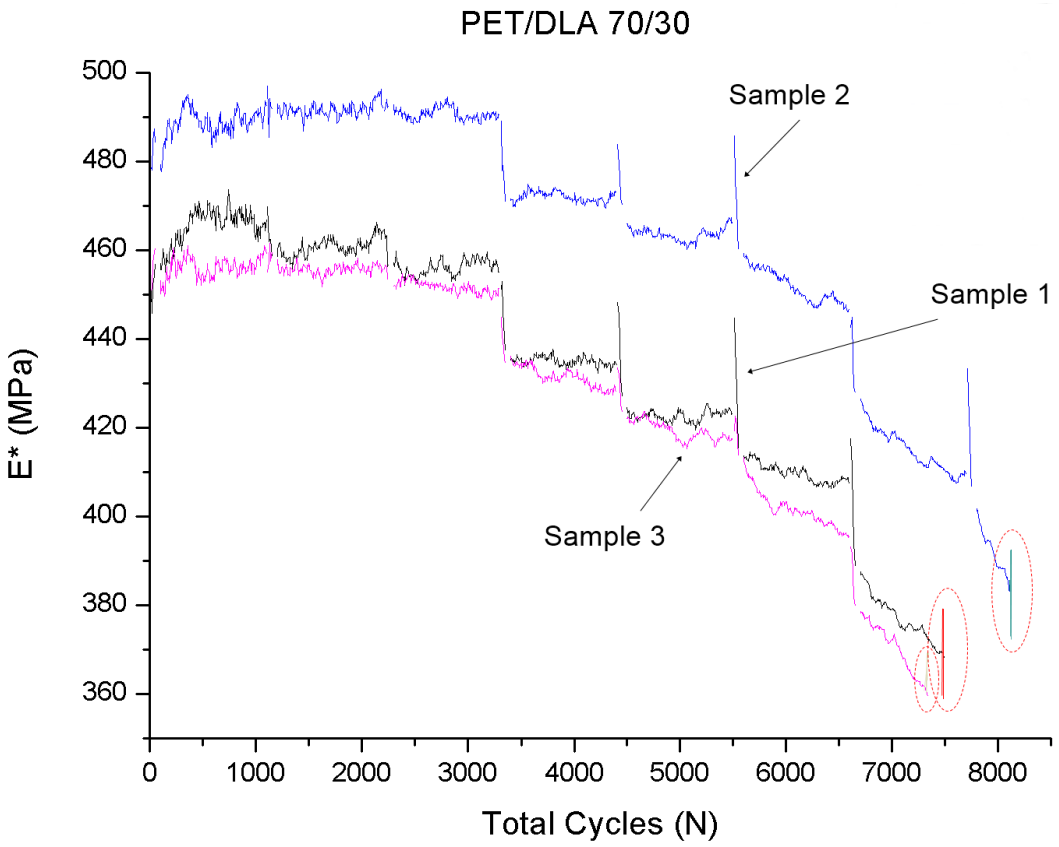

Fig. 3.2. Representation to see where the difference in E* is higher than 5%

Steps	E*1 (MPa)	E*2 (MPa)	Difference at the end of the step (%)
1 (5%)	455,56412	467,09159	2,467923964
2 (10%)	459,60502	464,83841	1,125850847
3 (15%)	457,26427	454,89988	-0,519761789
4 (20%)	435,31776	434,01227	-0,300795709
5 (25%)	424,62414	423,00771	-0,382127753
6 (30%)	413,7942	407,41884	-1,564816502
7 (35%)	387,56821	368,1218	-5,282601441

Table 3.2. a. Calculations for sample no. 1

Steps	E*1 (MPa)	E*2 (MPa)	Difference at the end of the step (%)
1 (5%)	479,22658	492,55194	2,705371172
2 (10%)	493,0036	491,95537	-0,213073541
3 (15%)	492,86296	490,69444	-0,441929011
4 (20%)	471,21967	473,36875	0,453997737
5 (25%)	466,01821	465,97197	-0,009923038
6 (30%)	459,34307	446,69095	-2,832409909
7 (35%)	426,35481	409,47476	-4,12236605
8 (40%)	401,72876	381,51156	-5,299237075

Table 3.2. b. Calculations for sample no. 2

Steps	E*1 (MPa)	E*2 (MPa)	Difference at the end of the step (%)
1 (5%)	453,14626	459,16623	1,311065781

2 (10%)	456,65123	456,03918	-0,134209828
3 (15%)	452,04052	451,53005	-0,113055218
4 (20%)	436,0294	427,9997	-1,876098304
5 (25%)	422,13934	417,73692	-1,053873278
6 (30%)	413,33826	395,43379	-4,527805705
7 (35%)	378,4584	359,50413	-5,27233814

Table 3.2. c. Calculations for sample no. 3

Related to PU (Bionate 55D) the protocol followed is quite different because the settings had to be changed after several measures. The reason is explained in following paragraphs.

The first settings that I used to set the loading protocol are shown in Table 3.3. The value of UTS was obtained from the static tensile test (54.4 MPa).

UTS		4Hz 5%	4Hz 10%	4Hz 15%	3Hz 20%	3Hz 25%	3Hz 30%	2HZ 35%	2HZ 40%	1HZ 45%	1HZ 50%
54,4	Load	2,72	5,44	8,16	10,88	13,60	16,32	19,04	21,76	24,48	27,20
	Amplitude	2,225	4,451	6,676	8,902	11,127	13,353	15,578	17,804	20,029	22,255
	Fmax	4,945	9,891	14,836	19,782	24,727	29,673	34,618	39,564	44,509	49,455
	Fmin	0,495	0,989	1,484	1,978	2,473	2,967	3,462	3,956	4,451	4,945

Table 3.3. Parameters calculated and introduced in the stepwise increasing load test (SILT). All values are in MPa.

The Fig.3.3 a-b shows the results which have been recorded.

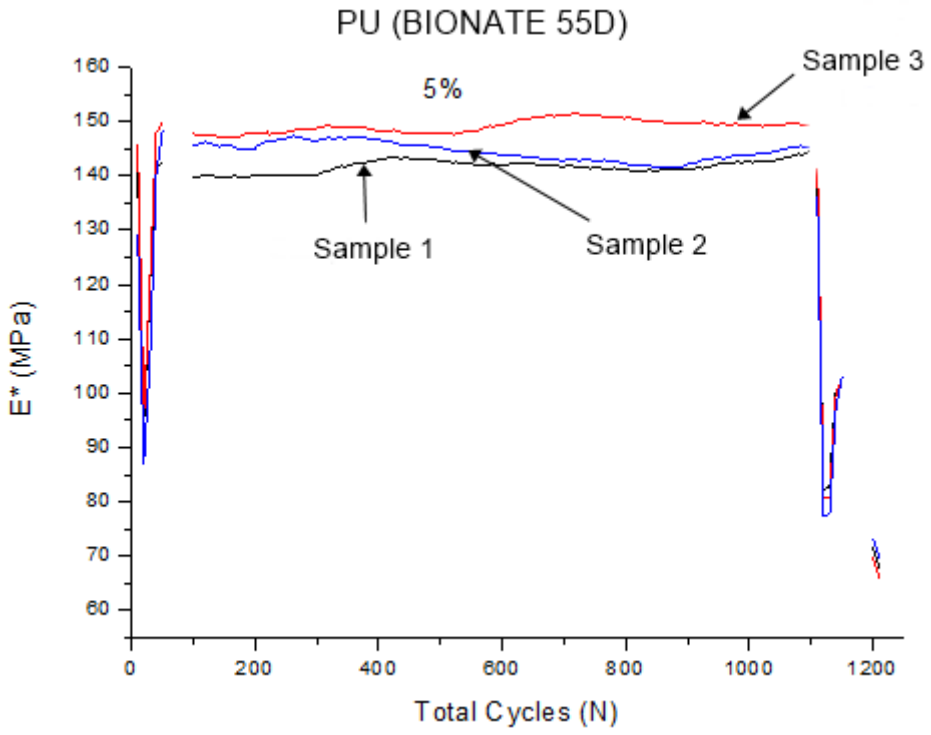

a) Pattern of change in dynamic modulus

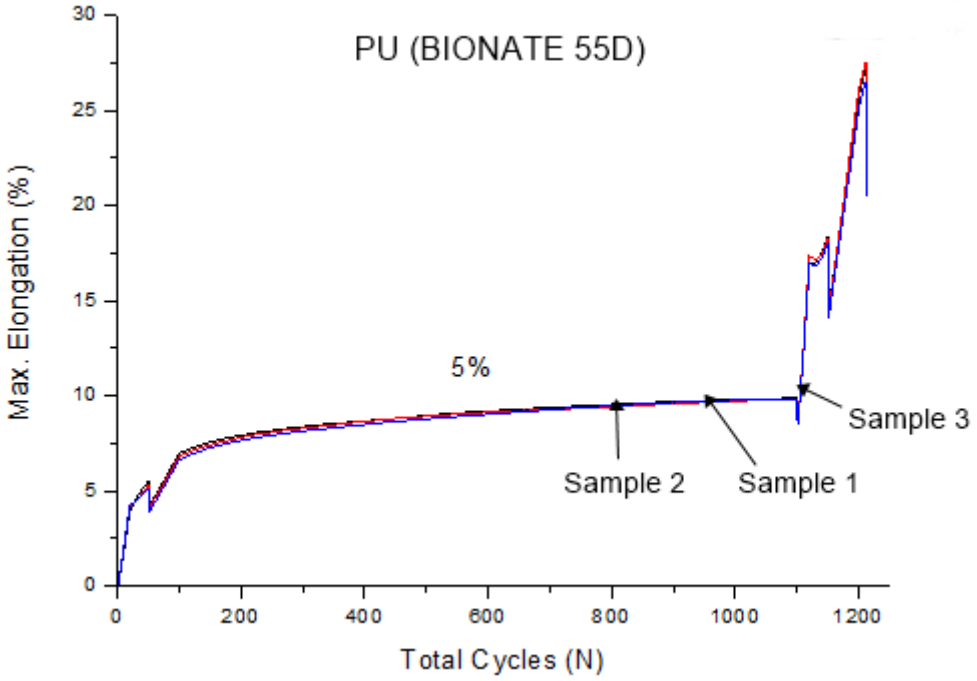

b) Pattern of change in strain

Fig. 3.3 a-b. Patterns of change in the strain and dynamic modulus for PU (Bionate 55D) at room temperature = 23ºC

The results demonstrate that the machine stopped because after the first step the specimens have been exceeded more than 5% of dynamic modulus. As it is not very useful to get information from only one step reached and compare with other materials, it was decided to change the loading protocol described at the beginning of the experiment to try to find if the material could reach more steps at lower loads. Sometimes, the second step is not achieved because in the first step there a lot of noise in the measurements and that cause the machine stops. That's why it should be a good idea to ensure that the reason of the stop is due to the noise or because the material can't reach more steps.

The changes in the protocol are shown in Table 3.4, where now the % of UTS are lower than before, thus, new loads are low too.

UTS		4Hz 2,5%	4Hz 5,0%	4Hz 7,5%	4Hz 10,0%	4Hz 12,5%
54,4	Load	1,36	2,72	4,08	5,44	6,80
	Amplitude	1,113	2,225	3,338	4,451	5,564
	Fmax	2,473	4,945	7,418	9,891	12,364
	Fmin	0,247	0,495	0,742	0,989	1,236

Table. 3.4 New parameters calculated and introduced in the stepwise increasing load test (SILT). All values are in MPa.

1st sample: the machine stops in the first step at 2.5% because it reaches more than 5% of dynamic modulus.

2nd sample: the machine also stops in the first step at 2.5% because it reaches more than 5% of dynamic modulus again.

As more results couldn't have been gotten for the rest of the steps because the machine stopped every time in the same step (at 2.5 5 of UTS), the option, which is able to find if the difference between cycles is higher than 5% of dynamic modulus, has been turned off to see how the sample would have behaved and then, the difference of dynamic modulus in every step have been calculated manually to see if the machine stopped in the first step because of the noise that can be seen in the following graphs (Fig.3.4 a-b).

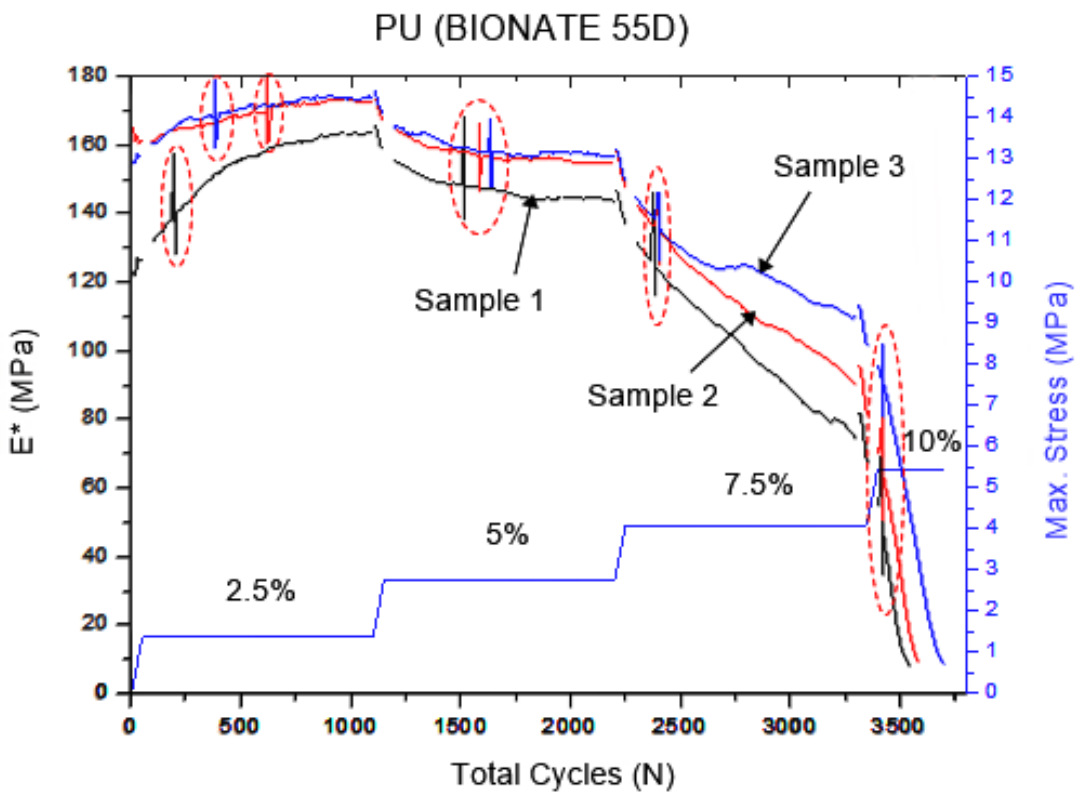

a) Pattern of change in the stress and dynamic modulus

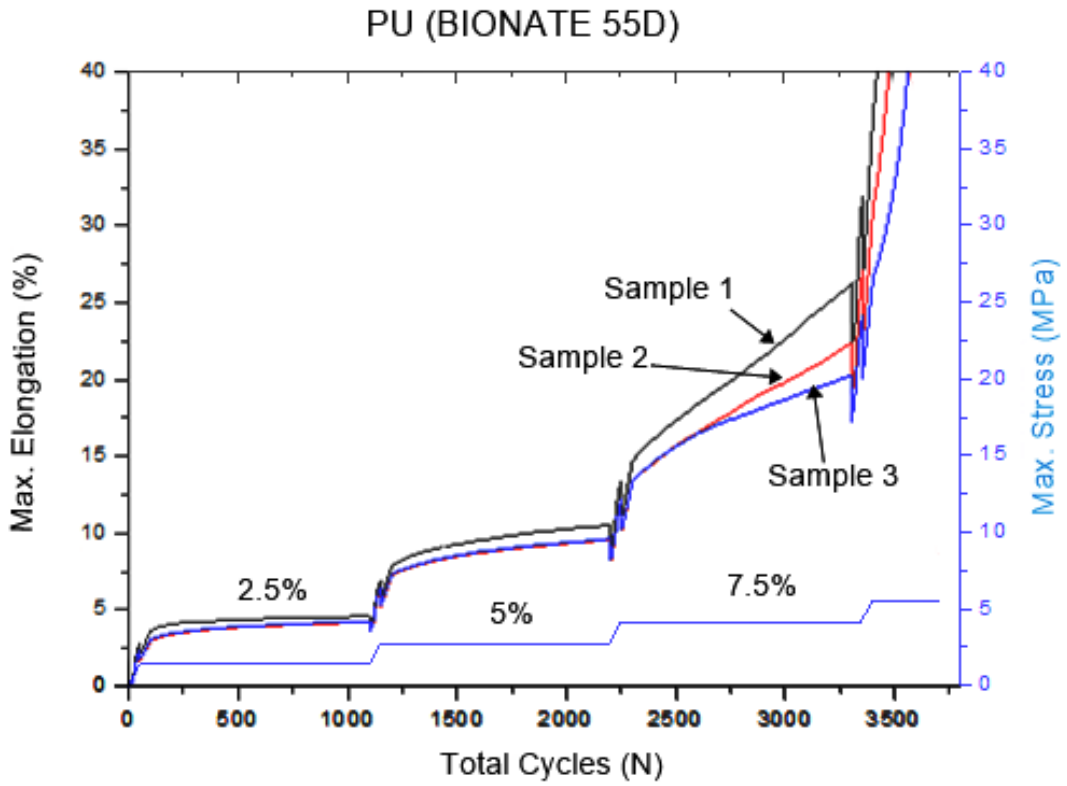

b) Pattern of change in the stress and strain

Fig. 3.4 a-b. Patterns of change in the stress, strain and dynamic modulus for PU (Bionate 55D) at room temperature = 23ºC

As shown in Fig. 3.4 a-b, for all samples, the dynamic modulus exponentially decreases again with increasing load level and number of cycles (N). However, the maximum stress (σ_{max}) and maximum strain (max. elongation = ε_{max}) grow stagedly with increasing cycles number.

Comparing Fig.3.3 a. and 3.4 a, it is very clear that, although all samples reach the 4th step (10% of UTS = 5.44 MPa) in Fig. 3.4.a, the dynamic modulus finishes to be stable in the 2nd step (5% of UTS = 2.72 MPa in Fig. 3.4 a) because after that it starts to drop dramatically. There are also noise at the beginning of the 1st step (2.5% of UTS in Fig.3.4 a) because the beginning should simulate a horizontal line, which would mean it would be a stable process. It can be ensured that the proper step is that one which reach 5% of UTS, regardless of the protocol followed because in both settings the most stable step is at 5% of UTS = 2.72 MPa. It should be noted that in Fig. 3.4 a, the specimens have reached more than 5% of dynamic modulus in the most stable step while in the Fig.3.3 a. haven't, as it has been calculated. This fact can be produced due to the noise in the first step (2.5% of UTS) may influence the second one, altering the final results. Because of the weak reproducibility of samples, it could be another reason for that fact.

Related to the maximum elongation, the Fig.3.4 b reveals that the material begins creeping slowly in the 2nd step (at 5% of UTS) but when it reaches the 3rd

one (7.5% of UTS) it creeps too much. Consequently, the step at 5% of UTS is still the most suitable for the investigation.

The difference of dynamic modulus (E*) has been calculated again for every step and as can be seen (Fig.3.4 a), each step has the same vertical line as before.

E*1 = dynamic modulus at the beginning of every step

E*2 = dynamic modulus at the end of every step

Steps	E*1 (MPa)	E*2 (MPa)	Difference at the end of the step (%)
1 (2,5%)	131,63496	163,51446	19,49644327
2 (5%)	155,66934	143,67232	-8,350271
3 (7,5%)	131,62607	74,1589	-77,49193081
4 (10%)	56,06407	8,13417	-589,2414393

Table 3.5. a. Calculations for sample no. 1

Steps	E*1 (MPa)	E*2 (MPa)	Difference at the end of the step (%)
1 (2,5%)	161,22067	172,55207	6,566943822
2 (5%)	164,46108	154,71809	-6,297256871
3 (7,5%)	142,6719	90,24051	-58,10183692
4 (10%)	71,4889	9,21883	-675,4663905

Table 3.5. b. Calculations for sample no. 2

Steps	E*1 (MPa)	E*2 (MPa)	Difference at the end of the step (%)
1 (2,5%)	160,16851	173,50187	7,684848131
2 (5%)	165,71286	156,31089	-6,014911709
3 (7,5%)	144,61833	109,76702	-31,75025576
4 (10%)	95,59264	8,4214	-1035,11541

Table 3.5. c. Calculations for sample no. 3

Focussing the attention of Tables 3.2 and 3.5 it has been seen that some differences at the end of the steps are negative in % because, as I mentioned before, the dynamic modulus exponentially decreases with increasing load level and number of cycles (N), since the end of one step is lower than the beginning. If the absolute change of the stiffness within a single stress level drops up to 5%, then the load value, σ_L (Table 3.6) assigned to this step level can be used for another experiment, such as long term dynamic loading (referred to as “dynamic creep”) of polymers during a single load testing (SLT), which is outlined in next section.

The load value for PU is very clear because it can only reach that step without dropping up to 5% in its stiffness but in the case of PET-DLA (70/30), the choice is not so easy. 3.12 MPa has been chosen as the load value for SLT because the last stable step for that material was the 5th one at 25% of UTS = 3.90 MPa and due to the weak reproducibility of the specimens it is more convenient to choose a lower level to achieve as many results as possible.

Material	σ_L (MPa)
PET-DLA (70/30)	3.12

PU (Bionate 55D)	2.72

Table 3.6. Load values, σ_L, derived from SILT test corresponding to the dynamic modulus drop up to 5% within a single load level

The strain- and stress-signal has been recorded in order to receive the hysteresis loop for both materials (Fig.3.5 a-b). The damping of the materials have induced a phase-shifting between the two signals.

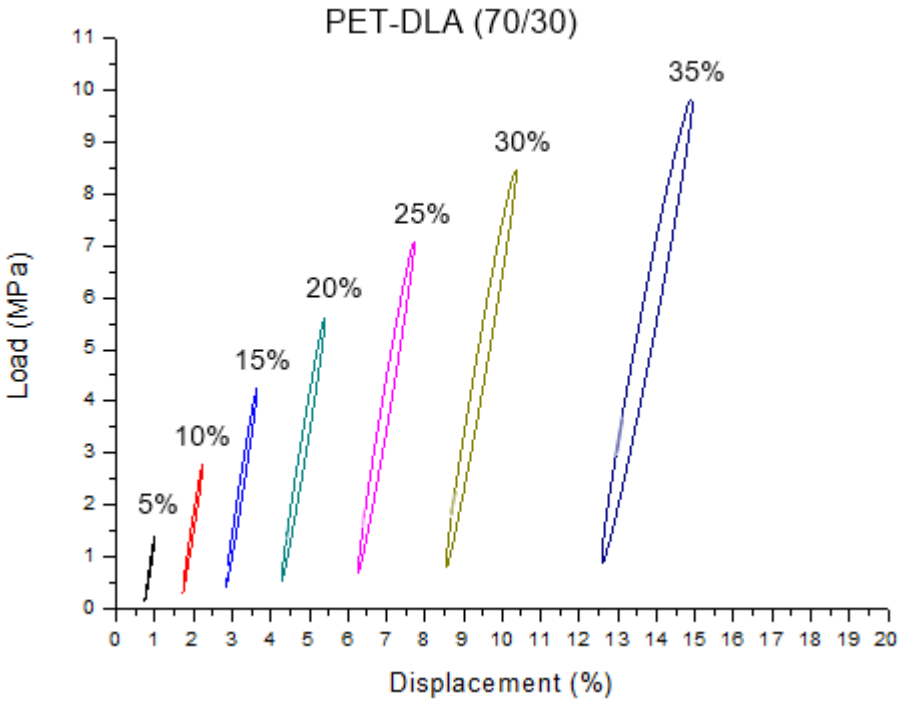

a) Hysteresis loops for PET-DLA (70/30)

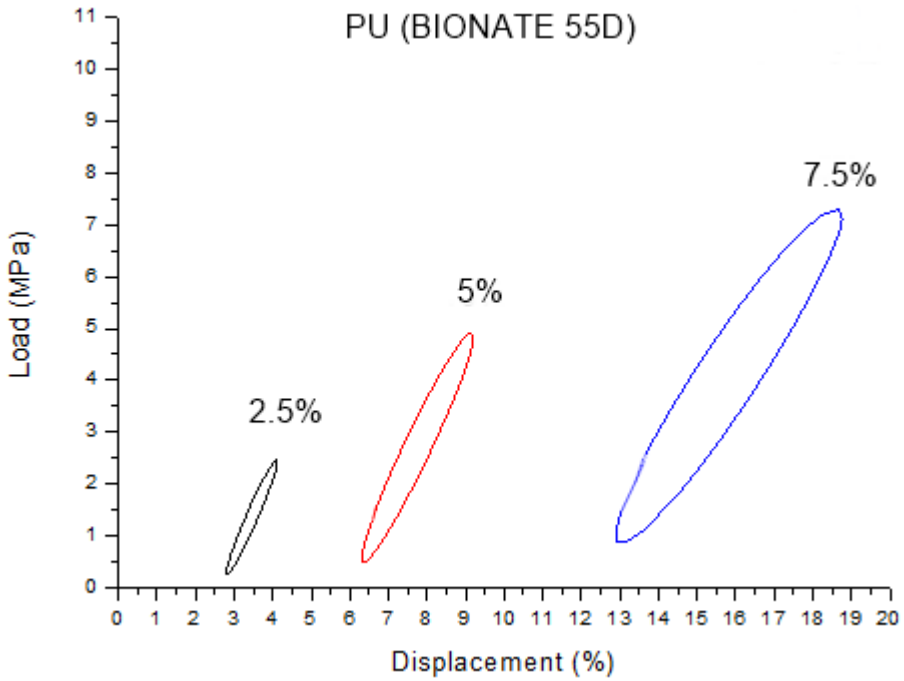

b) Hysteresis loops for PU

Fig. 3.5 a-b. Representative hysteresis loop for each load level (numbers of loops refers to percent of UTS) tested at room temperature of 23 ºC.

Both graphs are in the same scale to be compared between them and they were made with an average of all samples. As is shown in Fig.3.5 a-b, when subjected to strain-controlled cyclic loading, the stress-strain response of a material changes with the number of applied cycles. The material behaviour is linear viscoelastic because the strain has a phase-shifting to the stress, which means the relationship between stress and strain depends on time and thus, the hysteresis loops show an ellipse. It is said to cyclically harden because the maximum stress increases with each successive cycle. Cyclic hardening indicates increased resistance to deformation.

Comparing the materials, it can be observed, in Fig.3.5 a, a lower displacement and a larger area of the hysteresis loops than in Fig.3.5 b. That indicates the PET-DLA (70/30) has a higher hard segment content than PU (Bionate 55D), that means higher crystallinity and higher stiffness. The area of the hysteresis loop increases with incrementing load level for each polymer and that is due to the materials are creeping.

Although both materials reached steps at 40% and 10% of UTS, respectively, they has been overlooked because they weren't completed and the hysteresis loops couldn't have been drawn.

In view of the results achieved, the PET-DLA (70/30) multiblock copolymer showcases good properties to be used in the biomedical applications, especially for heart devices, because it can withstand high loads without breaking during cyclic loads due to his stiffness, given by the hard segments, and his elasticity, given by the soft segments which let the material elongate in a huge range of values.

3.2 Dynamic creep of polymers during single load test (SLT)

There is a great importance of knowing how the creep properties will be in elastomers which are expected to stay with their steady structure while they are under long term loading. Creep may be defined as a time-dependent deformation (length change) at certain temperature and constant stress (Fig. 3.6) [72]. Atom movements are involved during creep deformation. It occurs by grain-boundary sliding, that is, adjacent crystals move as a unit relative to each other (some are still relaxed) blending elastic and plastic region. This stage is called immediate elastic deformation region, where the strain speed is relatively high. Then a stable rate of creep starts to be steady.

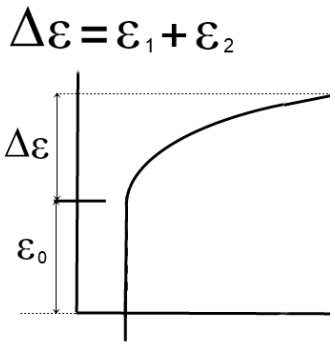

Fig. 3.6. Representation of a creep curve. ε_0 = the immediate elastic deformation (recoverable); ε_1 = the delayed elastic deformation (recoverable); ε_2 = material flow (unrecoverable); $\Delta\varepsilon$ = absolute creep

In fatigue test, a dynamic loading is applied as a sinusoidal force pattern. When strain increases, it is referred to as “dynamic creep” and for its assessment, certain stresses are applied, which has been obtained from the SILT as it was mentioned in previous section. These stresses was shown before in Table 3.6 and the load values were selected in which no damage of materials had been expected.

Returning to the results, Fig. 3.7 shows the dynamic creep curve of PU (Bionate 55D) during constant loading of 2.72 MPa (single load test, SLT) for a period of 1000000 cycles in air at room temperature T=23ºC and a frequency of f=1.33 Hz and additionally the dynamic creep curve of PET-DLA (70/30) during a constant loading of 3.12 MPa in the same conditions.

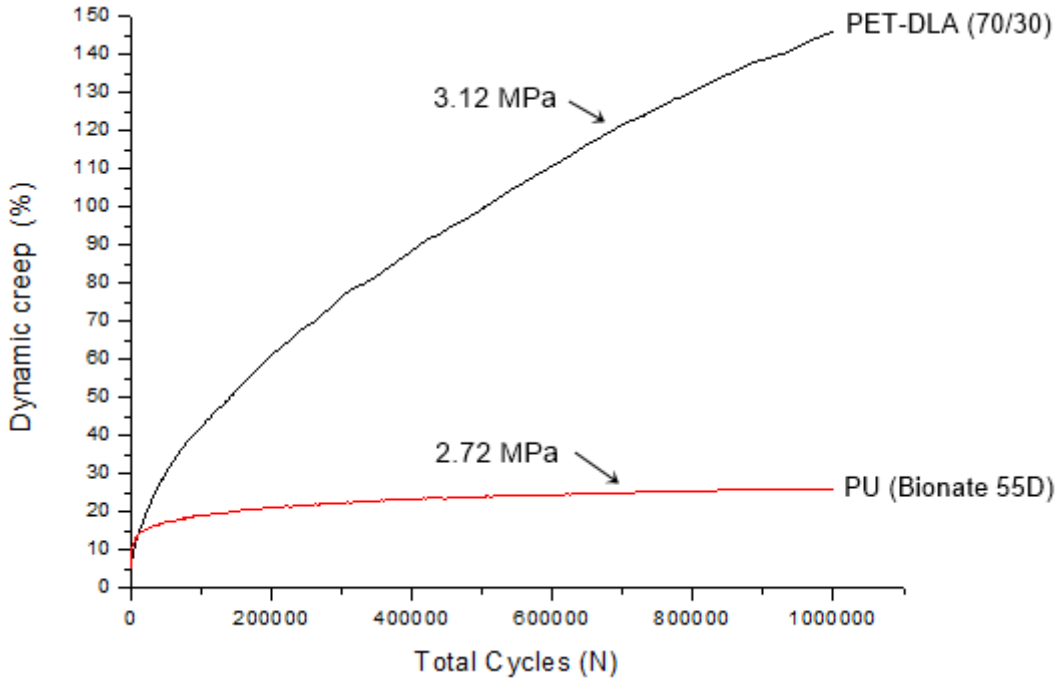

Fig. 3.7. Dynamic creep (ε_d) curves for PU (Bionate 55D) and PET-DLA (70/30) samples (load values (σ_L) for each polymer are indicated in the picture). Test frequency: 1.33 Hz, room temperature T=23ºC and number of cycles (N) = 1000000.

Absolute creep ($\Delta\varepsilon$) values for both materials are shown in Fig. 3.8.

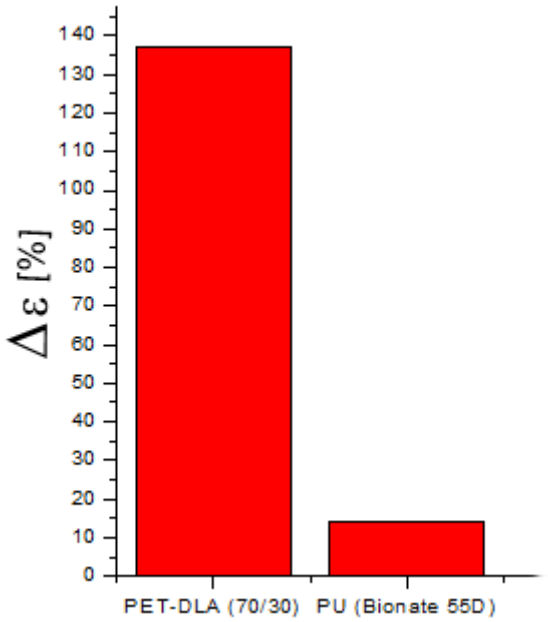

Fig. 3.8. Absolute creep (Δε) values for both polymers from the previous conditions

In Fig. 3.7., it is shown that for the softer polymer (PU), the immediate elastic deformation is larger than in the case of stiffer polymer (PET-DLA (70/30)). PU (Bionate 55D) possess a weak creep but the multiblock copolymer has a greater creep compliance and a greater rate of change in this characteristics with time. The difference between both polymers in the absolute creep (Δε), which was formulated in Fig. 3.6, is quite considerably. That can be corroborated by the Fig. 3.7 because it's seen that PU (Bionate 55D) creeps at the beginning but then it becomes stable. On the other hand, PET-DLA (70/30) doesn't creep instantaneously as PU does, but it creeps during all experiment without becoming stable.

For each polymer, the changes in the area and slope of hysteresis loop, taken at different cycles (Fig. 3.9), demonstrate that the influence of hard/soft segment concentration is not negligible.

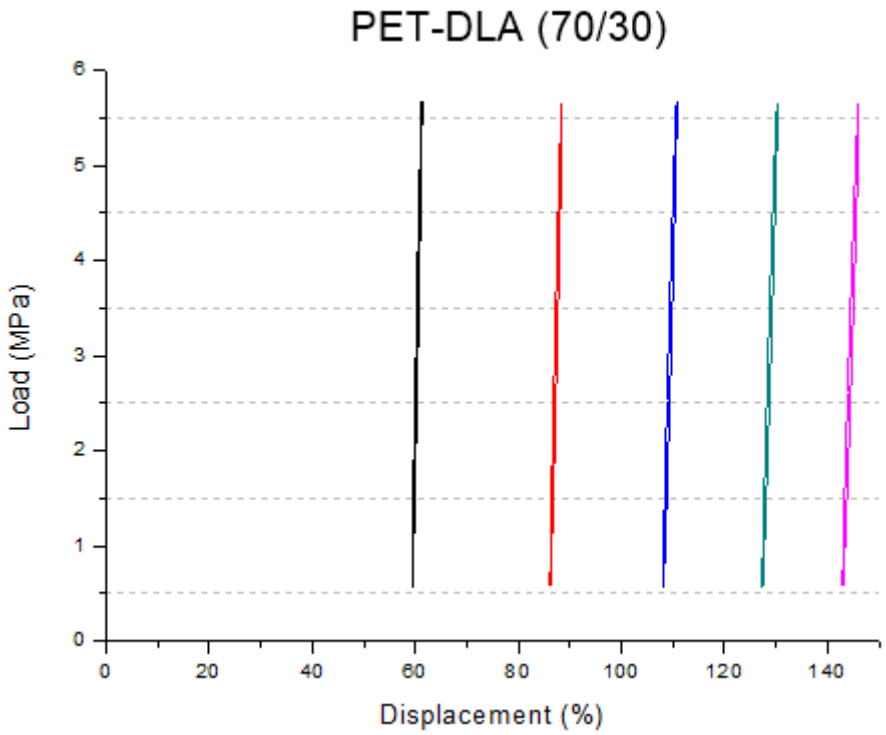
PET-DLA (70/30)
Load (MPa)
Displacement (%)
0
1
2
3
4
5
6
0
20
40
60
80
100
120
140

a)

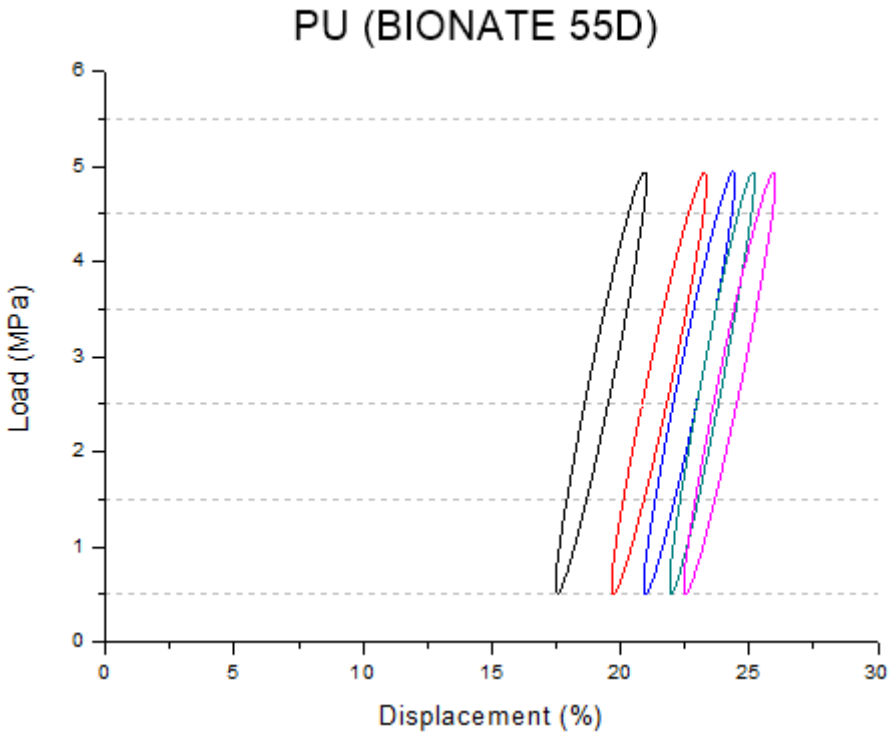
PU (BIONATE 55D)
Load (MPa)
Displacement (%)
0
1
2
3
4
5
6
0
5
10
15
20
25
30

b)

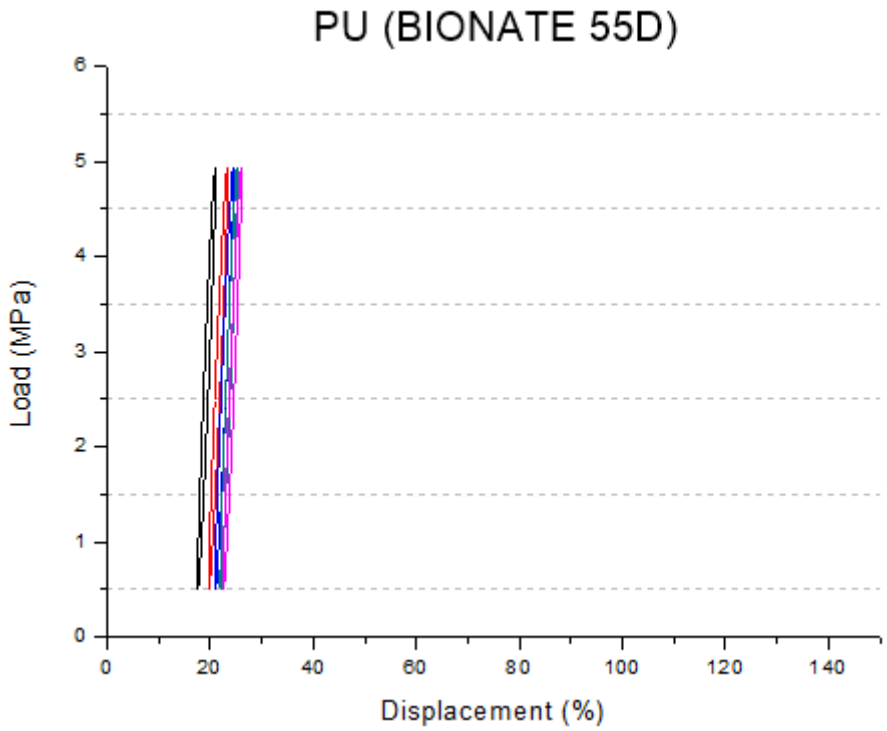

c)

Fig. 3.9. a) Hysteresis loops of PET-DLA (70/30); b) Hysteresis loops of PU (Bionate 55D); c) Hysteresis loops of PU (Bionate 55D) but drawn on the same scale as Fig. 3.9.a. All hysteresis loops are taken at the cycles no. 200000, 400000, 600000, 800000 and 1000000.

The Fig. 3.9.c. was drawn to compare it with the Fig. 3.9.a. because they have to be on the same scale. In Fig. 3.9.b. it can be seen that the polymer shows a very large area which can give an evidence on a large dissipation (high damping) but when both materials are drawn on the same scale it is shown that PU (Bionate 55D) has lower displacement and less area than PET-DLA (70/30). That's why PET-DLA (70/30) has a higher value of damping and it can be verified in the Fig. 3.7. where it is shown that this multiblock copolymer creeps during all test and doesn't become steady. The shift between loops provides insight of the creeping because it is related to the displacement. In Fig. 3.9.b. the first loop at cycle no. 200000 has a quite bit shift from the rest of loops due to the immediate elastic deformation has been steeper than in the case of PET-DLA (70/30). Thus, it creeps immediately in first cycles but then, when it turns into stable way the hysteresis loops show a less shift between them until the last two loops are almost the same.

Creep resistance is not only influenced by stress and duration, but also important parameters like temperature or environment should be investigated. To carry out the study of the dynamic creep of the studied materials in the presence of a liquid environment and at elevated temperature, a special environmental chamber has been used (Fig. 3.10).

To simulate the inside of the body, the samples have been immersed in simulated body fluid (SBF) at constant temperature of 23 and 37ºC during certain

defined cycles. The specimens has been investigated in 3 different situations: in air at 23ºC, immersed in SBF at 23ºC and in the presence of SBF but at 37ºC (Fig. 3.11). Previous conditions let know if the investigated materials are influenced by these parameters.

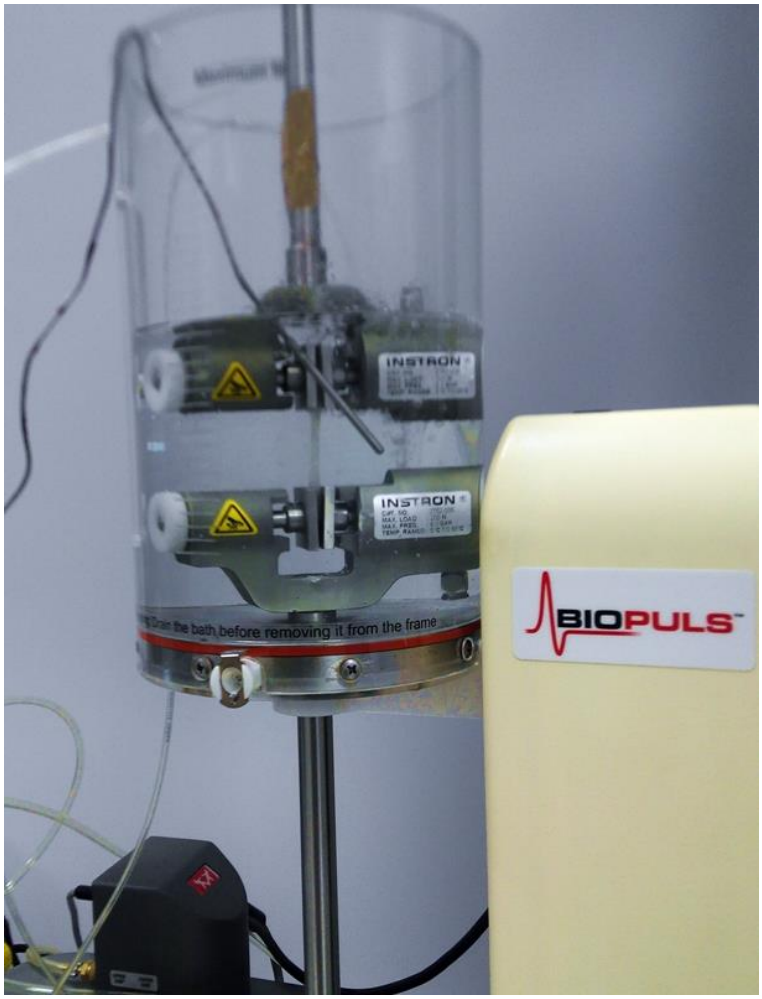

Fig. 3.10. The environmental chamber used in fatigue test with SBF

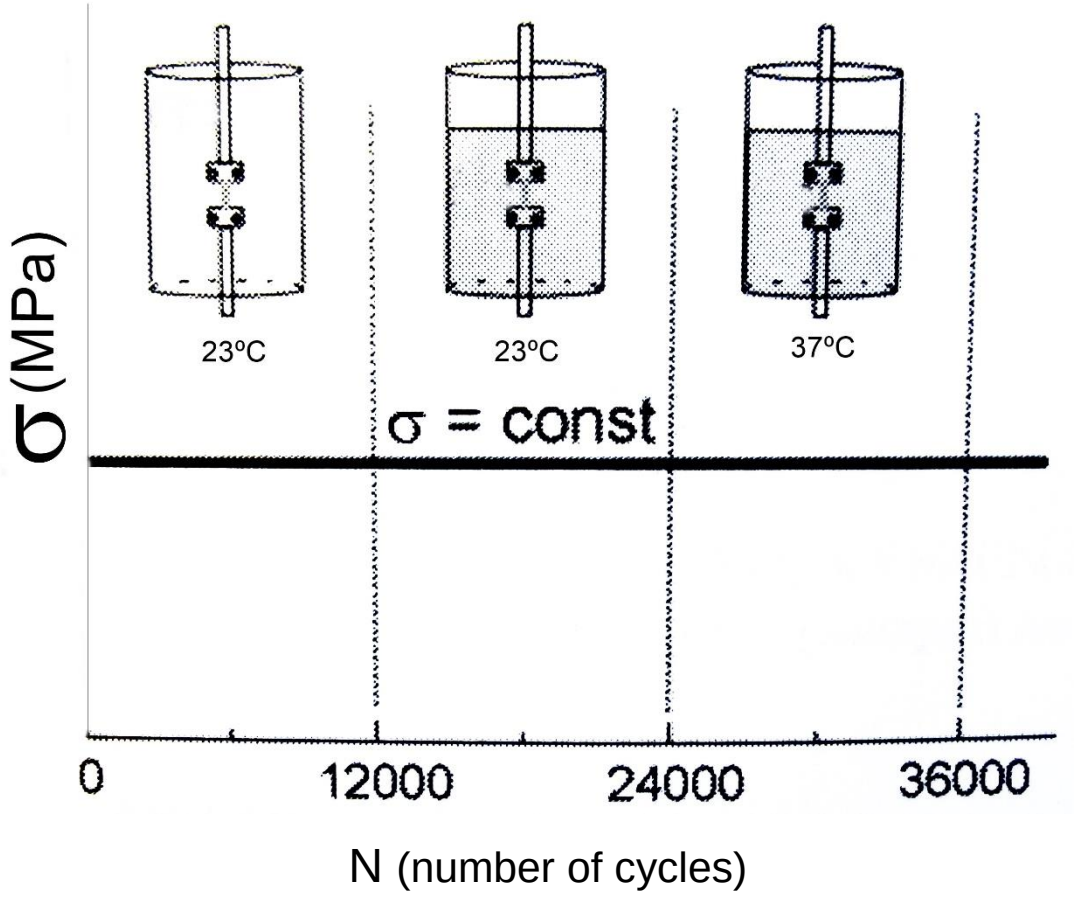

Fig. 3.11. Representation of different investigated situations in the environmental chamber

Before performing fatigue tests (SILT and SLT) in SBF, it is needed to measure again a new value of UTS for both materials at 37ºC, because as it was described during this project, behaviour of elastomers depends on the temperature and they probably change their mechanical properties. The temperature has to be below 40ºC because from this value materials begin to be very sensitive.

A new static tensile test was performed but now the temperature is 37ºC. It was reached using a specific heat chamber (Fig. 3.12.) which let stretch samples within it. Specimens were preheated at 37ºC during at least 35 min to stabilise their temperature before testing. The method used is the same as in previous static tensile test.

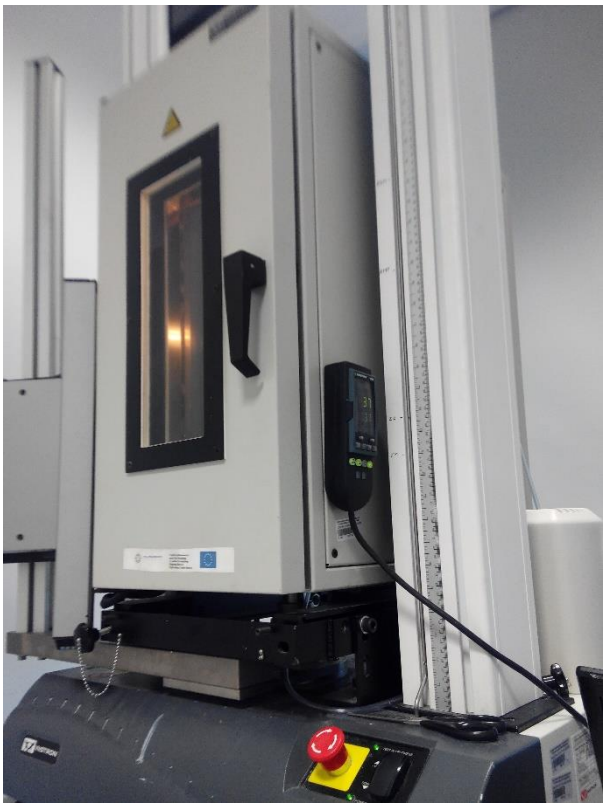

Fig. 3.12. Special heat chamber to heat all samples before and during the static tensile test at 37ºC

The results obtained for PET-DLA (70/30) are shown in Fig. 3.13. and Table 3.7.

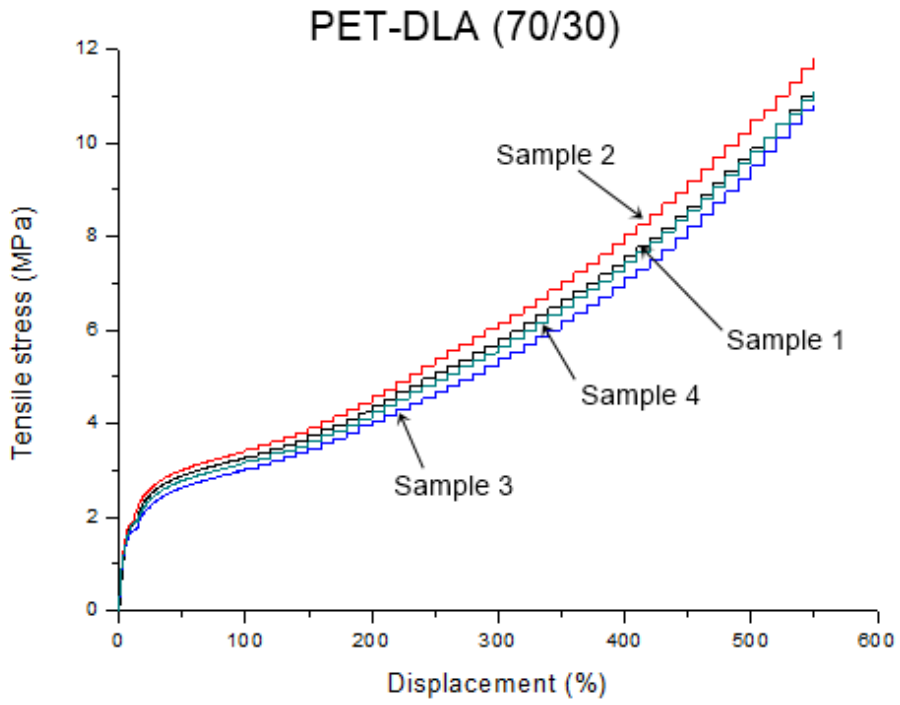

a)

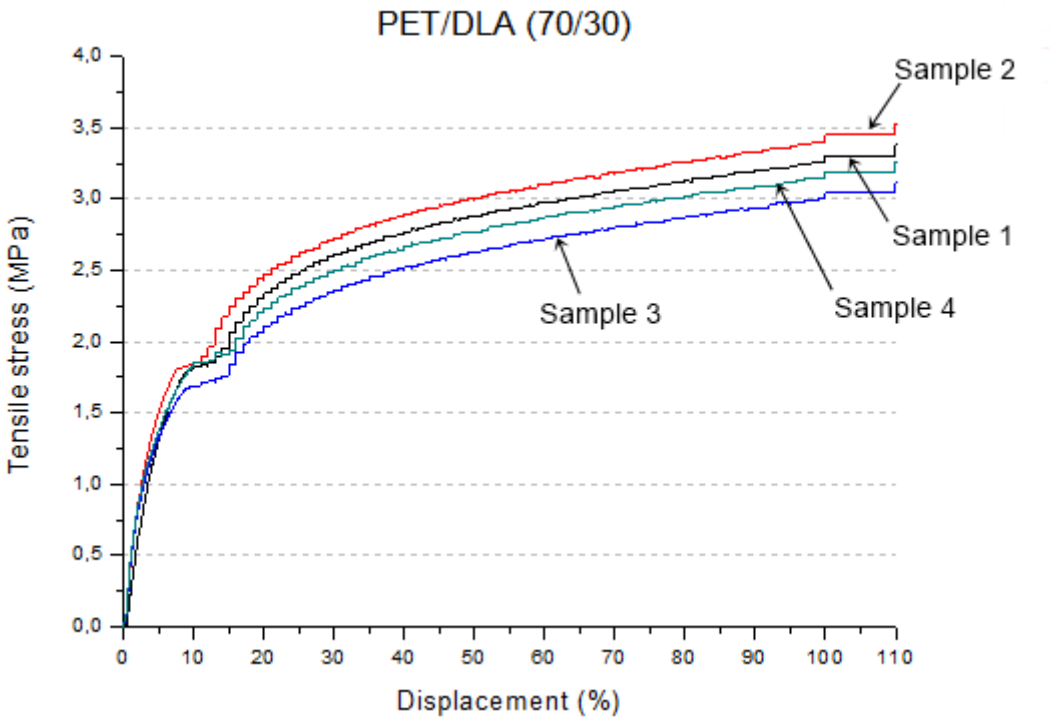

b)

Fig. 3.13. a) Stress-strain curves for PET-DLA (70/30) (measurements performed with a crosshead speed of 10 mm/min) at 37ºC. b) Zoom of the stress-strain curves for PET-DLA (70/30) (measurements performed with a crosshead speed of 10 mm/min) at 37ºC.

If Fig. 3.13 b) is compared to the Fig. 2.2 (static tensile test at 23ºC) there is a significant difference in the shape of the curves. At 37ºC, the samples don't break because they start to creep until high values of tensile stress. The experiments were stopped at 550% of elongation because samples could have continued stretching but in that case the clamps of the machine had been barged into the heat chamber.

The new UTS (3.23 MPa) which has been chosen in that experiment was the value of Young Modulus at 100 % of elongation (Table 3.7). The contrast of tensile stress values are very meaningful because at 37ºC they are almost one fifth of the first static tensile test at 24ºC. Thus, the temperature is a crucial factor to be determined due to its big influence in elastomers.

The next table (Table 3.7) shows the most important data which are in the graph:

Sample	Young Modulus (MPa)	Tensile strength (MPa)
1	7.5	13
2	11	12
3	7.2	11

4	8.2	11
Average	**8.475**	**11.75**

Sample	Young Modulus at 0,05 % - 0,3 % of elongation) (MPa)	Young Modulus at 0,25 % - 1 % of elongation) (MPa)	Young Modulus (at 100 % of elongation) (MPa)	Young Modulus (at 50 % of elongation) (MPa)
1	13	190	3,3	5,7
2	31	110	3,4	6,0
3	27	140	3,0	5,3
4	32	140	3,2	5,5
Average	**25.75**	**120**	**3.225**	**5.625**

Table 3.7. Values which have been collected from the static tensile test for PET-DLA (70/30) at 37ºC

Additionally, the results obtained for PU (Bionate 55D) are shown in Fig. 3.14. and Table 3.8.

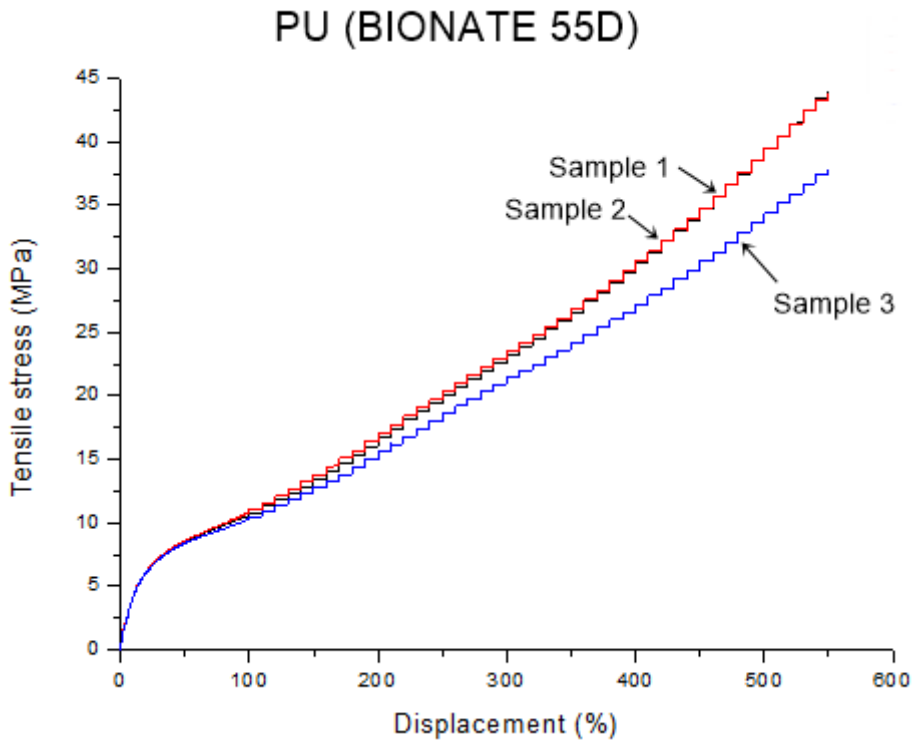

a)

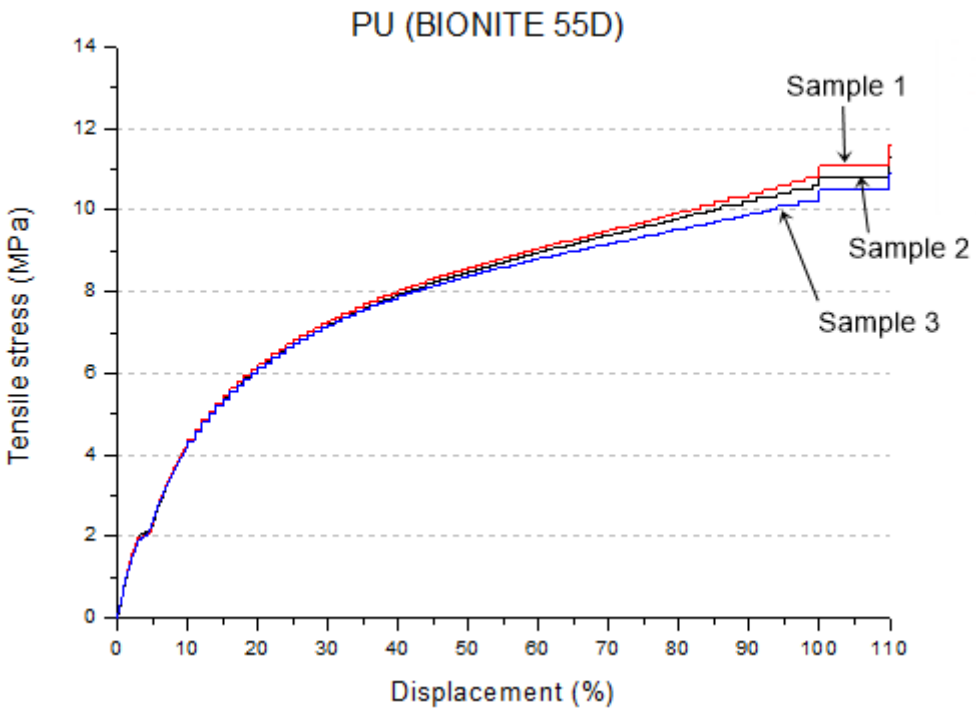

b)

Fig. 3.14. a) Stress-strain curves for PU (Bionate 55D) (measurements performed with a crosshead speed of 10 mm/min) at 37ºC. b) Zoom of the stress-strain curves for PU (Bionate 55D) (measurements performed with a crosshead speed of 10 mm/min) at 37ºC.

In that case, the shape of the Fig. 3.14 a) is very similar to Fig. 2.3, but like in the same situation as PET-DLA (70/30) samples, the material doesn't break. The new value of UTS were chosen from Table 3.8 as the Young Modulus at 100% of elongation (10.67 MPa). If this value is compared with the last one at 24ºC (54.6 MPa), it is seen that at 37ºC is the fifth part.

The following table (Table 3.8) shows the most important data which are in the graph:

Sample	Young Modulus (MPa)	Tensile strength (MPa)
1	15	44
2	16	44
3	22	38
Average	**17.667**	**42**

Sample	Young Modulus at 0,05 % - 0,3 % of elongation) (MPa)	Young Modulus at 0,25 % - 1 % of elongation) (MPa)	Young Modulus (at 100 % of elongation) (MPa)	Young Modulus (at 50 % of elongation) (MPa)
1	79	110	11	17
2	83	120	11	17
3	81	120	10	17
Average	**81**	**116.667**	**10.667**	**17**

Table 3.8. Values which have been collected from the static tensile test for PU (Bionate 55D) at 37ºC

After these static tests, the fatigue ones were performed. Two samples of each material were tested at 24ºC in air and SBF and consecutively at 37ºC in SBF.

The results in SILT related to PU (Bionate 55D) have been the following:

The settings that it was used to set the loading protocol at room temperature are the same as Table 3.4 because the temperature is going to be 23ºC but samples are inside SBF. The value of UTS has been 54.4 MPa.

The Fig.3.15 a-b shows the results which have been recorded.

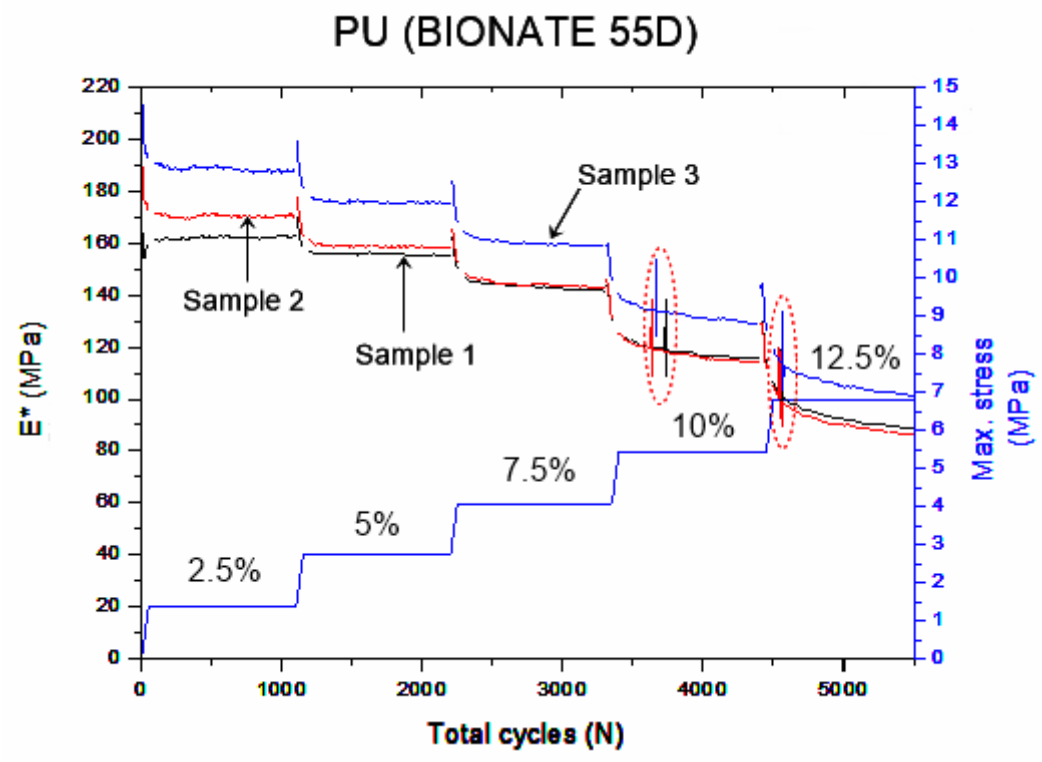

a)

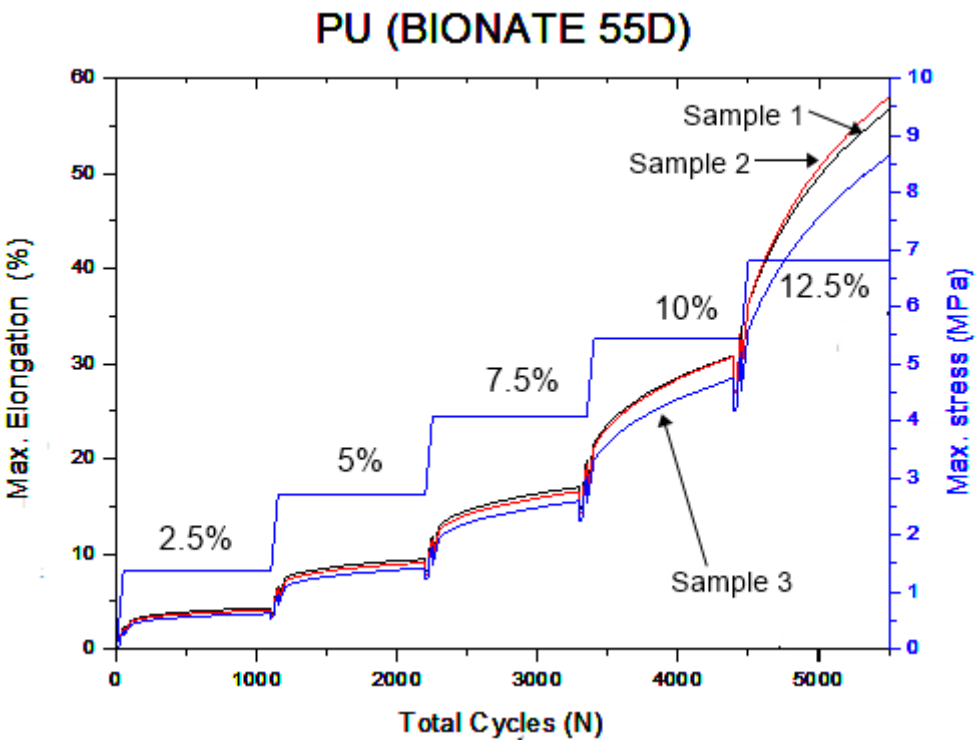

b)

Fig. 3.15. a) Pattern of change in the stress and dynamic modulus. b) Pattern of change in the stress and strain. Test performed at room temperature T=23ºC

As it was explained before, the difference of dynamic modulus in every step have been calculated manually to see if the machine stopped in the first step because of the noise. The Fig. 3.15. a) shows that the difference is bigger than 5% of dynamic modulus in the 4th step (10% of UTS = 5.44 MPa). That means that the load value from the 3rd step (4.08 MPa) will be used for SLT. In fact, in Fig. 3.15. b) it is observable that the 4th step creeps very quickly. However, although the 3rd also creeps, it is more stable than the following ones.

The results for SLT will be shown later to see the differences between conditions.

The settings that it was used to set the loading protocol for SILT at 37ºC are shown in Table 3.9 because the temperature has changed the value of UTS which is now 10.67 MPa.

UTS		4Hz 2,50%	4Hz 5,00%	4Hz 7,50%	4Hz 10,00%	4Hz 12,50%	4Hz 15,00%	4HZ 17,50%	3HZ 20,00%	3HZ 22,50%	3HZ 25,00%
10,67	Load	0,27	0,53	0,80	1,07	1,33	1,60	1,87	2,13	2,40	2,67
	Amplitude	0,218	0,437	0,655	0,873	1,091	1,310	1,528	1,746	1,964	2,183
	Fmax	0,485	0,970	1,455	1,940	2,425	2,910	3,395	3,880	4,365	4,850
	Fmin	0,048	0,097	0,145	0,194	0,242	0,291	0,339	0,388	0,436	0,485

Table 3.9. Parameters calculated and introduced in the stepwise increasing load test (SILT). All values are in MPa.

In that experiment the option to detect the difference of dynamic modulus was turned on and the machine stopped when that value was higher than 5%. Due to the lack of specimens, instead of 3 only 2 samples were investigated. Fig. 3.16 a-b represents the results obtained.

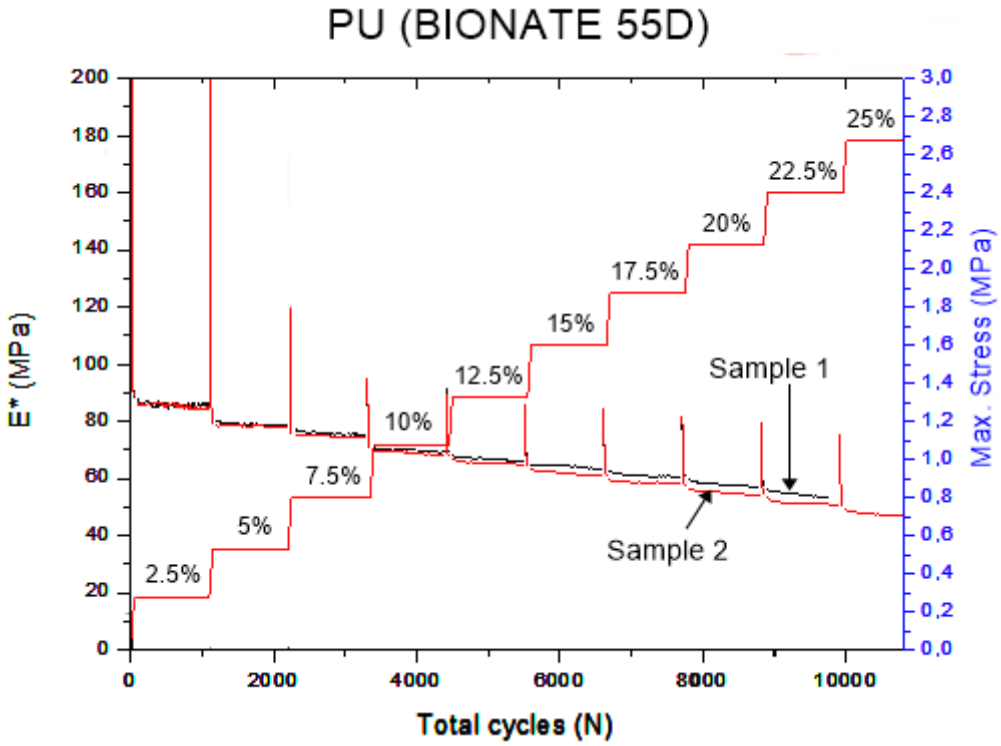

a)

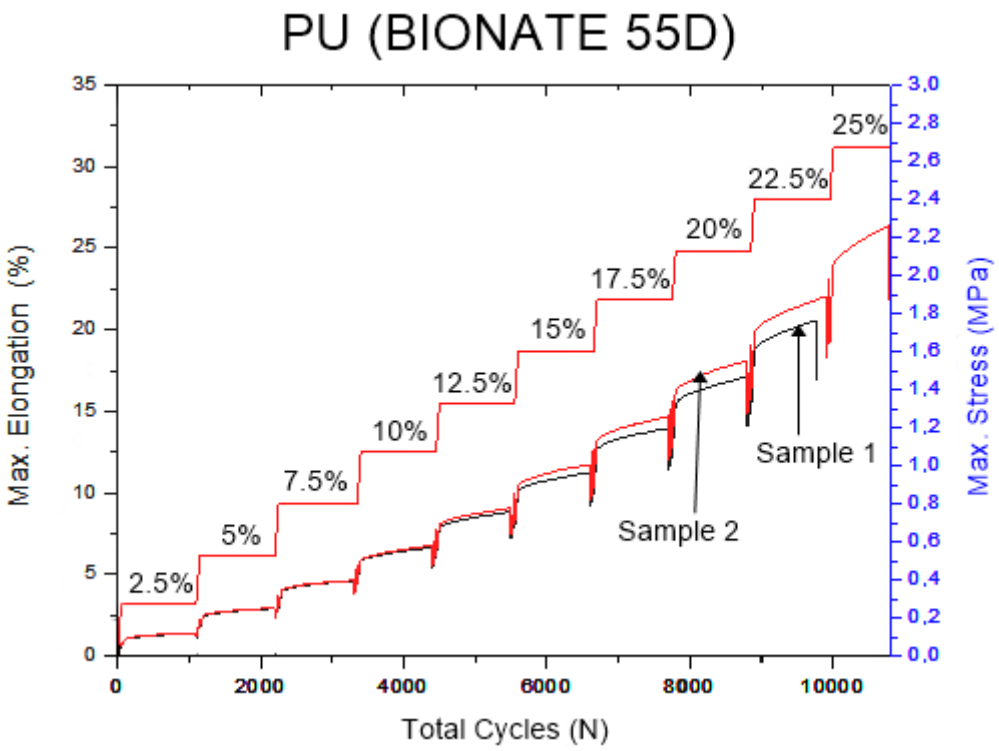

b)

Fig. 3.16. a) Pattern of change in the stress and dynamic modulus. b) Pattern of change in the stress and strain. Test performed at temperature T=37ºC.

The Fig. 3.16. a) shows one sample finished at the last step at 25% of UTS (2.67 MPa) but the another one did it at 22.5% of UTS (2.40 MPa). For that reason, the value of next SLT will be taken from the step before the one that sample 1 finished, it means it will be 2.13 MPa (at 20% of UTS).

The sample no. 1 could have finished at the same step that the second specimen but maybe the investigated area was worse and it is better to choose the 8th step to be sure that both samples reached it without any problem.

The load values in SLT for the 3 conditions are:

Condition for PU (Bionate 55D)	σ_L (MPa)
23ºC (air)	2.72
23ºC (SBF)	4.08
37ºC (SBF)	2.13

Table 3.10. Load values (σ_L [MPa]) used in SLT for PU (Bionate 55D)

Fig. 3.17. shows the results obtained in both experiments. There is a quite difference between samples, probably produced by tiny defects inside the specimens. One can observe that PU (Bionate 55D) doesn't change its curve due the SBF, however the temperature influences it because when SBF was increased at 37ºC, the sample needed less load value to creep at the same level as at 23ºC. If the load had been increased in the last condition, it will probably creep rapidly.

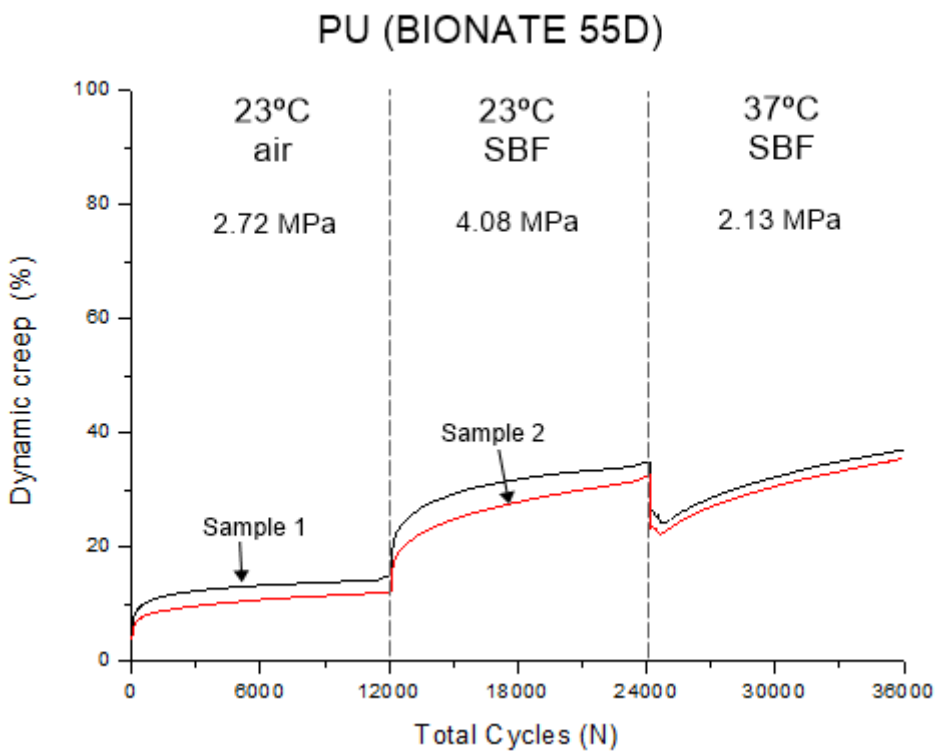

Fig. 3.19. Dynamic creep (ε_d) curve for PU (Bionate 55D) under different temperatures and environmental conditions. Test frequency: 1.33 Hz

Related to PET-DLA (70/30), the new UTS (3.23 MPa), which has been chosen from the static tensile test at 37ºC, was the value of Young Modulus at 100 % of elongation.

With that load value (Table 3.11), a new SLT test was performed at 37ºC and the result (Fig. 3.18) obtained was:

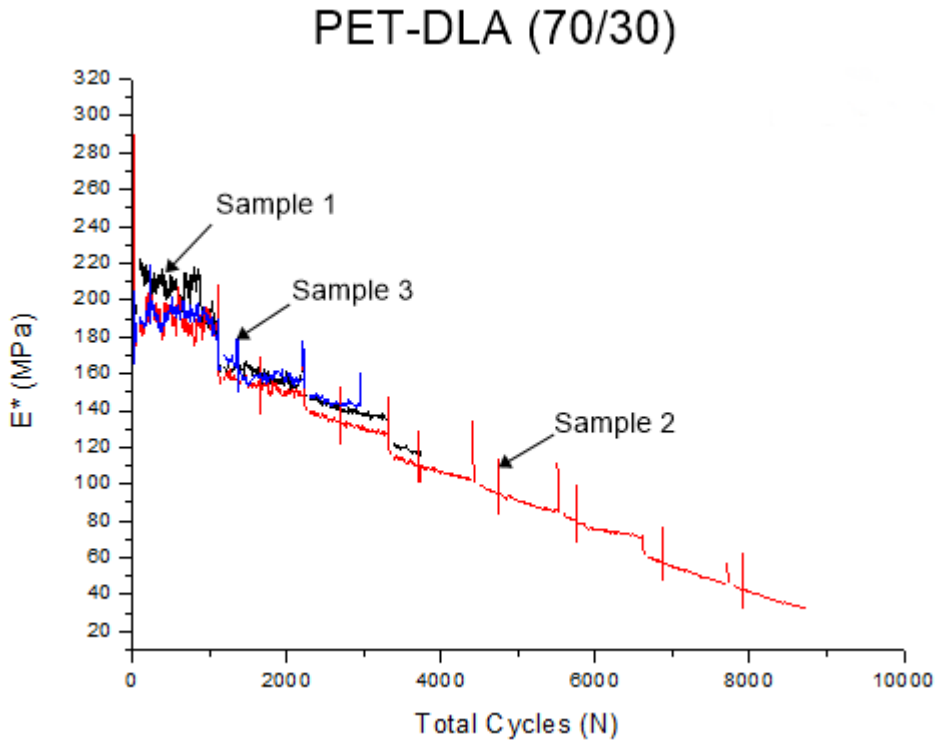

Fig. 3.18. Pattern of change in dynamic modulus at 37ºC

Although the difference of dynamic modulus was higher than 5% in the first step, it is seen that there is a lot of noise in the results and the second step (at 10% of UTS) is the most stable.

For the last SLT experiment, one sample is measured at 3 different conditions using the UTS value from Table 3.1. The problem is that as the previous graph shows, the material at 37ºC in SBF only reaches the second step with little probability. For SLT at 23ºC, the load value used was at 20% of UTS (3.12 MPa) but if that value is used now for 37ºC, the sample won't withstand that load (look at data in Table 3.11).

Thus, it was decided to choose a lower load value to see how the material would behave. That new value is 1.56 MPa (at 10% of UTS from Table 3.1) where the load is almost the same as in Table 3.11 but at 50% of UTS. If in SLT at 37ºC the step at 50% hadn't been reached, it is probably that in that case neither.

UTS		4Hz 5%	4Hz 10%	4Hz 15%	3Hz 20%	3Hz 25%	3Hz 30%	2HZ 35%	2HZ 40%	1HZ 45%	1HZ 50%
3,23	Load	0,16	0,32	0,48	0,65	0,81	0,97	1,13	1,29	1,45	1,62
	Amplitude	0,132	0,264	0,396	0,529	0,661	0,793	0,925	1,057	1,189	1,321
	Fmax	0,294	0,587	0,881	1,175	1,468	1,762	2,055	2,349	2,643	2,936
	Fmin	0,029	0,059	0,088	0,117	0,147	0,176	0,206	0,235	0,264	0,294

Table 3.11. Parameters calculated and introduced in the stepwise increasing load test (SILT) at 37ºC. All values are in MPa

Using a load value of 1.56 MPa at 3 different conditions, the results is shown in the following graph (Fig. 3.19):

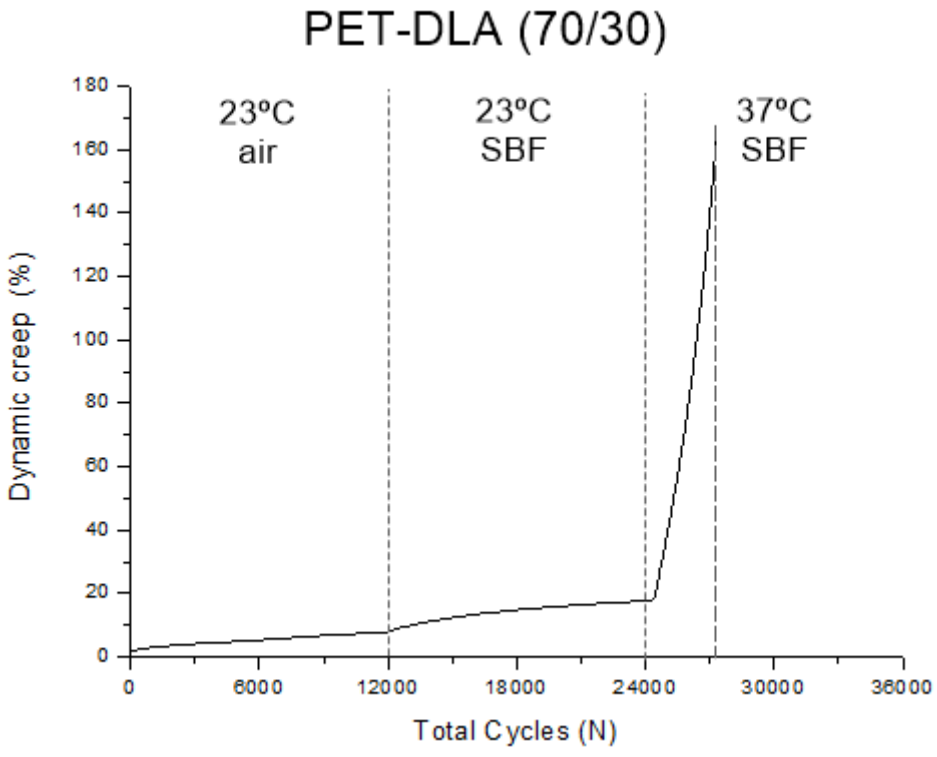

Fig. 3.19. Dynamic creep (ε_d) curve for PET-DLA (70/30) under different temperatures and environmental conditions. Constant loading of 1.56 MPa. Test frequency: 1.33 Hz

2L of SBF was used at 23ºC and two other were heated at 37ºC. After 24000 cycles there is a little error because all process was manually and it was needed to remove the SBF at 23ºC from the chamber and pour SBF at 37ºC into it.

The second SBF was heated in the laboratory at 37ºC but when it was poured into the chamber the temperature has decreased 2 ºC during the first liquid was removed. Using the heater inside the chamber the SBF started to heat but very slowly so it was heating from cycle no. 25000 (at 35ºC) to cycle no. 27200 (at 37ºC) and when the proper temperature was reached, the machine stopped because the maximum limit of it was exceeded.

As the last step hadn't been finished, it was decided to use the UTS value obtained in the static tensile test at 37ºC to see the behaviour of the material.

The first graph shows the most stable step is at 10% of UTS, with a load value of 0.32 MPa. The experiment was repeated again but with that value in the last step. The result wasn't as good as it was thought because the noise amplitude was higher than the material. Thus, the result wasn't a sinusoidal as the following picture (Fig. 3.20) proves:

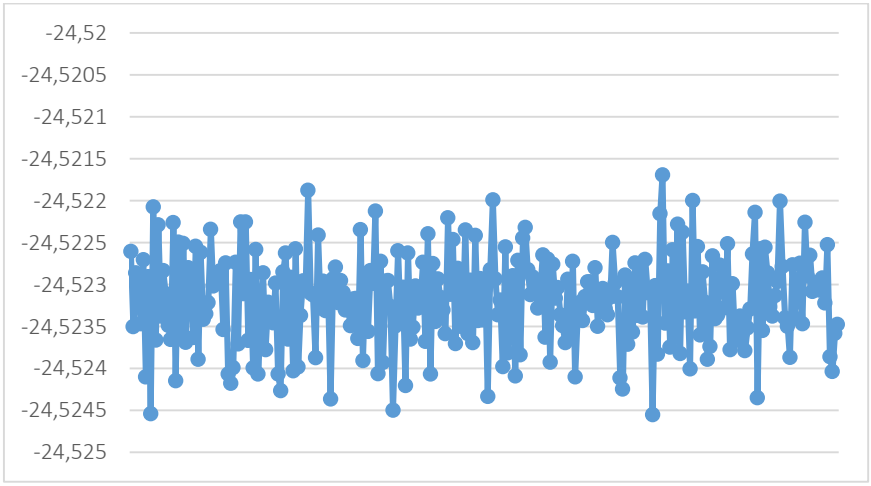

a)

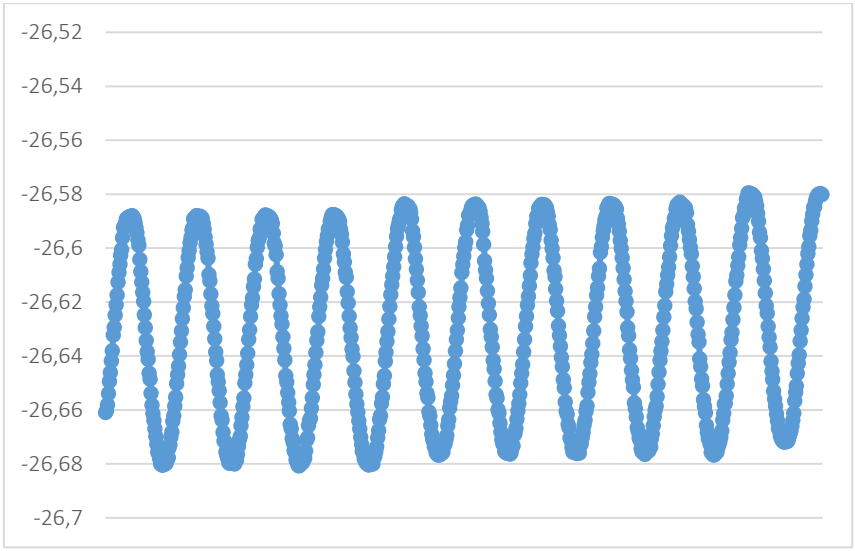

b)

Fig. 3.20. a) Representation of the real result of displacement (only noise) in the last condition (37ºC and 1.56 MPa). Data were randomly chosen from the results in the last condition. b) Representation of how the result should be

The left numbers are the displacement (mm) detected in the machine. In that case is only noise, probably produced by bubbles in SBF. The next graph (Fig. 3.21) shows that the machine didn't even move in the final step because the load value was too small compared to the noise:

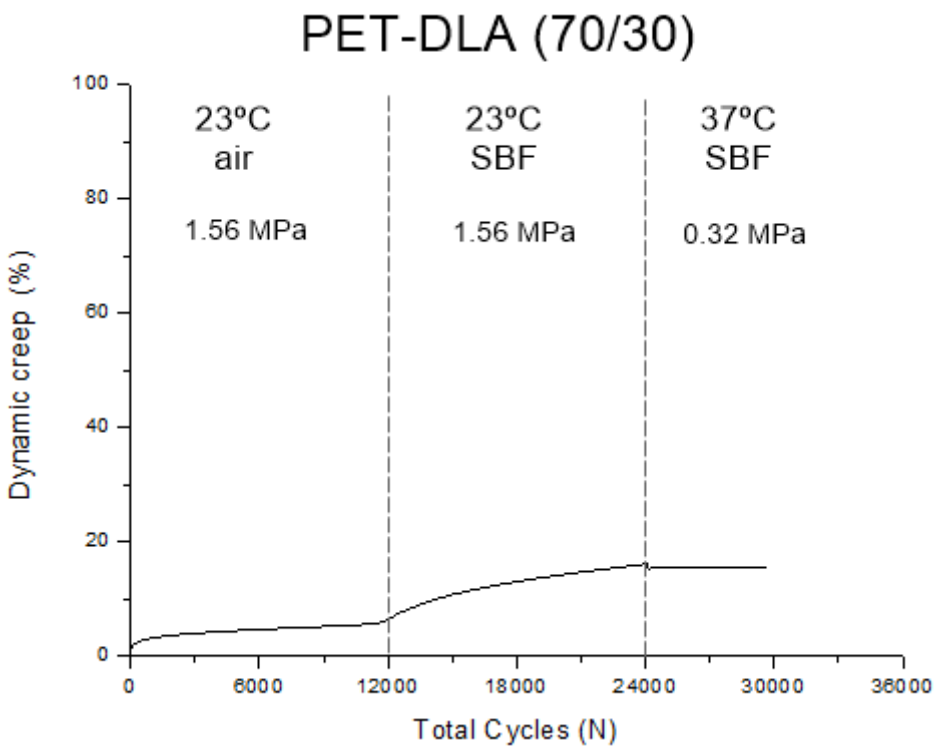

Fig. 3.21. Dynamic creep (ε_d) curve for PET-DLA (70/30) under different temperatures and environmental conditions. Test frequency: 1.33 Hz

It was decided to increase the load value at least at 20% of UTS (0.65 MPa) in the same sample to observe the behaviour in SBF at 37ºC. And the result (Fig. 3.22) obtained was:

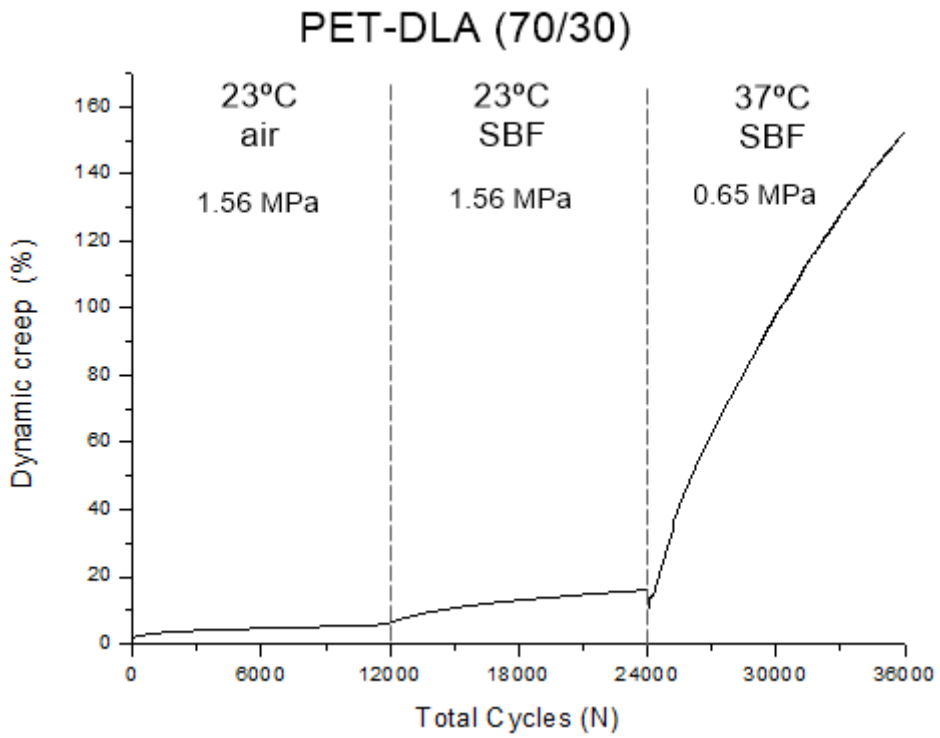

Fig. 3.22. Dynamic creep (ε_d) curve for PET-DLA (70/30) under different temperatures and environmental conditions. Test frequency: 1.33 Hz

Now, Fig. 3.22. lets know how the material is going to behave under these conditions. It is clear that it creeps a lot compared to the rest conditions although it is subjected to lower loads.

In that case, performing more tests should be assessed to see if material has a good reproducibility because Fig. 3.22 and Fig. 3.19 can't be compared since they have different load values at the end of the experiment (0.65 and 1.56 MPa respectively).

CONCLUSIONS

Thermoplastic elastomers (TPEs) consist of thermoplastic end blocks and an elastic midblock. As regards their structure and behaviour, they belong to a material class that is positioned between plastics (thermoplastics) and rubber (elastomer) and have gradually been developed into a material class of their own.

Similar to thermoplastics, TPEs become plastic when heated and elastic when cooled down again. In elastomers, this behaviour is due to chemical cross-linking. In TPEs, it is the result of physical cross-linking, and any changes in behaviour caused by heating are reversible. When the material is cooled down, new cross-links are established, which bond the elastic blocks into rigid three-dimensional networks. This means that TPEs show elastic properties that are similar to those of elastomers, while allowing for repeat deformation and recovery as known from thermoplastics. Thermoplastic elastomers are thus free-flowing and formable.

Due to their excellent stability and inertness they have become mayor key synthetic polymers used for biomedical applications.

This research work shows that different combinations of thermoplastic materials can be used to imitate the heart tissue. Polyurethane (PU (Bionate 55D)) and a multiblock polyester copolymer composed from hard segments of ethylene terephthalate sequences as in PET (70%) and soft segments of ethylene dilinoleate composed of dimmer fatty acid, dilinoleic acid (DLA) (30%), were the main materials used for this work, to replicate the same conditions as in the human body. Samples were produced by injection moulding and tested to study their mechanical properties. The main test is the fatigue test in which materials were subjected to different situations like temperature or environmental conditions because it showed how the material could change inside or outside the body.

The fatigue properties studied are especially important in terms of mimicking natural biostructural materials, because differences in morphology and nanostructure formations contribute to different mechanical properties and behaviours.

The use highly hydrophobic DLA yields transparent materials of expected high durability matching well the requirements of materials working under load bearing applications, such as heart assisting devices or other blood contacting devices.

Based on the results obtained it can be concluded that both materials are quite good to be implemented as heart assisting devices, although PET-DLA is a relatively new material which needs to be investigated further after these results to draw practical conclusions.

REFERENCES

1- Langer, R & Vacanti JP, Tissue Engineering. Science, vol.260, p. 920-926, 1993
2- Bone [anatomy], Microsoft® Encarta® Online Encyclopedia 2008
3- Physiology of the Heart written by Arnold M. Katz
4- Cardiac Tissue Engineering: Principles, Materials, and Applications written by Smadar Cohen,Emil Ruvinov,Yulia Sapir. Chapter 2: 7-9
5- Handbook of Cardiac Anatomy, Physiology, and Devices written by Paul A. Iaizzo “Anatomy of the Human Heart” Anthony J. Weinhaus and Kenneth P. Roberts 64-66
6- http://biology.about.com/od/anatomy/a/aa022808a.htm
7- http://www.ncbi.nlm.nih.gov/books/NBK9961/
8- Cardiovascular Physiology Concepts Second Edition. Published by Lippincott Williams & Wilkins, 2011, 60-92
9- Physiology written by Roger Thies,K.W. Barron, 75-91
10- Understanding Medical Physiology written by Bijlani, 137-170
11- Anatomy and Physiology' 2007 Ed.2007 Edition written by Martini, Frederic Et Al, 519-529
12- Cardiac conduction system - National Library of Medicine - http://www.nlm.nih.gov/
13- Four Steps of Cardiac Conduction - http://biology.about.com/
14- "Target Heart Rates - AHA". Target Heart Rates. American Heart Association. 4 Apr 2014. Retrieved 21 May 2014
15- Sherwood L. (2008). Human Physiology, From Cells to Systems p. 327.
16- The Encyclopedia of Men's Health written by Glenn S. Rothfeld,Deborah S. Romaine – p. 158
17- An Invitation to Health 2009-2010 Edition, written by Dianne Hales 117-118
18- Kolata, Gina (2001-04-24). 'Maximum' Heart Rate Theory Is Challenged. New York Times.
19- Precision Heart Rate Training written by Ed Burke p. 30
20- Atwal S, Porter J, MacDonald P (February 2002). "Cardiovascular effects of strenuous exercise in adult recreational hockey: the Hockey Heart Study". CMAJ 166 (3): 303–7.
21- Frequency of a Beating Heart. The Physics Factbook. Edited by Glenn Elert
22- The New Book of Popular Science. Connecticut: Grolier Inc, 1996.
23- Magill, Frank. Magill's Survey of Science. New Jersey: Salem, 1991.
24- Bender, Lionel. Human Body. New York: Crescent, 1992.
25- Lietz, Gerald & Anne White. Secrets of the Heart and Blood. Illinois: Gerrard, 1965.
26- Berkow, Robert. The Merck Manual of Medical Information. New Jersey: Merck, 1997.

27- What is Heart Rate Variability (HRV) - http://www.hrvhq.com/
28- Biomedical Engineering Department, Tlemcen University, Tlemcen, 13000, Algeria and Journal of Medical Engineering & Technology 08/2013;
29- Billman, George E. (2013). "The LF/HF ratio does not accurately measure cardiac sympatho-vagal balance". Frontiers in Physiology 4: 26.
30- Zierler KL: Mechanism of muscle contraction and its energetics. In: Mountcastle VB [ed]: Medical Physiology. 13th ed. Vol. 1, St. Louis, Mosby 1974.
31- Costanzo, Linda S. (2007). Physiology. Hagerstwon, MD: Lippincott Williams & Wilkins. p. 81
32- Analytical and Quantitative Cardiology edited by S. Sideman,Rafael Beyar. Chapter 29
33- Swanton's Cardiology written by R. Howard Swanton,Shrilla, p.587-593
34- Biomaterials: A Basic Introduction written by Qizhi Chen,George Thouas, p.324
35- Plastics Materials and Processes: A Concise Encyclopedia written by Charles A. Harper,Edward M. Petrie, p.152-153
36- Tencer, J., Frick, I. M., Oquist, B. W., Alm, P., Rippe, B. 1998. Size-selectivity of the glomerular barrier to high molecular weight proteins: upper size limitations of shunt pathways. Kidney Int. 53:709-715.
37- Polymeric Biomaterials, Revised and Expanded edited by Severian Dumitriu. Chapter 13
38- R. Yoda, J Biomater Sci Polym Ed, 9 (1998) 561-626
39- A. Nakamura, Y. Ikarashi, T. Tsuchiya, M. A. Kaniwa, M. Sato, K. Toyoda, M. Takahashi, N. Oshawa, T. Uchima, Biomaterials, 11 (1990) 92-94
40- M.G. Tucci, M. Mattioli Belmonte, E. Toschi, G.A. Pelliccioni, L. Checchi, C. Castaldini, G. Biagini, G. Piana, Biomaterials, 17 (1996) 517-522
41- Advances in Elastomers II: Composites and Nanocomposites written by P. M. Visakh,Sabu Thomas,Arup K. Chandra,Aji. P. Mathew, p. 228-239
42- PolyOne GLS Thermoplastic Elastomers - http://www.glstpes.com
43- Developments in Thermoplastic Elastomers written by K. E. Kear
44- Polymer processing methods - An easy guide - http://www.tangram.co.uk/
45- Thermoplastic processing - http://www.chemtrend.com/
46- Todd, Robert H.; Allen, Dell K.; Alting, Leo (1994). Manufacturing Processes Reference Guide. Industrial Press, Inc.
47- Our company - http://www.dsm.com/
48- Handbook of Fillers, Extenders, and Diluents edited by Michael Ash, Irene Ash
49- Encyclopedia of Tribology written by C. Kajdas,E. Wilusz,S
50- Polymeric Materials Encyclopedia, Twelve Volume Set written by Joseph C. Salamone
51- The name Terylene was formed by inversion of (polyeth)ylene ter(ephthalate) and dates to the 1940s. Oxford Dictionary. Terylene was first registered as a UK trademark in April 1946. UK Intellectual Property Office UK00000646992

52- A.K. van der Vegt & L.E. Govaert, Polymeren, van keten tot kunstof, ISBN 90-407-2388-5
53- Record of Polyethylenterephthalat in the GESTIS Substance Database of the IFA, accessed on 7 November 2007
54- J. G. Speight, Norbert Adolph Lange (2005). McGraw-Hill, ed. Lange's handbook of chemistry (16 ed.). p. 2.807–2.758. ISBN 0-07-143220-5.
55- C. C. Xu, R. W. Chan., Pore Architeture of Bovine Acellular Vocal Fold Scaffold, Tissue Engineering Part A., vol.14, p.1893-1903, 2008
56- 73. L. C. X., S. M. M.,S. H. Teoh, D. W. Hutmacher , Dynamics of in Vitro Polymer Degradation of Polycaprolactone Based Scaffolds: Accelerated versus Simulated Physiological Conditions, Biomedical Materials, vol.3-34108, 2008
57- T. Kokubo, H. Kushitani, S. Sakka, T. Kitsugi and T. Yamamuro, "Solutions able to reproduce in vivo surface-structure changes in bioactive glass-ceramic A-W", J. Biomed. Mater. Res., 24, 721-734 (1990)
58- Stress-strain curve - http://physics.tutorvista.com/
59- Mechanics of Materials written by Dr. B. C. Punmia, Ashok Kr. Jain, Arun Kr. Jain,Dr. B.C. Punmia,Ashok Kr. Jain,Arun Kr. Jain – chapter 2
60- http://imechanica.org/files/handout6.pdf
61- Metal Fatigue in Engineering written by Ralph I. Stephens, Ali Fatemi, Robert R. Stephens, Henry O. Fuchs
62- Elements of Metallurgy and Engineering Alloys edited by Flake C. Campbell
63- Nanostructured Elastomeric Biomaterials For Soft Tissue Reconstruction edited by Miroslawa El Fray
64- A.S. Argon. Topics in fracture and fatigueSpringer, New York (1992)
65- Fatigue test - http://www.instron.com/
66- Altstädt V. Hysteresismessungen zur Charakterisierung der mechanisch-dynamischen Eigenschaften von R-SMC. PhD Dissertation, University Kassel; 1987.
67- R. Renz, V. Altstädt, G.W. Ehrenstein. J Reinf Plast Compos, 7 (1988), p. 413–434
68- F. Orth, L. Hoffmann, H. Zilch-Bremer, G.W. Ehrenstein. Compos Struct, 24 (1993), p. 265–272
69- F. Raue, G.W. Ehrenstein. Macromol Symp, 148 (1999), pp. 229–240
70- I.M. Ward. An introduction to the mechanical properties of solid polymers J Wiley & Sons, Chichester (1993)
71- Zysk T. Zum statischen und dynamischen Werkstoffverhalten von Thermoplastischen Elastomeren, PhD Dissertation, University Erlangen; 1993.
72- Creep and Creep Failures. David N. French, Sc. D.President of David N. French, Inc., Metallurgists, Northborough, MA July 1991